



# Univerzita Tomáše Bati ve Zlíně

## Fakulta aplikované informatiky

**M.Sc. Juan Carlos Beltrán Prieto**

### **Zpracování glycerinové frakce**

**Treatment of glycerin fraction**

**Disertační práce**

Studijní program:

Inženýrská informatika

Studijní obor:

Automatické řízení a informatika

Školitel:

prof. Ing. Karel Kolomazník, DrSc.

Zlín, únor 2015

# ACKNOWLEDGEMENT

I would like to take the opportunity to thank very warmly all the people that helped me and supported me through the doctoral studies and during my daily life in the Czech Republic.

Special heartfelt gratitude and appreciation goes to my supervisor, prof. Ing. Karel Kolomazník, DrSc., Dr.h.c, for his enlightening guidance, devoted advice and commentaries that were of high value to complete this thesis research. His networking connections and solid industry relationships were truly important.

I would also like to recognize and extend my appreciation to the committee members, for taking their time to read the thesis and perform the evaluation.

Significant acknowledgements as well to the brilliant minds of researchers and academics from Tomas Bata University in Zlín, who contributed to several parts of the research through fruitful analysis, consultation, arguments, smart ideas and meetings, namely doc.Ing.Věra Kašpárková,CSc, Ing. Roman Slavík, Ph.D, prof. Ing. Roman Prokop, CSc, Ing. Jiří Pecha, and Mgr. Michaela Bařinová, Ph.D.

Prof. Jean Pierre Corriou, deserves also special thanks. His teachings helped me to understand the basics of process dynamics and control.

Acknowledgement is also extended to the organizations and institutions that financially supported me during my doctoral studies, namely The National Council on Science and Technology (CONACYT), Tomas Bata University in Zlín, Internal Grant Agency (IGA) and the CEBIA-Tech Regional Research Centre

Gratitude is also expressed to the laboratory colleagues, Ing. Veronika Friebrová, PhD, Ing. Lubomír Šánek, Mr. Karel Klein, Bc. Vladimír Dostál, and Ing. Pavel Kocurek, PhD. For making the environment in the laboratory a very warmful place to be.

Last but not least, sincere and deep recognition goes to my mother Lilia Prieto, my father Antonio Beltrán and my brother Luis Antonio for their encouragement, love and support.

Thank you all, this work is truly also yours

## ABSTRAKT

Současný nárůst množství přebytkového glycerinu v důsledku zvyšující se produkce bionafty vedl k intenzivnímu výzkumu v oblasti hledání nových aplikací glycerinu se zvláštním důrazem na vývoj produktů s vysokou užitnou hodnotou. Hlavní náplní práce byla parciální oxidace glycerinu na platinových elektrodách v roztocích oxidu manganičitého ( $\text{MnO}_2$ ) s využitím elektrochemických metod, konkrétně cyklické voltametrie a multipulzní ampérometrie. Rovněž byl řešen problém řízené oxidace glycerolu s využitím oxidu dusného. Pomocí vysokoúčinné kapalinové chromatografie (HPLC) byla vyvinuta metoda identifikace a kvantifikace oxidačních produktů glycerinu.

Byla navržena analytická řešení některých deterministických modelů oxidace glycerolu. Dále byl navržen fyzikálně-matematický model oxidace glycerolu, provedena jeho linearizace a byla stanovena přenosová funkce pro účely řízení. Byla pozorována dobrá shoda mezi numerickými daty (z matematického modelování), experimentálními daty a výstupy získanými pomocí příslušné přenosové funkce a impulzního vstupu. Výsledky ukázaly, že stanovená přenosová funkce systému plně popisuje daný proces.

**Klíčová slova:** anodická oxidace, glycerol, glyceraldehyd, platinová elektroda, přenosová funkce

## ABSTRACT

The recent increase in the amount of surplus glycerin as a result of biodiesel production has caused an intensive research aiming to find new applications for glycerin with special interest in the development of value added products. In this work, the partial oxidation of glycerin on platinum electrodes in presence of manganese dioxide ( $\text{MnO}_2$ ) by electrochemical methods was performed by means of cyclic voltammetry and multiple pulse amperometry techniques. The case of controlled oxidation of glycerol using nitrous oxide was also analyzed and explained. A method for the identification and quantification of glycerin oxidation products was developed by High Performance Liquid Chromatography (HPLC).

Proposal of analytical solutions of some deterministic models of glycerol oxidation was performed. The determination of the physical mathematical model for glycerol oxidation, performance of the linearization of the proposed model and determination of transfer function for control purposes was achieved. Agreement between numerical data (from mathematical modeling), experimental data and output using the respective transfer function and impulse input was observed. As a result, the determined transfer function of the system demonstrated to fully describe the process

**Keywords:** anodic oxidation, glycerol, glyceraldehyde, platinum electrode, transfer function

# CONTENT

<b>LIST OF FIGURES</b> .....	<b>7</b>
<b>LIST OF TABLES</b> .....	<b>11</b>
<b>LIST OF APPENDICES</b> .....	<b>12</b>
<b>LIST OF ABBREVIATIONS AND SYMBOLS</b> .....	<b>13</b>
<b>1 INTRODUCTION</b> .....	<b>16</b>
<b>2 STATE OF ART</b> .....	<b>18</b>
2.1 Biocatalysis.....	18
2.2 Heterogeneous catalysis .....	19
2.3 Homogeneous catalysis.....	21
2.4 Electrochemical oxidation.....	22
2.4.1 Anodic oxidation .....	23
2.5 Reasons for chemical process control .....	25
2.6 Evaluation of the state of the art.....	25
<b>3 AIMS OF THE THESIS</b> .....	<b>27</b>
<b>4 EXPLORATION OF THE PRODUCTION SYSTEM</b> .....	<b>28</b>
4.1 Modeling of the partial oxidation of glycerin.....	28
4.2 Kinetics model for glycerin oxidation - non linear model .....	32
4.3 Evaluation of the oxidation of adiabatic temperature .....	34
4.3.1 Estimation of thermodynamics parameters of the oxidation of glycerin to glyceraldehyde with H <sub>2</sub> O <sub>2</sub> .....	34
4.3.2 Estimation of thermodynamics parameters of the oxidation of glycerin to glyceraldehyde with airborne oxygen and nitrous oxide .....	37
<b>5 DETERMINATION OF TRANSFER FUNCTION FOR ISOTHERMAL CASE – ANODIC OXIDATION</b> .....	<b>41</b>
<b>6 DETERMINATION OF TRANSFER FUNCTION FOR ISOTHERMAL CASE – OXIDATION USING NO<sub>2</sub></b> .....	<b>47</b>
<b>7 NON-ISOTHERMAL REACTION SYSTEMS</b> .....	<b>57</b>
<b>8 A SIMPLIFIED MODEL FOR THE OXIDATION OF GLYCEROL INTO GLYCERALDEHYDE AND THE DETERMINATION OF TRANSFER FUNCTION</b> .....	<b>64</b>
<b>9 ANALYSIS OF THE OXIDATION OF GLYCEROL CONSIDERING CONSECUTIVE REVERSIBLE REACTION</b> .....	<b>70</b>

<b>10 EXPERIMENTAL MEASUREMENTS.....</b>	<b>75</b>
10.1 Liquid chromatography method .....	75
10. 1. 1 Instrument.....	75
10. 1. 2 Chemicals and reagents .....	75
10. 1. 3 Sample preparation for development of the HPLC method .....	75
10. 1. 4 Chromatographic method development .....	76
10. 1. 5 Chromatographic validation .....	76
10.2 Electrochemical experiments.....	77
10. 2. 1 Anodic oxidation .....	77
10. 2. 2 Instrument.....	77
10. 2. 3 Voltammetric measurements .....	77
10. 2. 4 Effect of varying glycerol and MnO <sub>2</sub> concentration .....	78
10. 2. 5 Effect of potential scan limits, scan rate and analysis of temperature variation.....	78
10. 2. 6 Oxidation of glycerol using multiple pulse amperometry.....	79
10.3 Approximate experiments oxidation of glycerol nitrous oxide .....	80
<b>11 RESULTS .....</b>	<b>84</b>
11.1 Chromatographic method development .....	84
11.2 Validation parameters.....	86
11.3 Analysis of cyclic voltammetric data.....	89
11.4 The analysis of glycerol and MnO <sub>2</sub> reaction order.....	90
11.5 The effect of potential scan limits on cyclic voltammogram .....	92
11.6 The effect of sweep rate variation on cyclic voltammogram.....	95
11.7 The effect of temperature on cyclic voltammogram .....	97
11.8 Oxidation at controlled potential by multiple pulse amperometry .....	98
11.9 Evaluation of kinetic parameters using mathematical statistic method .....	99
<b>12 CONTRIBUTION OF THE THESIS TO SCIENCE AND PRACTICE AND DISCUSSION.....</b>	<b>106</b>
<b>13 RECOMMENDATION FOR INDUSTRIAL APPLICATIONS .....</b>	<b>109</b>
<b>14 CONCLUSIONS .....</b>	<b>110</b>
<b>15 LITERATURE .....</b>	<b>111</b>
<b>APPENDICES .....</b>	<b>120</b>
<b>LIST OF AUTHOR PUBLICATIONS.....</b>	<b>132</b>
<b>CURRICULUM VITAE OF AUTHOR .....</b>	<b>135</b>

## LIST OF FIGURES

<b>Fig. 1</b>	Experimental setup of an electrochemical cell.....	24
<b>Fig. 2</b>	Representation of an electrode reaction occurring in the electrode .....	24
<b>Fig. 3</b>	Response of (a) stable; and (b) unstable systems .....	25
<b>Fig. 4</b>	Simplified model of anodic oxidation.....	29
<b>Fig. 5</b>	Dimensionless plot of glycerol and products using values of $k_1=0.04$ , $k_2=0.18$ , $k_3=0.01 \text{ h}^{-1}$ in the analytical solution.....	31
<b>Fig. 6</b>	Dimensionless plot of glycerol and products using values of $k_1=0.01$ , $k_2=0.05$ , $k_3=0.02 \text{ h}^{-1}$ in the analytical solution.....	31
<b>Fig. 7</b>	Dimensionless plot of time needed to reach the maximum concentration of glyceraldehyde. ....	32
<b>Fig. 8</b>	Concentration profile for reactants and product with $k_2/k_1=1$ and $R_0/G_0=1.2$ .....	33
<b>Fig. 9</b>	Concentration profile for reactants and product with $k_2/k_1=3$ and $R_0/G_0=0.5$ .....	33
<b>Fig. 10</b>	Concentration profile for reactants and product with $k_2/k_1=10$ and $R_0/G_0=0.5$ .....	34
<b>Fig. 11</b>	Scheme of the system describing the input, state variable and output.	41
<b>Fig. 12</b>	Scheme of the oxidation of glycerol with $\text{NO}_2$ describing the input, state variable and output. ....	47
<b>Fig. 13</b>	Step response for the system of glycerol oxidation with $\text{NO}_2$ . Input $u_1=F$ to respective outputs $y_1=A \square$ ; $y_2=R \circ$ ; $y_3=G \diamond$ ; $y_4=K \Delta$ . ....	55
<b>Fig. 14</b>	Step response for the system of glycerol oxidation with $\text{NO}_2$ . Input $u_2=C_{G0}$ to respective outputs $y_1=A \square$ ; $y_2=R \circ$ ; $y_3=G \diamond$ ; $y_4=K \Delta$ .....	55
<b>Fig. 15</b>	Step response for the system of glycerol oxidation using $\text{NO}_2$ . Input $u_3=C_{R0}$ to respective outputs $y_1=A \square$ ; $y_2=R \circ$ ; $y_3=G \diamond$ ; $y_4=K \Delta$ .....	56
<b>Fig. 16</b>	Non-isothermal reaction system for the conversion of glycerol (G) into glycerol oxidation products (GO).....	57
<b>Fig. 17</b>	Scheme of the system describing the input, state variable and output.	57
<b>Fig. 18</b>	Scheme of the system describing the input, state variable and output.	64
<b>Fig. 19</b>	Scheme of chemical reactor for anodic oxidation of glycerol in which glyceraldehyde is the main product.....	65
<b>Fig. 20</b>	Profile of temperature in function of time for glycerol oxidation to glyceraldehyde.....	66

<b>Fig. 21</b>	Profile of reaction temperature in function of time and $a_G$ for glycerol oxidation to glyceraldehyde... ..	66
<b>Fig. 22</b>	Profile of reaction temperature in function of $a_G$ and mass flow input of glycerol for glycerol oxidation to glyceraldehyde .....	67
<b>Fig. 23</b>	Full mechanism of anodic oxidation with reversible reactions .....	70
<b>Fig. 24</b>	Description of the system including the input, state variable and output .....	70
<b>Fig. 25</b>	Output of the system for concentration of oxidation products based on the respective transfer functions ( $\diamond CB$ ; $\Delta CC$ ; $*CD$ ; $\bullet CE$ ; $—CF$ ) .....	73
<b>Fig. 26</b>	Output of the system for concentration of glycerol.....	74
<b>Fig. 27</b>	Devices used for electrochemical experiments. a)EmStat Potentiostat. b)electrochemical cell, c)working electrode, d)reference electrode, e)counter electrode. ....	78
<b>Fig. 28</b>	HPLC chromatogram and cyclic voltammogram after 3 hours of controlled potential.....	79
<b>Fig. 29</b>	HPLC chromatogram after 4 hours of controlled potential.....	80
<b>Fig. 30</b>	HPLC chromatogram after 5 hours of controlled potential.....	80
<b>Fig. 31</b>	Temperature vs time plot for the oxidation of glycerol in ammonium nitrate... ..	82
<b>Fig. 32</b>	Influence of flow rate and concentration of mobile phase on resolution between glyceraldehyde and glyceric acid.....	85
<b>Fig. 33</b>	Influence of flow rate and concentration of mobile phase on resolution between glycolic acid and dihydroxyacetone. ....	85
<b>Fig. 34</b>	HPLC analysis at optimized conditions: Temperature: 30 °C, mobile phase: 3mM H <sub>2</sub> SO <sub>4</sub> flow rate: 0.5mL/min. The elution order is 1. Mesoxalic acid, 2.Tartronic acid, 3.Glyceraldehyde, 4.glycerol, 5. Glyceric acid, 6.Glycolic acid, 7.Dihydroxyacetone.....	86
<b>Fig. 35</b>	Sensitivity test for quantification of glyceric acid in RI detector .....	89
<b>Fig. 36</b>	Cyclic voltammogram analysis of Pt electrode in the presence of MnO <sub>2</sub> and glycerol + MnO <sub>2</sub> .....	90
<b>Fig. 37</b>	Analysis of the variation of glycerol concentration on the current density (j) at different potentials for glycerol solutions (15-124 mM) in 14mM MnO <sub>2</sub> .....	91
<b>Fig. 38</b>	Inductive effect of the glycerol molecule .....	91

- Fig. 39** Log of peak current vs log of oxidant concentration for partial oxidation of glycerol.....92
- Fig. 40** Cyclic voltammogram for glycerol oxidation varying forward potential limit. a) 0 V, b) 0.5 V, c) 1 V, e) 1.5 V in 0.0625 M glycerol + 0.014 M MnO<sub>2</sub> (25 °C, 0.05 V/s)... ..93
- Fig. 41** Cyclic voltammogram for glycerol oxidation varying forward potential limit. (dotted line -1.5 to 1.3 V; dashed line (---) -1.5 to 1.5 V) in 0.0625 M glycerol + 0.014 M MnO<sub>2</sub> (25 °C, 0.05 V/s)... ..94
- Fig. 42** The effect of varying the negative potential limit on cyclic voltammograms at 25 °C and 0.05 V/s. a) -1 V, b) -1.2 V, c) -1.35, d) -1.5 V .....94
- Fig. 43** Effect of varying the sweep rate on the voltammograms of a platinum electrode in 0.0625 M glycerol + 0.014 M MnO<sub>2</sub> (25 °C). Solid line: 0.01 V·s<sup>-1</sup>; dash dot line: 0.03 V·s<sup>-1</sup>; round dot line: 0.05 V·s<sup>-1</sup>; long dash line: 0.07 V·s<sup>-1</sup>; square dot line: 0.1 V·s<sup>-1</sup> .....95
- Fig. 44** Plot of peak potential against the logarithm of sweep rate for platinum electrode in 0.0625 M glycerol + 0.014 M MnO<sub>2</sub> (25 °C). a) Peak I, b) Peak 2, c) Peak 3.....96
- Fig. 45** Dependence on anodic peak current on the applied scan rate obtained from cyclic voltammetry .....96
- Fig. 46** Plot of current peak against sweep rate potential that shows the possibility of adsorbed species.....97
- Fig. 47** Arrhenius plot for glycerol oxidation. (■) peak I; (●) peak II; (\*) peak III.....97
- Fig. 48** Current vs time plot at controlled potential using multiple pulse amperometry a) without pulse steps of ±1.5V b) including pulse steps of ±1.5V for 1 s each.....98
- Fig. 49** Plot of glycerol and products formed (glyceric acid, glyceraldehyde, glycolic acid, tartronic acid, mesoxalic acid) (dimensionless) vs time of oxidation .....99
- Fig. 50** Comparison between numerical results and experimental data for the partial electrochemical oxidation of glycerol. The products are (■) glyceraldehyde, (▲) glyceric acid, and (◆) glycolic acid... ..101
- Fig. 51** Products concentration profile. Comparison between numerical results and experimental data for the mechanism described in Fig 23. (■) glyceraldehyde, (▲) glyceric acid, (◆) glycolic acid, (●)tartronic acid, (\*) mesoxalic acid.....102

<b>Fig. 52</b>	Glycerol concentration profile. Comparison between numerical results and experimental data for the mechanism described in Fig 23 .....	102
<b>Fig. 53</b>	Estimation of the output (products formed $\square C_B$ ; $\blacktriangle C_C$ ; $\blacktriangledown C_D$ ; $\diamond C_E$ ; $-C_F$ ) after impulse input during anodic oxidation of glycerol.....	104
<b>Fig. 54</b>	Estimation of the concentration of glycerol (output) to an impulse input during electrooxidation of glycerol .....	105
<b>Fig. 55</b>	Technique: Multiple pulse amperometry, E1:1.05V, t1=2s, E2:-1.5V, t2=1s, E3:1.5V, t3=1s, reaction time 2h .....	120
<b>Fig. 56</b>	Technique: Multiple pulse amperometry, E1:1.05V, t1=2s, E2:-1.5V, t2=1s, E3:1.5V, t3=1s, reaction time 5h .....	120
<b>Fig. 57</b>	Technique: Multiple pulse amperometry, E1:0.7V, t1=2s, E2:-1.5V, t2=1s, E3:1.5V, t3=1s, reaction time 16h .....	121
<b>Fig. 58</b>	Technique: Multiple pulse amperometry, E1:0.7V, t1=2s, E2:-1.5V, t2=1s, E3:1.5V, t3=1s, reaction time 11h .....	121
<b>Fig. 59</b>	Technique: Multiple pulse amperometry, E1:1.05V, t1=2s, E2:1.5V, t2=1s, E3:0.7V, t3=1s, reaction time 13h .....	122
<b>Fig. 60</b>	Technique: Multiple pulse amperometry, E1:1.05V, t1=2s, E2:-1.5V, t2=1s, E3:1.5V, t3=1s, reaction time 14h, 100 rpm, 63 °C .....	122
<b>Fig. 61</b>	Technique: Multiple pulse amperometry, E1:1.05V, t1=2s, E2:-1.5V, t2=1s, E3:1.5V, t3=1s, reaction time 7h .....	123
<b>Fig. 62</b>	Technique: Multiple pulse amperometry, E1:1.05V, t1=2s, E2:-1.5V, t2=1s, E3:1.5V, t3=1s, reaction time 4h .....	123
<b>Fig. 63</b>	Step response of the system considering the estimated transfer functions for glycerol reacted (a) and products formed (b) ( $\square C_B$ ; $\blacktriangle C_C$ ; $\blacktriangledown C_D$ ; $\diamond C_E$ ; $-C_F$ ) .....	129
<b>Fig. 64</b>	Proposal of closed-loop PID controllers for the stabilization of the anodic oxidation system .....	130
<b>Fig. 65</b>	Dynamic response of feedback loop. Estimation of the output response (solid line: glycerol; products formed $\square C_B$ ; $\blacktriangle C_C$ ; $\blacktriangledown C_D$ ; $\diamond C_E$ ; $-C_F$ ) after step input .....	131

## LIST OF TABLES

<b>Table 1</b>	Bond enthalpies for glycerol, H <sub>2</sub> O <sub>2</sub> , glyceraldehyde and H <sub>2</sub> O from references [65], [66], [67]. .....36
<b>Table 2</b>	Enthalpy change due to the vaporization stage for glycerol, H <sub>2</sub> O <sub>2</sub> , glyceraldehyde and H <sub>2</sub> O. Values were obtained from reference [68]. .....36
<b>Table 3</b>	Bond energies for glycerol, N <sub>2</sub> O, O <sub>2</sub> , glyceraldehyde, N <sub>2</sub> , and H <sub>2</sub> O. Values from references [65], [66], [67]. .....39
<b>Table 4</b>	Enthalpy change due to the vaporization stage for glycerol, H <sub>2</sub> O <sub>2</sub> , glyceraldehyde and H <sub>2</sub> O e.g. [68]. .....39
<b>Table 5</b>	Record of temperature variation after addition of NH <sub>4</sub> NO <sub>3</sub> . .....82
<b>Table 6</b>	Summary of conditions allowing the identification of all the standards analyzed with the respective resolution achieved .....86
<b>Table 7</b>	Standard curves for glycerol oxidation products .....87
<b>Table 8</b>	Intra-day precision Test of the HPLC method for the determination of glycerol oxidation products (UV detector) .....87
<b>Table 9</b>	Intra-day precision Test of the HPLC method for the determination of glycerol oxidation products (RI detector). .....88
<b>Table 10</b>	Sensitivity analysis of UV and RI detectors .....88
<b>Table 11</b>	Reaction order with respect to glycerol and MnO <sub>2</sub> for the electrooxidation of glycerol .....92
<b>Table 12</b>	Apparent activation energy ( $\Delta E^*$ ) for the forward scan peaks detected .....98
<b>Table 13</b>	Closed-loop calculations of controller parameters .....130

## LIST OF APPENDICES

<b>Appendix A</b> HPLC chromatogram of some anodic oxidation experiments .....	120
<b>Appendix B</b> List of selected experiments performed for the evaluation of parameters affecting the anodic oxidation of glycerol and influence on selectivity and conversion to glyceraldehyde.....	124
<b>Appendix C</b> Program developed in Matlab for the simulation of chemical reaction in series $A \rightarrow B \rightarrow C \rightarrow D$ .....	125
<b>Appendix D</b> Incorporation of PID controllers. ....	129

## LIST OF ABBREVIATIONS AND SYMBOLS

Abbreviations	Description
pH	potential of hydrogen
<i>et al.</i>	<i>et alibi.</i> (and others)
i.e.	id est (that is).
NAD <sup>+</sup>	Nicotinamide adenine dinucleotide
<i>sp.</i>	specie
MWCNTs	multi-walled carbon nano tubes
TEMPO	2,2,6,6-tetramethylpiperidin-1-yl)oxidanyl
scCO <sub>2</sub>	supercritical carbon dioxide
HPLC	High performance liquid chromatography
RI	refractive index
UV	ultraviolet
S/N	signal to noise ratio
<i>e.g.</i>	exempli gratia (for example)
Symbol	Description
g	grams
°C	Celsius
h	hour
L	Liter
Au	Gold
Pt	Platinum
Pd	Palladium
Rh	Rhodium
Co	Cobalt
Bi	Bismuth
TiO <sub>2</sub>	Titanium dioxide
OH <sup>-</sup>	Hydroxyl radical
H <sup>+</sup>	Hydrogen
% w/w	weight/weight percent
NaOH	Sodium hydroxide

$\text{PdCl}_4^{-2}$	tetrachloropalladate
K	Kelvin
C	Carbon
$\text{CO}_2$	Carbon dioxide
MPa	Megapascals
Sb	Antimon
$\text{H}_2\text{O}_2$	Hydrogen peroxide
NaOCl	Sodium hypochlorite
DHA	Dihydroxyacetone
NaOH	Sodium hydroxide
M	Molar
$\text{HClO}_4$	Perchloric acid
V	Voltage
rhe	reversible hydrogen electrode
$\text{Na}_2\text{SO}_4$	Sodium sulfate
$\text{KMnO}_4$	Potassium permanganate
Ru–Ir	Ruthenium – iridium
Sn	Stannum
$\text{N}_2\text{O}$	Nitrous oxide
$k_n$	rate constant ( $n>0$ )
$\text{C}_3\text{H}_8\text{O}_3$	Glycerol
$\text{C}_3\text{H}_6\text{O}_3$	Glyceraldehyde
$n_r$	number of mols
$\bar{C}_p$	specific heat of the reaction blend
kJ	Kilojoules
$(\Delta H)_r$	enthalpy of reaction
$\Delta H_{\text{vap}}$	enthalpy change due to vaporization
N	Nitrogen
O	Oxygen
T	temperature of reaction blend
A	state matrix
$a_{nm}$	elements of matrix A
B	control matrix
$b_{nm}$	elements of matrix B
$G(s)$	transfer function
$g_{nm}$	elements of transfer function
U	input variables
Y	output variables
X	state variables
$F_i$	input flow of glycerol
$T_i$	inlet temperature of glycerol

$T_j$	mean temperature in the jacket
$\rho$	density
$T_{j0}$	initial temperature of coolant
$T_j$	temperature of coolant at exit
$U$	overall heat transfer coefficient
$\Delta H$	heat of reaction
$t^*$	dimensionless time
$\dot{V}$	volume flow rate
s	second
m	meter
$H_2SO_4$	sulfuric acid
$k$	capacity factor
$\alpha$	selectivity
$N$	efficiency
$Rs$	resolution
$t_{B,A}$	retention time of compounds B,A
Ag/AgCl/KCl (sat.)	Silver/silver chloride/saturated KCl electrode
$MnO_2$	manganese dioxide
$MW_P$	molecular weight of product
$MW_G$	molecular weight of glycerol
$r^2$	coefficient of determination
$CV$	coefficient of variation
$\Delta E^*$	apparent activation energy
$F$	flow
$C_{A,B,C}$	concentration of A, B, C...
$V$	volume

# 1 INTRODUCTION

Petroleum fuels play an important role in industrial growth, transportation, agricultural sectors and in many other key areas of human activity. However, the ever-increasing demand for energy and the limits of the world's fossil fuel reserves make the task of producing an alternative fuel to fulfill the energy demands of the world essential, see *e.g.*, [1] and [2]. In addition, the problems that nowadays affect the use of fossil fuels include the increase of petroleum prices, which complicates economic sustainability, dissemination of pollutants dangerous for human health, and global warming caused by greenhouse gas emissions, as expressed in [3] and [4]. Currently, non-renewable resources such as oil, coal, and gas are the main raw materials for fuel production, see *e.g.* [5]. However, the increase of fuel prices has made the consumer look for cheaper and ecological alternatives. Biodiesel has emerged as an environmentally friendly substitute for fossil fuels to reduce the adverse ecological and health impacts of diesel engine emissions because it is produced from renewable sources such as vegetable oils or animal fats as discussed in [6].

The processes used for the production of biodiesel are pyrolysis, microemulsification, and transesterification. Of these processes, biodiesel is normally produced at industrial scale from triglycerides via a transesterification reaction with alcohols such as methanol or ethanol in the presence of an alkali catalyst, see *e.g.*, [7]. During consecutive reactions, the triglyceride is first converted into a diglyceride, then to a monoglyceride and finally to glycerol. The transesterification reaction of 1 mol of triolein (i.e. 885.5 g), used as a model triacylglycerol, with 3 mol of methanol (96.1 g) produces 1 mol of glycerol (92.1 g) and three mol of methyl oleate (889.5 g) in the case of 100 % conversion. Therefore, one of the most important challenges associated with the growing industry of biodiesel is the valorization of the high amounts of glycerol that are produced.

Owing to the functionality of the glycerol molecule, great efforts are being put into utilization of surplus glycerol in the synthesis of chemicals with higher added value, as described in [8]. Glycerol, or 1,2,3-propanetriol, is considered a versatile compound. Many different applications have been documented, for example in the manufacture of epichlorohydrin [9], the utilization as ingredient in livestock feed or in the synthesis of glycerol derivatives such as aldehydes, carboxylic acids, and ketones, frequently used in the preparation of new chemicals for cosmetics, medicine or food industry purposes. Among the most important valuable oxygenates are glyceraldehyde, dihydroxyacetone, glyceric acid, hydroxypyruvic acid, tartronic acid, mesoxalic acid, glycolic acid, and glyoxylic acid. However, glycerol conversion and selectivity for a specific product vary according to the reaction conditions (temperature, concentration of

reactants, solvent used, ratio of glycerol and catalyst, or mass-transfer conditions), configuration of the reactor, nature of the support, relationship between the rate of product desorption and subsequent oxidation to other glycerol derivative, and the selection of a specific oxidation method, which implies the use of a defining catalyst, microorganisms, chemical reagents or electrochemical conditions.

Moreover, the management of chemical reactors associated with exothermic reactions such as oxidation of organic substances is among the most challenging tasks of chemical reactor engineering. The design of an algorithm must be based on the stage before – the exploration of the production system – which includes research on their own reaction kinetics coupled with transport processes, especially the heat of reaction, which in case of oxidation of glycerol is considerable. The problem is complicated by the heterogeneity of the reaction mixture accompanying the products formed.

The control of oxidation reaction is a prerequisite for successful and safe industrial applications of this promising manufacturing technology. The task of the oxidation of glycerol oxidation products results from the urgent need for efficient processing of glycerin excess in biodiesel production. So far, this task has not been solved even for a practical sense.

In the present research, an alternative for partial oxidation of glycerol, namely anodic oxidation was studied, which was performed in the presence of platinum electrode and manganese dioxide. Estimation of the reaction enthalpy of the oxidation of glycerol to glyceraldehyde was realized and the kinetic model for anodic and catalytic oxidation using airborne oxygen and nitrous oxide was proposed. In addition, the determination of the transfer function for both systems under study was carried out.

## 2 STATE OF THE ART

The oxidation of glycerol is considered to be one of the most important alternatives of glycerol processing because it leads to the formation of aldehydes, carboxylic acids, and ketones, frequently used in the preparation of new chemicals for cosmetics, medicine or food industry purposes. However, the rate of glycerol conversion and the selectivity to a specific compound are strongly influenced by the reaction conditions, oxidation reagent employed, the reactor setup, the presence of glycerol derivatives formed during the oxidation and more important, the particular method of oxidation used. Therefore, the understanding of the effect of these parameters on the reaction system and the physical and chemical phenomena taking place in the oxidation reaction is important to be able to design a simple and effective control scheme of the process and maximize the output. For this reason I summarize comprehensive information about the main ways of partial oxidation of glycerol, namely biocatalysis, heterogeneous catalysis, homogeneous catalysis and electrochemical oxidation. However, more detailed information about these processes can be found in a recent publication [10].

### 2.1 Biocatalysis

The capacity of several microorganisms for using glycerol as a carbon substrate enables them to produce biomass and metabolites through a diversity of environmentally friendly processes, based on aerobic and anaerobic fermentation. Enzymes like glycerol dehydrogenase, glycerol kinase, glycerol dehydratase and methanol dehydrogenase are directly linked to the biotransformation of glycerol, see *e.g.*, [11]. The use of glycerol dehydrogenase from the gram-negative bacterium *Gluconobacter oxydans* for the production of dihydroxyacetone has been reported by several authors [12]–[16]. In addition, the behavior of the aerobic culture during the bioreaction has been described by mathematical modeling as in references [15] and [17]. A patent developed by Wolf in [18] reported the production of glyceraldehyde via the reaction of glycerol with a methanol dehydrogenase purified from *Methylobacterium organophilum*. The culture medium for the bioconversion contained up to 20 % glycerol with pH in the range of 5 to 11, and the temperature ranging from 5 to 50 °C under aerobic conditions. A maximum conversion of 35 % of glycerol was reported in a period of 24 h. In many cases, attempts to increase the yield of the desired product are made by optimizing the media components, the use of recombinant strains, and the modification of fermentation conditions.

As the glycerol molecule is a small uncharged molecule, it can cross the inner membrane of the cell through an integral membrane protein (glycerol uptake facilitator, in the case of *Escherichia coli*) that enables facilitated diffusion. Once inside the cell, glycerol can be metabolized to glycerol-3-phosphate by

glycerol kinase. Therefore, it has the potential to be substituted for common and bigger carbohydrates used in the fermentation process, such as glucose, starch or sucrose, as stated in reference [11].

Enzymatic production of glyceric acid from glycerol has been achieved through oxidative fermentation by the action of acetic acid bacteria such as *Acetobacter* and *Gluconobacter* strains in a jar fermenter. A bioconversion of  $136.5 \text{ g}\cdot\text{L}^{-1}$  was obtained when using *Gluconobacter frateurii* and  $101.8 \text{ g}\cdot\text{L}^{-1}$  with *Acetobacter Fropicallis* [19]. For the production of succinic acid, Lee *et al.* [20] proposed the addition of yeast extract in glucose fermentation to enhance the conversion to the desired product. Bizzini *et al.* [21] reported the formation of dihydroxyacetone phosphate by *Enterococcus faecalis* when using glycerol as a carbon source. In their work, they proposed two different pathways of glycerol metabolism according to the phosphorylation–oxidation pattern under aerobic and anaerobic conditions. Under anaerobic conditions, glycerol is oxidized by glycerol dehydrogenase and then phosphorylated by dihydroxyacetone kinase, whereas under aerobic fermentation, the majority of the *Enterococcus faecalis* strains metabolize glycerol by phosphorylation through the action of a glycerol kinase and then oxidation by glycerol-3-phosphate oxidase. Similarly, Joseph *et al.* [22] reported that a gram-positive bacterium like *Listeria monocytogenes* essentially needs a glycerol kinase for glycerol uptake and metabolism.

A nanoparticle-supported enzyme system was described in [23] for the biotransformation of glycerol into dihydroxyacetone (yielding 160 g per g of immobilized enzyme) in the presence of the cofactor  $\text{NAD}^+$  using glycerol dehydrogenase from *Cellulomonas sp.* This revealed the possibility of producing value-added chemicals from biorenewable resources with in situ cofactor regeneration through reaction pathways that are non-native to living organisms.

## 2.2 Heterogeneous catalysis

The heterogeneous catalytic oxidation of glycerol with molecular oxygen is considered to be one of the most attractive routes for production of glycerol derivatives from the industrial point of view. Several works have reported the selective oxidation of glycerol into fine chemicals using monometallic and bimetallic catalysts, mainly Au, Pt, Pd, Rh, Co, and Bi, supported on carbon, graphite or  $\text{TiO}_2$  among others. Metallic catalysts for the oxidation of the primary hydroxyl group are usually based on gold, palladium, and platinum nanoparticles, as shown in [24]–[28]. Pd and Pt are characterized by having the lowest hydrogenolysis activity of Group VIII metals and maintaining good hydrogenation and dehydrogenation activity. However, alcohol oxidation in aqueous phase using gold as catalyst was more selective and less prone to metal leaching and deactivation caused by overoxidation and self-poisoning by strongly adsorbed by-products in comparison to Pt and Pd, according to [29].

Among the parameters that affect the yield and selectivity for a specific glycerol derivative produced by means of heterogeneous catalysis, the most important are: the methods of synthesis of supported catalysts, temperature, pH, mass-transfer conditions, concentration and physicochemical properties of the catalyst used, partial pressure of oxygen, and type of reactor. In addition, the presence of an alkaline medium favors glycerol deprotonation, the first step in the oxidation process, which is considered essential for the oxidation of the primary alcohol, as described in references [24]–[26]. Kimura [30] used a bimetallic (platinum–bismuth) catalyst and 30 % conversion and 20 % selectivity for dihydroxyacetone were achieved. Similarly, as stated in [31], pH conditions have been reported to strongly influence the selectivity. Carrettin *et al.* [26] reported that the presence of radical  $\text{OH}^\cdot$  aids in the removal of the  $\text{H}^+$  from a primary alcohol and a 56 % conversion to sodium glycerate using 1 % w/w Au/graphite in the presence of NaOH was obtained.

García *et al.* [32] reported the use of 5 % Pd catalyst on activated charcoal for a high glycerol conversion (90–100 %) and yield of glyceric acid (70 %) in alkaline media. The catalyst was synthesized by the impregnation method with an acidic solution of  $\text{PdCl}_4^{2-}$  ions at 298 K for 5 h. The impregnation of the carrier metal was followed by reduction using 37 % formaldehyde under basic conditions and subsequent drying at 333 K under vacuum. Hu *et al.* [33] performed a detailed study on the kinetic parameters for given reaction conditions (temperature, pressure, initial reactants concentration) of the glycerol oxidation reaction mechanism over Pt–Bi/C catalyst including all reaction steps. After analysis of the concentration of glycerol derivatives and turnover rates, a simplified reaction network was proposed considering the concentration of glycerol, glyceric acid, dihydroxyacetone, and  $\text{CO}_2$ , which can be used for chemical reactor design, modeling, simulation, and optimization of the desired product.

Wörz *et al.* [34] reported that product adsorption influences the selective deactivation during the oxidation of glycerol, decreasing the activity of the catalyst and product selectivity. In their work, the formation of glyceric acid during bimetallic Pt–Bi/C catalysis in acid media blocked the active sites that are mainly responsible for high selectivity to dihydroxyacetone; Hu *et al.* [35] optimized the method of catalyst preparation and the reaction conditions to achieve higher oxidation rates and selectivity towards dihydroxyacetone. The yield of dihydroxyacetone was reported to be 48 % after 80 % glycerol conversion. As boiling has to be avoided, the reaction temperature should be kept under 100°C, and the preferred temperature was 80°C. Oxygen pressure values in the range of 0.2–0.35 MPa and an initial pH of 2 were also determined to be optimum values.

Rodríguez *et al.* [36] found out that the oxygen content on the surface is one of the key factors influencing catalyst activity. Higher selectivity towards glyceric acid (62 %) and dihydroxyacetone (22 %) was observed at 40°C and 0.3 MPa or 60 °C and 1 MPa, independently of the number of oxygenated surface groups present.

Problems of inhibition of glycerol oxidation over 1.6 % w/w Au/TiO<sub>2</sub> catalyst by glyceric acid, acting as a reactive intermediate, were reported by Zope and Davis [37]. They proposed that the formation of chelating intermediates like ketones, enones or compounds with a β-dicarbonyl structure via bonding of hydroxyl radicals to secondary carbon atoms blocks the active sites after adsorption onto the catalyst surface. Reactions carried out using Pt and Pd as catalyst have demonstrated the drawback of oxygen poisoning which is proportional to the oxygen partial pressure, see *e.g.*, [38]. According to [39], the use of low partial pressures of oxygen has been recommended to overcome oxygen dissolution.

Nie and co-workers [40] reported the use of multi-walled carbon nano tubes (MWCNTs) as support for Pt, Pt–Bi, and Pt–Sb. They found that the selectivity for dihydroxyacetone (51.4 %) was enhanced in a base-free aqueous solution by using Pt–Sb alloy in MWCNTs with a high conversion rate (90 %). Glyceric acid was obtained with 67.4 % selectivity when using Pt catalyst at similar conversion rates. They proposed that Sb acts as a site-blocker and semiconductor and therefore as a promoter of Pt. The Pt–Sb alloy also decreased C–C splitting. The presence of glyceric acid was also beneficial by blocking active sites that can lead to the overoxidation of dihydroxyacetone.

### 2.3 Homogeneous catalysis

The oxidation of alcohols by means of homogeneous catalysis often requires the use of oxidizing reagents in stoichiometric amounts. However, as reported in reference [41], these oxidants are commonly halogenated organic solvents and generate hazardous or toxic waste. For this reason, this area has been barely studied and in some cases, it is combined with heterogeneous oxidation. One of the preferred oxidants is H<sub>2</sub>O<sub>2</sub> as water is the only by-product of the reaction. For example, the oxidation of ethanol using H<sub>2</sub>O<sub>2</sub> catalyzed by ferrous ion (Fenton's reagent) in acid media leading to acetaldehyde was studied by Kolthoff and Medalia [42]. The oxidation of glycitols such as mannitol and glycerol with Fenton reagent produced glycoaldehyde, which was progressively oxidized to glyoxal, see *e.g.*, [43]. Ciriminna and Pagliaro [44] reported the selective conversion of glycerol to ketomalic acid using 2,2,6,6-tetramethylpiperidin-1-yl)oxidanyl (TEMPO) as a catalyst and NaOCl as a stoichiometric oxidant under very mild conditions. With the addition of TEMPO, most of the glycerol was converted into ketomalic acid during the

first half hour of reaction. Intermediate products like tartronic acid and dihydroxyacetone were progressively oxidized to achieve 98 % selectivity for ketomalonic acid after 3 h of reaction. By performing the oxidation over sol-gel silica xerogels doped with nitroxyl radical, the authors found that a similar high-yield conversion and selectivity were achieved. The catalyst showed high stability at pH 10 and was recycled seven times without loss of activity.

The use of a soluble catalyst containing manganese in the presence of H<sub>2</sub>O<sub>2</sub> at room temperature was described by Shul'pin and coworkers [45]. The main product reported was DHA, with a yield of 45 %. Oxidation of DHA to glycolic acid in the absence of glycerol proceeded in 60 % yield.

## 2.4 Electrochemical oxidation

The electrochemical oxidation of glycerol comprises a heterogeneous redox reaction where electrodes provide the electron source for reduction at the cathode and the electron sink for oxidation at the anode surface, associating intra and intermolecular electron transfers and incorporating the breaking and making of covalent bonds, as explained in [46].

Schnaidt *et al.*[47] investigated the mechanism and kinetics of the oxidation and adsorption of glycerol, glyceraldehyde, and glyceric acid on a Pt thin-film electrode. In their study, they were able to simultaneously measure the Faradaic current under controlled mass-transport conditions and to characterize the adsorbed products by in situ attenuated total reflection Fourier-transform infrared spectroscopy and the volatile reaction products by on-line differential electrochemical mass spectrometry. They reported glyceric acid as the final product in the electrochemical oxidation of glycerol, and glyceraldehyde as an intermediate in the formation of adsorbed carbon monoxide. An study in alkaline medium was performed by Kwon *et al.* [48] using gold catalyst, which has been employed extensively in investigations of alcohol oxidation, see *e.g.*, [24]. In their work, they confirmed that base and gold catalysts make active and selective oxidation catalysts through the first step – deprotonation catalyzed by the base, followed by the second step – deprotonation catalyzed by gold. Higher oxidation activity on gold catalyst was attributed to the high gold resistance to the formation of poisoning surface oxides. However, complete understanding of the factors responsible for this high catalytic activity is still under study.

The oxidation of glycerol to glyceric acid by silver oxide catalyst formed in situ on an anodic surface in aqueous basic medium was reported by Kyriacou and Tougas, [49]. In their work, a linear dependency of temperature and NaOH concentration on the oxidation rate was described. A temperature below 45°C and NaOH concentration of 10 % were recommended. Roquet *et al.* [50] reported the electrooxidation of glycerol in the presence of platinum electrode in

acid medium (0.1 M HClO<sub>4</sub>) using programmed-potential electrolysis and cyclic voltammetry. The conversion of glycerol was 38 %, and led to the formation of glyceraldehyde as the primary product after 44.5 h of electrolysis at a potential range of 0.75 V *rhe*<sup>-1</sup>(reversible hydrogen electrode). The electrolysis of manganous oxide salts in acid solution to obtain manganic oxide salts for subsequent oxidation of glycerol to glyceraldehyde at a lead anode was described by Lang [51].

The oxidation of glycerol derivatives has also been studied recently by Manea and co-workers [52], who carried out a systematic study on the oxidation and determination of oxalic acid using cyclic voltammetry, linear scan voltammetry and chronoamperometry in the presence of a prepared exfoliated graphite–polystyrene composite electrode in 0.1 M Na<sub>2</sub>SO<sub>4</sub>. The results demonstrated that the proposed voltammetric method was accurate compared with the quantification obtained using the KMnO<sub>4</sub> titration method. Production of hydrogen by electrochemical reforming after complete oxidation of glycerol using Pt on Ru–Ir oxide as anode was reported by Marshall and Haverkamp [53]. Therefore, cyclic voltammetry used in combination with the catalytic reaction data gave more detailed information on the active surface characterization and oxidation mechanism.

Binary carbide such as nickel–tungsten has also been used as an anode electrocatalyst. It was found that the activity was strongly dependent on the method of catalyst preparation, as the presence of surface species and bulk phases are affected by this process see *e.g.*, [54]. Other studies for alcohol electrooxidation have reported the use of Pt–Sn, *e.g.* [55],[56] and Pt–Au, *e.g.* [57] particles supported on carbon. Several factors, namely surface oxygen-containing species, lattice parameters, electron transfer from Sn or Au to Pt and ohmic effects, which depend on Sn or Au content, have been found to be promoters of catalyst activity.

#### **2.4.1 Anodic oxidation**

Electrochemistry is a concept generally used to describe the study of chemical reactions that proceeds due to the flow of an electric charge and having electrolysis as one of the main manifestations, *e.g.* [46]. Fig. 1 describes a general experimental setup of an electrochemical cell. An electrochemical cell is a system comprising the electrodes, electrolyte, and electroactive compound (organic molecule) in which organic electrode processes, namely anodic or cathodic reaction, take place.

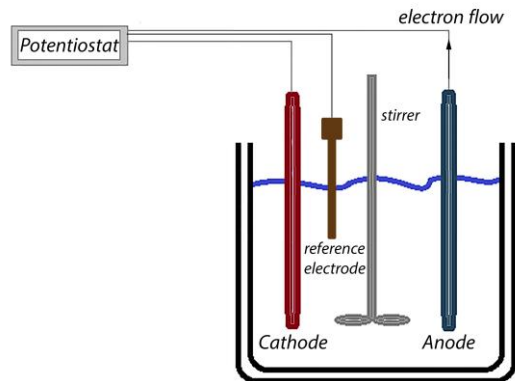


**Fig 1:** Experimental setup of an electrochemical cell.

When a voltage is applied to the cell, there is a movement of electrical charge from the anode to the cathode, followed by a mass transport of the electroactive compound (A) to the electrode interface. Then, transfer of electrons from the electrode to the reactant molecule occurs, resulting in the formation of a new product (B), which finally migrates to the bulk solution. This electrode reaction is presented in Fig. 2. As described in [58], it is important to notice that the above described process is dependent on the voltage applied, the reactivity of the electroactive compound, the electrodes used, experimental conditions, i.e. temperature or stirring, current density, concentration of catholyte among others. When performing transient or relaxation studies in electrochemistry, it is necessary to analyze the variation of the electrode potential, the concentration of electroactive compounds at the electrode-solution interface and the current according to the time required for the interface to change from equilibrium to steady state. Voltammetric techniques involve the study of the current variation in function of the potential. Linear sweep and cyclic voltammetry are two of the main voltammetric techniques. In cyclic voltammetry, a triangular potential-time waveform with equal positive and negative slope is used. The potential sweep rate is the rate by which the potential changes with time.

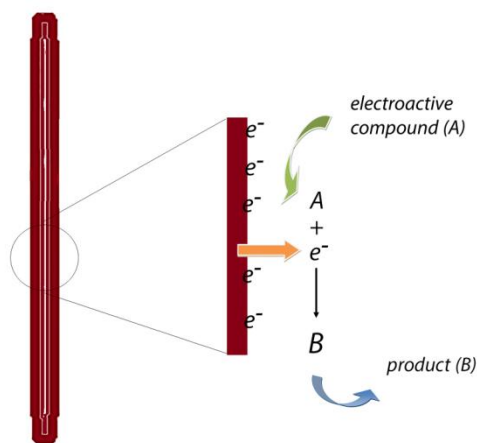


**Fig. 2:** Representation of an electrode reaction occurring in the electrode.

## 2.5 Reasons for chemical process control

Among the main needs that a control system is called to satisfy, the most important are to minimize the influence of external disturbances, to ensure the stability of the chemical process and to optimizing the performance of the chemical process according to reference [59]. Disturbances normally denote any effect from the surroundings of the system that is out of reach of the human operator. As a result, a control mechanism is required to maintain the desirable conditions by adjusting specific variables in the system to guarantee the safety, product quality and profit optimization, as stated in [60].

The importance in control stability is presented in Fig. 3. The system described in (a) is stable or self-regulating. Therefore, there is no need of an external intervention for its stabilization. However, the system presented in (b) is a classical example of an unstable system as the variable does not return to its initial value after it is disturbed by external influences and therefore it requires an external control.

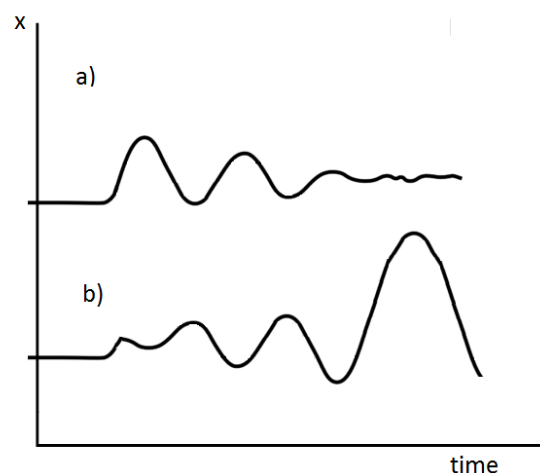


**Fig. 3:** Response of (a) stable; and (b) unstable systems.

Therefore, the controller ensures the stability of the system operation in the presence of external disturbances that tend to take the system away from the desired point.

## 2.6 Evaluation of the state of the art

It can be concluded from the bibliographical search that there is no reported industrial implementation of partial oxidation of glycerol. The majority of existing literature sources deal with laboratory preparations with the main objective of finding optimal reaction conditions in order to achieve high selectivity and yield of the desired products, particularly glyceraldehyde. With

the exception of the work performed by Roquet and coworkers in 1994 [61], all the studies concluded that the yield was poor, which brings considerable difficulties in isolation of pure components. Most of cited papers concern the preparation method without performing a quantitative description of the reaction kinetics derived from the idea of reaction micromechanism. The demanding partial oxidation, including the isolation of pure products, result in very high prices of the products. Nowadays, great research effort is put into selection of particular oxidation technologies as well as their optimization, which goes hand in hand with the demands for control of the oxidation reaction. As far as I am concerned, on the base of my comprehensive literature study, there are no reports in the literature dealing particularly with control of partial oxidation of glycerin.

For the purpose of the implementation of an automated system for technological processes it is necessary to engage in the exploration of the production system in the first stage, which involves the mathematical modeling of a particular system, which in our case is complicated due to the presence of mixture of glycerin and its partial oxidation products. Our main task is the attempt to find such reaction conditions, when we get the maximum production glycerinaldehyde.

Based on the study, firstly it will be presented the description of reaction kinetics including the system of differential equations as a part of the irreplaceable step concerning the exploration of the production system. The above task includes the evaluation of kinetic parameters like reaction rate constants. Important are also the reaction enthalpy and adiabatic temperature for the exothermal reaction. As described in [59], the absence of this step makes it practically impossible to successfully perform the subsequent particular project of an automated control system, which is also the main task of my dissertation.

### **3 AIMS OF THE THESIS**

- 1) Determine the vector differential equations that describe the anodic oxidation of glycerol including its solution and following simulation calculation.
- 2) Design of non-linear kinetics of glycerin oxidation using various oxidizing agents, especially nitrous oxide ( $N_2O$ ).
- 3) Develop the solutions of non-linear kinetics oxidation and simulation of the reaction system for calculation of theoretical yield of glyceraldehyde.
- 4) Determine the transfer functions for glycerol oxidation in
  - a) anodic oxidation,
  - b) isothermal case-oxidation with nitrous oxide,
  - c) non isothermal and non adiabatic oxidation of glycerol.
- 5) Develop a quantitative experimental method for analysis of reaction blend products using liquid chromatography.
- 6) Analyze the kinetic data, using anodic oxidation and their mathematical statistic treatment for the determination of rate constants.
- 7) Elaborate a summary of key results achieved and recommendation for industrial practice.

## 4 EXPLORATION OF THE PRODUCTION SYSTEM

Several valuable glycerol derivatives find wide application in pharmaceutical and cosmetic industries. Their utilization as grafting agents, which is another promising use of these substances, can shift these products towards lower price levels. Additional efforts should be put into the design of chemical reactors for oxidation and reduction reactions, which are not only challenging in terms of design but also of operation. For example, the kinetics of the reaction can be affected by intermediates that are attached to the catalyst owing to the presence of multiple reaction pathways. Nowadays, these intermediates are of considerable importance in the production of plastics monomers. As an example, the oxidation of cyclohexane produces a mixture of cyclohexanol and cyclohexanone, a basic raw material for caprolactam and polyamide production. Management of chemical reactors associated with exothermic reactions such as the oxidation of organic substances is among the most challenging tasks of chemical reactor engineering. The control of oxidation is a prerequisite for successful and safe industrial applications of this promising manufacturing technology. Design of control algorithms should be based on the upstream stage – exploration of the production system, which includes research on the reaction kinetics of the system coupled with transport processes, especially of the heat of reaction, which in the case of glycerol oxidation is considerable. The problem is complicated because of the complexity of the reaction mixture after the oxidation, having small concentration of glyceraldehyde. In such cases, a purification step is always necessary. Dynamic models consisting of one or more differential equations-ordinary differential equations and/or partial differential equations- often combined with one or more algebraic relations. For control process analysis, a dynamic model is obtained from the application of unsteady-state conservation relations such as mass and energy balance, *e.g.* [62]. These models are frequently nonlinear, where multiple solutions are possible, while commonly used control strategies are based on linear systems theory. Therefore, the linearization process of nonlinear models for control system design and analysis purposes is an important tool in process control, *e.g.*[63]

The implementation of an automated system for the control of technological processes consists of several steps. The step of exploration of the production system is absolutely irreplaceable, *i.e.* it cannot be omitted should the implementation of automated control lead to the desired effect. It mainly concerns generation of products with the required utility value while keeping acceptable economics of the process, compliance with safety conditions of industrial production in order to protect health of employees and last but not least compliance with environmental protection regulations. In the case of

partial oxidation of glycerin it is necessary to carry out a chemical-engineering analysis of particular reaction, formulate a quantitative reaction kinetics model based on the estimation of the reaction mechanism and determine whether the system in question is a lumped parameter model, i.e. the state values are only a function of time and thus the system is described by a system of total differential equations, or a distributed parameter model in which the state values are not only a function of time, but also position. In the latter case the system is described by a system of partial differential equations. Taking into account the practical aspect, it is necessary to determine the inputs, outputs and state values. The chemical-engineering analysis also results in finding the key control point. The subsequent model-based simulation calculations can allow selecting the most suitable proposal of a control algorithm for partial oxidation of glycerin to the desired oxidation products. From the comprehensive bibliographical research on the current state of glycerin oxidation, two technologies of partial oxidation of glycerin with promising practical application have been found, namely catalytic and anodic oxidation.

#### 4.1 Modeling of the partial oxidation of glycerin

The oxidation kinetics is based on the idea of the reaction mechanism, quantitative description of the dependences of the reaction rates on the concentration of the reacting components. The description is realized by vector differential equation, the solutions of which are time dependent of the concentrations of the oxidation intermediate products. Generally, glycerol oxidation is accompanied by various relatively complex simultaneous reactions resulting in a complicated blend of intermediate products. Relatively simple mechanism can be assumed if oxidation of glycerol is carried out with the use of anodic oxidation, where the main products are glyceraldehyde, glyceric acid and glycolic acid. The vector equation is linear in this case and can be solved analytically using Laplace transform. This assumption will be verified in the experimental part of the thesis. Therefore, the mechanism of the anodic glycerin oxidation can be described by the scheme presented in Fig. 4.

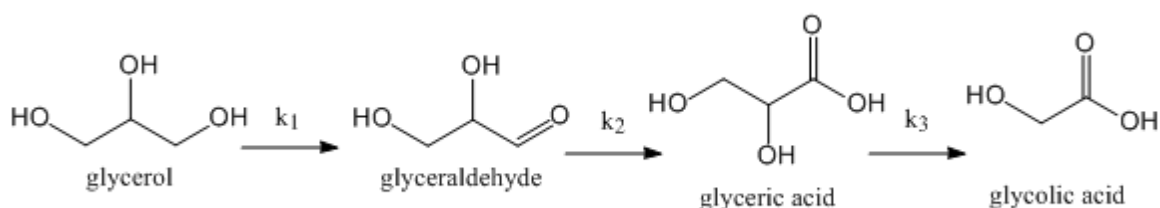


**Fig. 4:** Simplified model of anodic oxidation.

The kinetic model is represented by the following system of differential equations:

$$\frac{dC_A}{dt} = -k_1 C_A \quad (1)$$

$$\frac{dC_B}{dt} = k_1 C_A - k_2 C_B \quad (2)$$

$$\frac{dC_C}{dt} = k_2 C_B - k_3 C_C \quad (3)$$

$$\frac{dC_D}{dt} = k_3 C_C \quad (4)$$

The above mentioned equations represent a vector differential equation:

$$\dot{C} = A \cdot C \quad (5)$$

$$C(0) = C_0 \quad (6)$$

By application of the Laplace transform we get:

$$sC_L - C_0 = A \cdot C_L \quad (7)$$

$$C_L = (sI - A)^{-1} C_0 \quad (8)$$

$$(sI - A)^{-1} C_0 = \begin{pmatrix} \frac{\frac{C_{A0}}{s+k_1}}{C_{A0}k_1} \\ \frac{C_{A0}k_1}{(s+k_1)(s+k_2)} \\ \frac{C_{A0}k_1k_2}{(s+k_1)(s+k_2)(s+k_3)} \\ \frac{C_{A0}k_1k_2k_3}{s(s+k_1)(s+k_2)(s+k_3)} \end{pmatrix} = \begin{pmatrix} C_{AL} \\ C_{BL} \\ C_{CL} \\ C_{DL} \end{pmatrix} \quad (9)$$

Considering the next set of dimensionless equations:

$$C_A^* = \frac{C_A}{C_{A0}}; C_B^* = \frac{C_B}{C_{0A}}; C_C^* = \frac{C_C}{C_{0A}}; C_D^* = \frac{C_D}{C_{0A}} \quad (10)$$

The analytical solution of the previous set of equations is presented in (11) to (14)

$$C_A^* = e^{-k_1 t} \quad (11)$$

$$C_B^* = \frac{k_1}{k_1 - k_2} (e^{-k_2 t} - e^{-k_1 t}) \quad (12)$$

$$C_C^* = k_1 k_2 \left[ \frac{e^{-k_1 t}}{(k_3 - k_1)(k_2 - k_1)} + \frac{e^{-k_2 t}}{(k_3 - k_2)(k_1 - k_2)} + \frac{e^{-k_3 t}}{(k_2 - k_3)(k_1 - k_3)} \right] \quad (13)$$

$$C_D^* = 1 - k_1 k_2 k_3 \left[ \frac{e^{-k_3 t}}{k_3(k_2 - k_3)(k_1 - k_3)} + \frac{e^{-k_2 t}}{k_2(k_3 - k_2)(k_1 - k_2)} + \frac{e^{-k_1 t}}{k_1(k_3 - k_1)(k_2 - k_1)} \right] \quad (14)$$

where the terms  $C_A^*$ ,  $C_B^*$ ,  $C_C^*$ , and  $C_D^*$  represents the dimensionless concentration of glycerol, glyceraldehyde, glyceric acid, and glycolic acid respectively.

Following Fig. 5 and Fig. 6 show the kinetics profile curves for arbitrary constants values of  $k_1$ ,  $k_2$  and  $k_3$ . Values of  $k_1=0.04\text{ h}^{-1}$ ,  $k_2=0.18\text{ h}^{-1}$ , and  $k_3=0.01\text{ h}^{-1}$  were used to obtain Fig. 5 and values of  $k_1=0.01\text{ h}^{-1}$ ,  $k_2=0.05\text{ h}^{-1}$ , and  $k_3=0.02\text{ h}^{-1}$  were selected to obtain Fig. 6

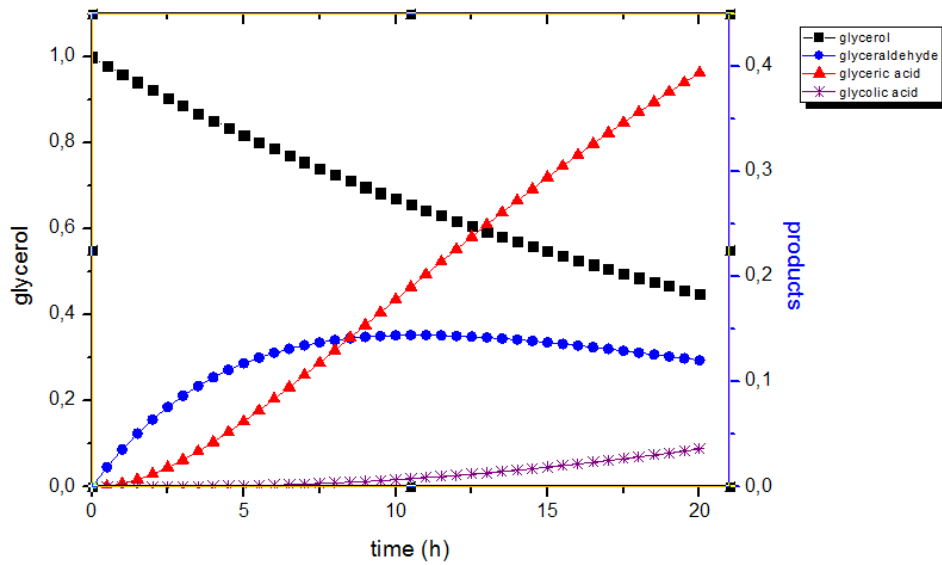


**Fig. 5:** Dimensionless plot of glycerol and products using values of  $k_1=0.04$ ,  $k_2=0.18$ ,  $k_3=0.01\text{ h}^{-1}$  in the analytical solution.

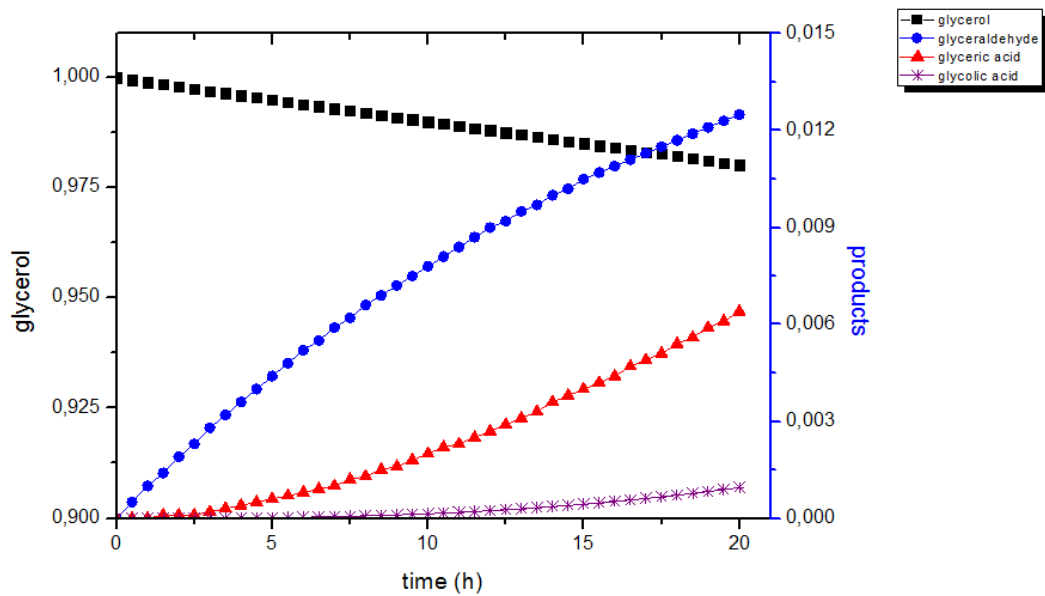


**Fig. 6:** Dimensionless plot of glycerol and products using values of  $k_1=0.01$ ,  $k_2=0.05$ ,  $k_3=0.02\text{ h}^{-1}$  in the analytical solution.

## 4.2 Kinetics model for glycerin oxidation - non linear model

The analysis of a non linear system is presented by the oxidation of glycerin with nitrous oxide (laughing gas), hydrogen peroxide or airborne oxide. As an example, I present the nitrous oxide as oxidation agent. A simplified oxidation mechanism is supposed according to the equations described in (15):



where  $G$  is glycerin concentration,  $R$  stands for nitrous oxide concentration and  $K$  is the glyceric acid concentration. Quantitative description is the following:

$$\frac{dA}{dt} = k_1 \cdot G \cdot R - k_2 \cdot A \cdot R \quad (16)$$

$$\frac{dR}{dt} = -k_1 \cdot G \cdot R - k_2 \cdot A \cdot R \quad (17)$$

$$\frac{dG}{dt} = -k_1 \cdot G \cdot R \quad (18)$$

$$\frac{dK}{dt} = k_2 \cdot A \cdot R \quad (19)$$

The stated equations (16)-(19) were solved according to the algorithm developed by Fürst, (unpublished results). Dimensionless presentations of the time dependent curves are shown in the Fig. 7

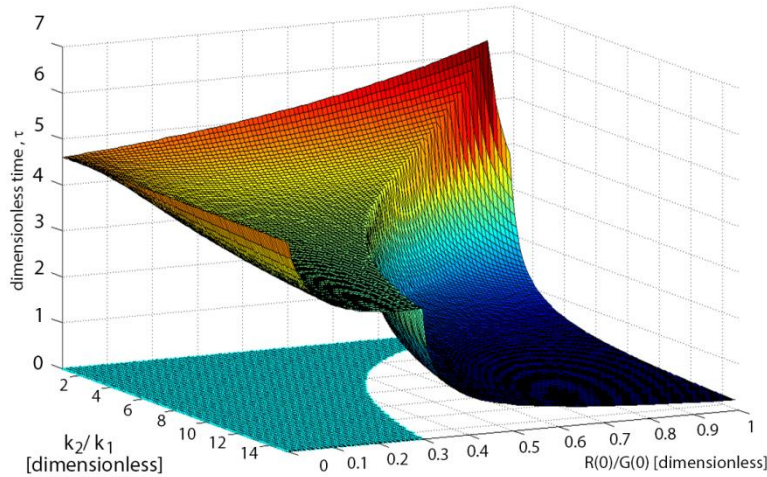


**Fig 7:** Dimensionless plot of time needed to reach the maximum concentration of glyceraldehyde.

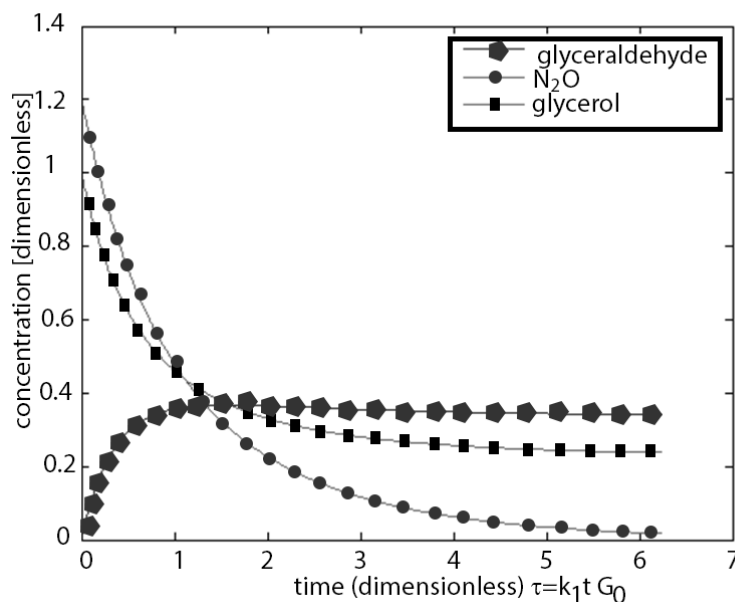


**Fig 8:** Concentration profile for reactants and product with  $k_2/k_1=1$  and  $R_0/G_0=1.2$ .

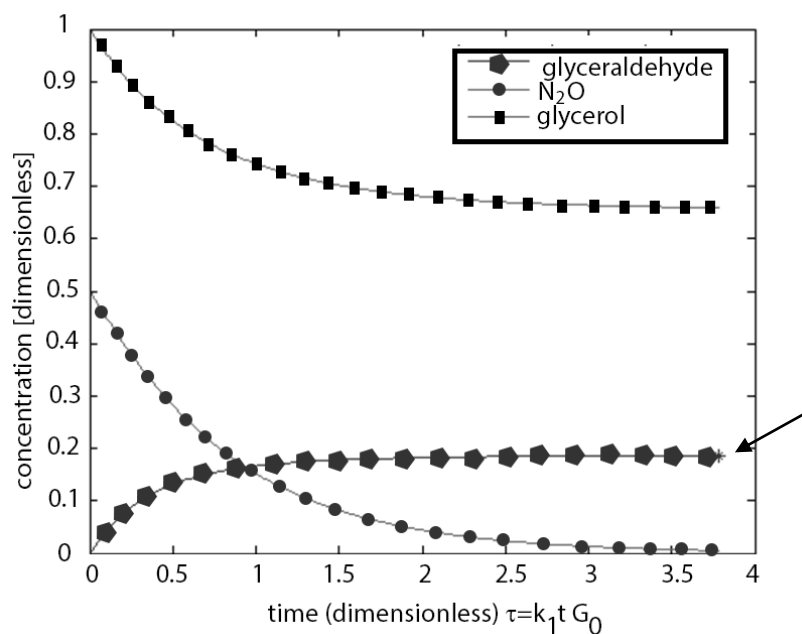


**Fig 9:** Concentration profile for reactants and product with  $k_2/k_1=3$  and  $R_0/G_0=0.5$ .

Asterisks in Figures 9 and 10 (pointed out with an arrow) denote maximum yields of glyceralddehyde for specific initial concentration of nitrous oxide and ratios rate constants  $k_2/k_1$ .

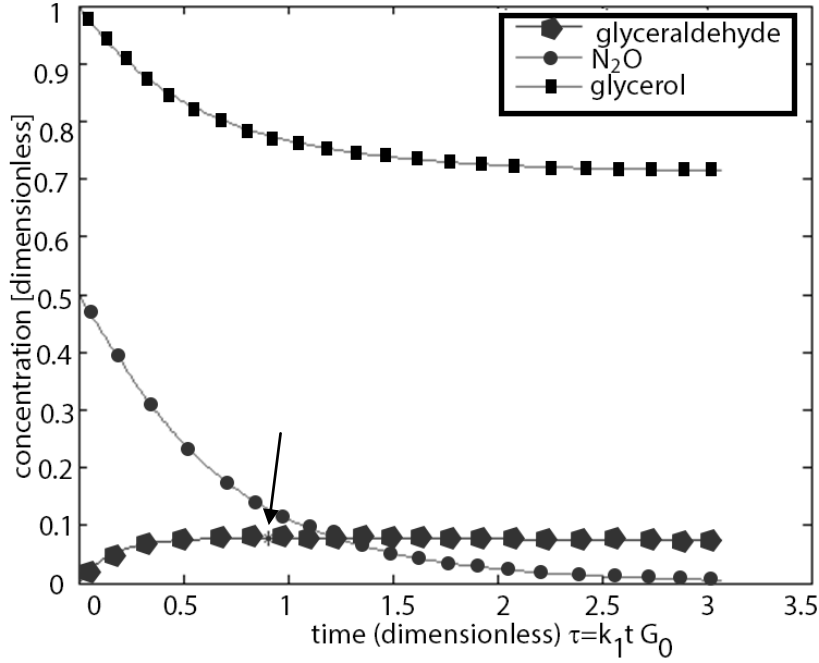


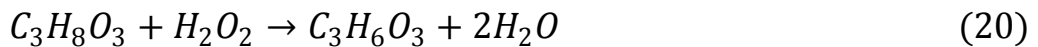
**Fig 10:** Concentration profile for reactants and product with  $k_2/k_1=10$  and  $R_0/G_0=0.5$ .

### 4.3 Evaluation of the oxidation of adiabatic temperature

The knowledge and control of the heat released from a chemical reaction is essential and extremely important for the safety of the process at laboratory level and further scale-up of chemical processes. In order to determine the engineering design parameters, as such as the required jacket temperature, the adiabatic temperature variation of the process and the total condenser design heat load, it is required the determination of the process heats

Two different proposed models of oxidation of glycerol are discussed. The first one considering the reaction of glycerol with hydrogen peroxide ( $H_2O_2$ ) and production of glyceraldehyde and the second one with airborne oxygen and nitrous oxide. The models were considered to analyze the variation of adiabatic temperature in the oxidation of glycerol.

#### 4.3.1 Estimation of thermodynamics parameters of the oxidation of glycerin to glyceraldehyde with $H_2O_2$



Using the reaction from equation (20) as a first model of study, the calculation of adiabatic temperature difference is performed using equation (21):

$$\Delta T = \frac{-(\Delta H)_r - 2(\Delta H)_{H_2O}^{vap}}{n_r \cdot \bar{C}_{p_{reactionblend}}} \quad (21)$$

The term  $n_r$  corresponds to the number of mols in the reaction blend,  $\bar{C}_p$  represents the specific heat of the reaction blend and can be calculated using equation (22) and the numerator represents the enthalpy of the reaction and of enthalpy of vaporization of water ( $40.74 \text{ kJ}\cdot\text{mol}^{-1}$ )

$$\bar{C}_{p_{\text{reactionblend}}} = \frac{1}{3}\bar{C}_{p_{\text{glyceralde hyde}}} + \frac{2}{3}\bar{C}_{p_{\text{H}_2\text{O}}} \quad (22)$$

In order to evaluate the enthalpy change of the reaction, two different methods are discussed. The first one involves the use of values obtained from thermodynamic tables and the second method was using the bond energy.

Based on thermodynamic tables [64], the values for the energy of formation of glycerol ( $-668.43 \text{ kJ}\cdot\text{mol}^{-1}$ ), glyceraldehyde ( $598.312 \text{ kJ}\cdot\text{mol}^{-1}$ )  $\text{H}_2\text{O}_2$  ( $-187.8 \text{ kJ}\cdot\text{mol}^{-1}$ ) and  $\text{H}_2\text{O}$  ( $-285.83 \text{ kJ}\cdot\text{mol}^{-1}$ ) were substituted on equation (23) to calculate the enthalpy of reaction. In this equation,  $n$  and  $m$  stands for the number of reactants and products respectively. The solution is presented through equations (24) to (26)

$$(\Delta H)_r = \sum_{i=1}^n (\Delta H)_{f_{\text{products}}}^{298 \text{ K}} - \sum_{i=1}^m (\Delta H)_{f_{\text{reactants}}}^{298 \text{ K}} \quad (23)$$

$$\begin{aligned} (\Delta H)_r = \\ [-598.312 \text{ kJ}\cdot\text{mol}^{-1} - 2 * 285.83 \text{ kJ}\cdot\text{mol}^{-1}] - [-668.43 \text{ kJ}\cdot \\ \text{mol}^{-1} - 187.8 \text{ kJ}\cdot\text{mol}^{-1}] \end{aligned} \quad (24)$$

$$(\Delta H)_r = -1169.972 \text{ kJ}\cdot\text{mol}^{-1} + 856.23 \text{ kJ}\cdot\text{mol}^{-1} \quad (25)$$

$$(\Delta H)_r = -313.742 \text{ kJ}\cdot\text{mol}^{-1} \quad (26)$$

A second procedure to calculate the enthalpy of the reaction is based on bond energy. The bond energy is considered as the energy required to break a chemical bond of a mol of molecule into their individual atoms in the gas phase at zero Kelvin. In order to estimate the heat of reaction, it is necessary to sum the values of the bond energies (obtained from tables) required to break the bonds and subtract the sum of bond energies required to form the bonds.

The bond enthalpies required to break a mole of each molecules involved in the chemical reaction into gaseous C, H or O atoms are presented in Table 1.

**Table 1.** Bond enthalpies for glycerol, H<sub>2</sub>O<sub>2</sub>, glyceraldehyde and H<sub>2</sub>O from references [65], [66], [67]

Compound	Bond	Number of bonds	Bond enthalpy per bond (kJ·mol <sup>-1</sup> )	Sum of bond enthalpies (kJ·mol <sup>-1</sup> )	Net change (kJ·mol <sup>-1</sup> )
glycerol	C-H	5	414	2070	5197
	C-O	3	351	1053	
	O-H	3	460	1380	
	C-C	2	347	694	
H <sub>2</sub> O <sub>2</sub>	H-O	2	460	920	1062
	O-O	1	142	142	
glyceraldehyde	C-H	4	414	1656	4712
	C-O	2	351	702	
	O-H	2	460	920	
	C-C	2	347	694	
	C=O	1	740	740	
H <sub>2</sub> O	H-O	2	460	920	920

As it is possible to use bond enthalpies only in the gas state, and since the compounds in the chemical reaction are liquids, it is required to add an extra energy to convert from liquid to gas.

Table 2 shows the values for enthalpy change due to the vaporization stage  $\Delta H_{\text{vap}}$  (kJ·mol<sup>-1</sup>)

**Table 2.** Enthalpy change due to the vaporization stage for glycerol, H<sub>2</sub>O<sub>2</sub>, glyceraldehyde and H<sub>2</sub>O. Values were obtained from reference [68]

Compound	$\Delta H_{\text{vap}}$ (kJ·mol <sup>-1</sup> )
glycerol	91.7
H <sub>2</sub> O <sub>2</sub>	51.6
glyceraldehyde	88.11
H <sub>2</sub> O	41

Using the values obtained from Table 1 and 2, the enthalpy change of reaction is obtained in equations (27) to (31)

$$(\Delta H)_r = \sum_{i=1}^n (\Delta H)_{\text{bonds broken}} - \sum_{i=1}^m (\Delta H)_{\text{bonds formed}} \quad (27)$$

$$(\Delta H)_r = [(91.7 + 5197) + (51.6 + 1062)] - [(88.11 + 4712) + (2 * 41 + 1840)] \text{ kJ} \cdot \text{mol}^{-1} \quad (28)$$

$$(\Delta H)_r = \{[5288.7 + 1113.6] - [4800.11 + 1922]\} \text{ kJ} \cdot \text{mol}^{-1} \quad (29)$$

$$(\Delta H)_r = \{[6402.3 - 6722.11] \text{ kJ} \cdot \text{mol}^{-1}\} \quad (30)$$

$$(\Delta H)_r = -319.81 \text{ kJ} \cdot \text{mol}^{-1} \quad (31)$$

It is evident that the values for  $(\Delta H)_r$  obtained using equations (23) and (27) correspond accordingly. Considering an specific heat capacity value for glyceraldehyde similar to glycerol ( $0.219 \text{ kJ} \cdot \text{mol}^{-1} \text{K}^{-1}$ ) *e.g.* [69] and  $\text{H}_2\text{O}$  equal to  $0.0752 \text{ kJ} \cdot \text{mol}^{-1} \text{K}^{-1}$ , *e.g.* [70], the value of  $\bar{C}_p$  can be calculated from equation (22):

$$\bar{C}_{p_{\text{reactionblend}}} = \frac{1}{3} (0.219 \text{ kJ} \cdot \text{mol}^{-1} \text{K}^{-1}) + \frac{2}{3} (0.0752 \text{ kJ} \cdot \text{mol}^{-1} \text{K}^{-1}) \quad (32)$$

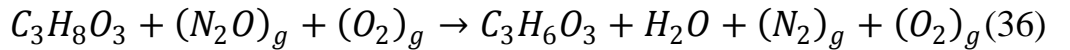
$$\bar{C}_{p_{\text{reactionblend}}} = 0.123 \text{ kJ} \cdot \text{mol}^{-1} \text{K}^{-1} \quad (33)$$

Therefore, in order to calculate the adiabatic temperature difference, the corresponding values of  $(\Delta H)_r$ , and  $\bar{C}_{p_{\text{reactionblend}}}$ ,  $n_r = 3$  and  $(\Delta H)_{\text{H}_2\text{O}}^{\text{vap}} = 40.72 \text{ kJ} \cdot \text{mol}^{-1}$  are substituted in equation (21):

$$\Delta T = \frac{[319.81 - 2(40.72)] \text{ kJ} \cdot \text{mol}^{-1}}{(3)(0.123 \text{ kJ} \cdot \text{mol}^{-1} \text{K}^{-1})} \quad (34)$$

$$\Delta T = 645.99 \text{ K} \quad (35)$$

#### 4.3.2 Estimation of thermodynamics parameters of the oxidation of glycerin to glyceraldehyde with airborne oxygen and nitrous oxide



Using the energy of formation of starting chemicals and products formed, the values for the energy of formation of glycerol ( $-668.43 \text{ kJ} \cdot \text{mol}^{-1}$ ),  $(\text{N}_2\text{O})_g$  ( $82.05 \text{ kJ} \cdot \text{mol}^{-1}$ ), glyceraldehyde ( $598.312 \text{ kJ} \cdot \text{mol}^{-1}$ ),  $\text{H}_2\text{O}$  ( $-285.83 \text{ kJ} \cdot \text{mol}^{-1}$ ) were used on equation (37) to calculate the enthalpy of reaction. The solution is presented through equations (38) to (40). The values of energy of formation were obtained from reference [64].

$$(\Delta H)_r = \sum_{i=1}^n (\Delta H)_{f_{\text{products}}}^{298 \text{ K}} - \sum_{i=1}^m (\Delta H)_{f_{\text{reactants}}}^{298 \text{ K}} \quad (37)$$

$$(\Delta H)_r = [-598.312 \text{ kJ} \cdot \text{mol}^{-1} + 0 - 285.83 \text{ kJ} \cdot \text{mol}^{-1}] - [-668.43 \text{ kJ} \cdot \text{mol}^{-1} + 82.05 \text{ kJ} \cdot \text{mol}^{-1}] \quad (38)$$

$$(\Delta H)_r = -884.142 \text{ kJ} \cdot \text{mol}^{-1} + 586.38 \text{ kJ} \cdot \text{mol}^{-1} \quad (39)$$

$$(\Delta H)_r = -297.762 \text{ kJ} \cdot \text{mol}^{-1} \quad (40)$$

According to the description of the first model of study, the bond enthalpies required to break a mole of each molecules involved in the chemical reaction into gaseous C, H, N or O atoms are calculated and presented in Table 3. The values for enthalpy change due to the vaporization stage are taken from Table 4 for glycerol, glyceraldehyde and H<sub>2</sub>O. The determination of the enthalpy of formation is described in the group of equations (41) to (44)

$$(\Delta H)_r = \{ [(91.7 + 5197) + (1143 )] - [(88.11 + 4712) + (950) + (41 + 920)] \} \text{ kJ} \cdot \text{mol}^{-1} \quad (41)$$

$$(\Delta H)_r = \{ [5288.7 + 1143] - [4800.11 + 950 + 961] \} \text{ kJ} \cdot \text{mol}^{-1} \quad (42)$$

$$(\Delta H)_r = \{ [6431.7 - 6711.11] \} \text{ kJ} \cdot \text{mol}^{-1} \quad (43)$$

$$(\Delta H)_r = -279.41 \text{ kJ} \cdot \text{mol}^{-1} \quad (44)$$

Given the numerical value expressed in (40), a calculation based on energies of formation for the same reaction gives -297.76 kJ·mol<sup>-1</sup>. Both values are comparably closer. With an error difference of 6%, which are normally caused due to the heat capacity between the reactants and products, normally ignored in bond enthalpies calculation.

The value of  $\bar{C}_p$  of the reaction blend is calculated as described in (45) with  $\bar{C}_{pN_2} = 0.0292 \text{ kJ} \cdot \text{mol}^{-1} \text{K}^{-1}$

$$\bar{C}_{p_{\text{reaction blend}}} = \bar{C}_{p_{\text{glyceralde hyde}}} + \bar{C}_{p_{N_2}} + \bar{C}_{p_{H_2O}} \quad (45)$$

$$\bar{C}_{p_{\text{reaction blend}}} = (0.219 + 0.0292 + 0.0752) \text{ kJ} \cdot \text{mol}^{-1} \text{K}^{-1} \quad (46)$$

$$\bar{C}_{p_{\text{reaction blend}}} = 0.3234 \text{ kJ} \cdot \text{mol}^{-1} \text{K}^{-1} \quad (47)$$

Using the values of  $(\Delta H)_r$  and  $\bar{C}_{p_{\text{reaction blend}}}$  calculated, and considering  $n_r = 3$  and  $(\Delta H)_{H_2O}^{vap} = 40.72 \text{ kJ} \cdot \text{mol}^{-1}$ , the adiabatic temperature difference was calculated as shown in next equations.

$$\Delta T = \frac{[279.41 - (40.72)] \text{ kJ} \cdot \text{mol}^{-1}}{(3)(0.3528 \text{ kJ} \cdot \text{mol}^{-1} \text{K}^{-1})} \quad (48)$$

$$\Delta T = 225.52 \text{ K} \quad \text{or} \quad \Delta T = 225.52 \text{ }^\circ\text{C} \quad (49)$$

**Table 3.** Bond energies for glycerol, N<sub>2</sub>O, O<sub>2</sub>, glyceraldehyde, N<sub>2</sub>, and H<sub>2</sub>O. Values from references [65], [66], [67]

Compound	Bond	Number of bonds	Bond enthalpy per bond (kJ·mol <sup>-1</sup> )	Sum of bond enthalpies (kJ·mol <sup>-1</sup> )	Net change (kJ·mol <sup>-1</sup> )
glycerol	C-H	5	414	2070	5197
	C-O	3	351	1053	
	O-H	3	460	1380	
	C-C	2	347	694	
N <sub>2</sub> O	N≡N	1	950	950	1143
	N-O	1	201	201	
	C-H	4	414	1656	
glyceraldehyde	C-O	2	351	702	4712
	O-H	2	460	920	
	C-C	2	347	694	
	C=O	1	740	740	
H <sub>2</sub> O	H-O	2	460	920	920

**Table 4.** Enthalpy change due to the vaporization stage for glycerol, H<sub>2</sub>O<sub>2</sub>, glyceraldehyde and H<sub>2</sub>O e.g. [68]

Compound	$\Delta H_{\text{vap}}$ (kJ·mol <sup>-1</sup> )
glycerol	91.7
N <sub>2</sub> O	16.53
glyceraldehyde	88.11
N <sub>2</sub>	5.57
H <sub>2</sub> O	41

It is important to consider that the numerical value obtained in equation (49) for the determination of adiabatic temperature (225.52) represents a difference in temperature and since a change in 1 °C is the same as a change in 1 K, it can be considered in both, Kelvin or Centigrade scale.

The estimation of adiabatic temperature rise during the highly exothermic reactions is the most common method used for the determination of hazardous behavior. As can be seen from the value obtained from (40),  $(\Delta H)_r = -297.762 \text{ kJ}\cdot\text{mol}^{-1}$ , the partial oxidation of glycerol is highly exothermic reaction. In exothermic reactions, the energy evolved may appear in many forms, but for practical purposes it is usually obtained in the form of heat. In view of the increasingly several legal and economic implications of disastrous explosion and catastrophic effects, it is essential to cool the reaction to eliminate runaway

conditions. As a result, intensive research has been performed aiming to avoid the danger from an explosion by reducing the heat caused by the reaction and keeping the control costs at an acceptable level. For example, the use of supercritical carbon dioxide (scCO<sub>2</sub>) as a reaction medium for oxidations has reported to be successful in achieving a reduction in the reaction temperature rise for H<sub>2</sub> combustion with O<sub>2</sub> from 209 to 42 K due to the pressure tunable heat capacity of scCO<sub>2</sub> (from 100-9000 kPa) by which the heat generated throughout the reaction was adsorbed *e.g.* [71].

Another possibility is related to the design of non-isothermal reactors, considering the inclusion of a heat exchanger and cooling water into the system, selection of the type of reactor (continuously stirred-tank reactor or tubular reactor), the use of cooling coil, the addition of a glyceraldehyde solution blend to the feeding stream or the optimization of the inlet temperature of the feed. In cases where it is not possible to include a heat exchanger to the reactor, the use of multistage operations with interstage cooling between adiabatic sections can be also helpful for heat removal. The temperature distribution will affect the yield of the glyceraldehyde production, which has to be maximized. Therefore, an efficient reactor heat removal system has to be used to prevent the degradation of the resulting compound or prevent overoxidation to glyceric acid. Moreover, if the heat released by the reaction is not removed fast enough, a severe non-uniform temperature distribution can occur within the reactor, which in turn will cause different rates of reaction.

The effect of heat and mass transfer becomes even more important for faster reaction rates, when they can become rate controlling in heterogeneous reactions. In addition, it might be possible to control the temperature distribution by varying the tube diameter, residence time and the cooling rate.

## 5 DETERMINATION OF TRANSFER FUNCTION FOR ISOTHERMAL CASE – ANODIC OXIDATION

The anodic oxidation of glycerol ( $C_A$ ) for the particular case of production of glyceraldehyde ( $C_B$ ), glyceric acid ( $C_C$ ) and glycolic acid ( $C_D$ ) is discussed firstly. The partial oxidation of glycerol is a dynamic system, the general model described in the following equation:

$$\begin{aligned} X &= F(X, U), \\ Y &= G(X, U), \end{aligned} \quad (50)$$

where  $X$  is the vector of state variables, the output variables vector is represented by  $Y$  and  $U$  is the vector of input variables. This model is nonlinear and for control purposes it is strictly necessary to model nonlinear dynamic systems linearized. Relatively simple linearization is the development of the functions into Taylor series, given the relatively narrow interval variations we consider only the first linear members of the Taylor series. A detailed description is the linearization described by Corriou [59]. The system of equation (50) is then as follows:

$$\begin{aligned} \Delta X &= A\Delta X + B\Delta U \\ \Delta Y &= C\Delta X + D\Delta U \end{aligned} \quad (51)$$

Using  $\Delta Y = \Delta X$ , we derive and obtain equation (52), where the Laplace figure  $X$  is represented as  $X_L$ . Using  $\Delta Y_L = \Delta X_L$  equation (53) is obtained.  $(sI - A)^{-1}B$  represents the transfer function.

$$s\Delta X_L = A\Delta X_L + B\Delta U_L \quad (52)$$

$$\Delta Y_L = (sI - A)^{-1}B\Delta U_L \quad (53)$$

In this case it is considered that the partial oxidation is carried out in a flow isothermal perfectly stirred reactor. The diagram of the system is presented in Fig. 11 having two inputs flow ( $F$ ) and initial concentration of glycerol ( $C_{A0}$ ), four state concentration variables ( $C_A, C_B, C_C,$  and  $C_D$ ) and the same four output variables ( $C_A, C_B, C_C,$  and  $C_D$ ) where A,B,C,D, represent glycerol, glyceraldehyde, glyceric acid and glycolic acid respectively.

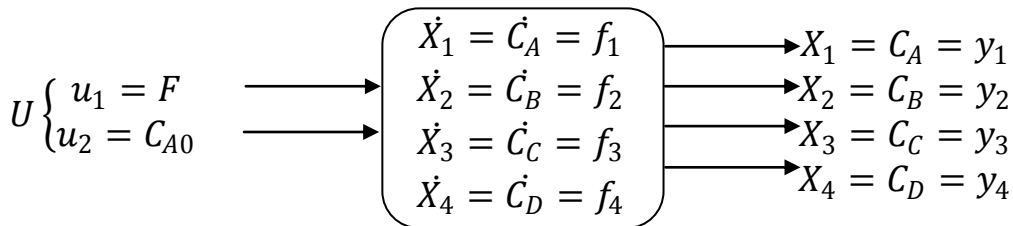


**Fig.11:** Scheme of the system describing the input, state variable and output.

The dynamic model of the previous system is based on the mass balance, including the chemical reactions and assuming a first order mechanism of the components (Equation (54))

$$\begin{aligned}
\frac{dC_A}{dt} &= \frac{F}{V}C_{A0} - k_1C_A - \frac{F}{V}C_A = f_1 \\
\frac{dC_B}{dt} &= k_1C_A - k_2C_B - \frac{F}{V}C_B = f_2 \\
\frac{dC_C}{dt} &= k_2C_B - k_3C_C - \frac{F}{V}C_C = f_3 \\
\frac{dC_D}{dt} &= k_3C_C - \frac{F}{V}C_D = f_4
\end{aligned} \tag{54}$$

The equations described in (54) are the vector components of the dynamic model of the system, which represents the anodic oxidation at constant voltage.

The previous equations are markedly nonlinear equations due to the element  $F/V$ . Therefore, it is necessary to perform linearization of the equations to obtain the equation represented in (55)

$$\begin{aligned}
\Delta \dot{X}_{4 \times 1} &= A_{4 \times 4} \Delta X_{4 \times 1} + B_{4 \times 2} \Delta U_{2 \times 1} \\
\Delta Y &= \Delta X
\end{aligned} \tag{55}$$

where A is the state matrix of dimension 4×4 and B is the control matrix of dimension 4×2. The elements of both matrices A and B are following:

$$\begin{aligned}
a_{11} &= \frac{\partial f_1^0}{\partial C_A} = -\left(k_1 + \frac{F^\circ}{V}\right); \quad a_{12} = \frac{\partial f_1^0}{\partial C_B} = 0; \quad a_{13} = \frac{\partial f_1^0}{\partial C_C} = 0; \\
a_{14} &= \frac{\partial f_1^0}{\partial C_D} = 0
\end{aligned} \tag{56}$$

$$\begin{aligned}
a_{21} &= \frac{\partial f_2^0}{\partial C_A} = k_1; \quad a_{22} = \frac{\partial f_2^0}{\partial C_B} = -\left(k_2 + \frac{F^\circ}{V}\right); \quad a_{23} = \frac{\partial f_2^0}{\partial C_C} = 0; \\
a_{24} &= \frac{\partial f_2^0}{\partial C_D} = 0
\end{aligned} \tag{57}$$

$$\begin{aligned}
a_{31} &= \frac{\partial f_3^0}{\partial C_A} = 0; \quad a_{32} = \frac{\partial f_3^0}{\partial C_B} = k_2; \quad a_{33} = \frac{\partial f_3^0}{\partial C_C} = -\left(k_3 + \frac{F^\circ}{V}\right); \\
a_{34} &= \frac{\partial f_3^0}{\partial C_D} = 0
\end{aligned} \tag{58}$$

$$\begin{aligned}
a_{41} &= \frac{\partial f_4^0}{\partial C_A} = 0; \quad a_{42} = \frac{\partial f_4^0}{\partial C_B} = 0; \quad a_{43} = \frac{\partial f_4^0}{\partial C_C} = k_3; \\
a_{44} &= \frac{\partial f_4^0}{\partial C_D} = -\frac{F^\circ}{V}
\end{aligned} \tag{59}$$

$$b_{11} = \frac{\partial f_1^0}{\partial F} = \frac{1}{V}(C_{A0} - C_A^0); \quad b_{12} = \frac{\partial f_1^0}{\partial C_{A0}} = \frac{F^\circ}{V} \tag{60}$$

$$b_{21} = \frac{\partial f_2^0}{\partial F} = -\frac{C_B^0}{V}; b_{22} = \frac{\partial f_2^0}{\partial C_{A0}} = 0 \quad (61)$$

$$b_{31} = \frac{\partial f_3^0}{\partial F} = -\frac{C_C^0}{V}; b_{32} = \frac{\partial f_3^0}{\partial C_{A0}} = 0 \quad (62)$$

$$b_{41} = \frac{\partial f_4^0}{\partial F} = -\frac{C_D^0}{V}; b_{42} = \frac{\partial f_4^0}{\partial C_{A0}} = 0 \quad (63)$$

The substitution of these relationships on equation (55) gives:

$$\begin{pmatrix} \frac{d\Delta C_A}{dt} \\ \frac{d\Delta C_B}{dt} \\ \frac{d\Delta C_C}{dt} \\ \frac{d\Delta C_D}{dt} \end{pmatrix} = \begin{pmatrix} -\left(k_1 + \frac{F^\circ}{V}\right) & 0 & 0 & 0 \\ k_1 & -\left(k_2 + \frac{F^\circ}{V}\right) & 0 & 0 \\ 0 & k_2 & -\left(k_3 + \frac{F^\circ}{V}\right) & 0 \\ 0 & 0 & k_3 & -\frac{F^\circ}{V} \end{pmatrix} \begin{pmatrix} \Delta C_A \\ \Delta C_B \\ \Delta C_C \\ \Delta C_D \end{pmatrix} + \begin{pmatrix} \frac{1}{V}(C_{A0} - C_A^0) & \frac{F^\circ}{V} \\ -\frac{C_B^0}{V} & 0 \\ -\frac{C_C^0}{V} & 0 \\ -\frac{C_D^0}{V} & 0 \end{pmatrix} \begin{pmatrix} \Delta F \\ \Delta C_{A0} \end{pmatrix} \quad (64)$$

The multiplication procedure leads to the next group of equations:

$$\frac{d\Delta C_A}{dt} = -\left(k_1 + \frac{F^\circ}{V}\right) \Delta C_A + \frac{1}{V}(C_{A0} - C_A^0) \Delta F + \frac{F^\circ}{V} \Delta C_{A0} \quad (65)$$

$$\frac{d\Delta C_B}{dt} = k_1 \Delta C_A - \left(k_2 + \frac{F^\circ}{V}\right) \Delta C_B - \frac{C_B^0}{V} \Delta F \quad (66)$$

$$\frac{d\Delta C_C}{dt} = k_2 \Delta C_B - \left(k_3 + \frac{F^\circ}{V}\right) \Delta C_C - \frac{C_C^0}{V} \Delta F \quad (67)$$

$$\frac{d\Delta C_D}{dt} = k_3 \Delta C_C - \frac{F^\circ}{V} \Delta C_D - \frac{C_D^0}{V} \Delta F \quad (68)$$

For the purpose of control, it is necessary to introduce the following dimensionless parameters

$$C_A^* = \frac{C_A}{C_A^0} \rightarrow C_A = C_A^* \cdot C_A^0 \quad (69)$$

$$C_B^* = \frac{C_B}{C_A^0} \rightarrow C_B = C_B^* \cdot C_A^0 \quad (70)$$

$$C_C^* = \frac{C_C}{C_A^0} \rightarrow C_C = C_C^* \cdot C_A^0 \quad (71)$$

$$C_D^* = \frac{C_D}{C_A^0} \rightarrow C_D = C_D^* \cdot C_A^0 \quad (72)$$

$$F^* = \frac{F}{F^0} \rightarrow F = F^* \cdot F^0; C_{A0}^* = \frac{C_{A0}}{C_A^0} \rightarrow C_{A0} = C_{A0}^* \cdot C_A^0 \quad (73)$$

The differential equations expressed in (65) to (68) take the form of equations (74) to (77) by substitution of the previous dimensionless dependencies

$$\frac{d\Delta C_A^* \cdot C_A^0}{dt} = -\left(k_1 + \frac{F^\circ}{V}\right) \Delta C_A^* \cdot C_A^0 + \frac{1}{V} (C_{A0} - C_A^0) \Delta F^* \cdot F^0 + \frac{F^\circ}{V} \Delta C_{A0}^* \cdot C_A^0 \quad (74)$$

$$\frac{d\Delta C_B^* \cdot C_A^0}{dt} = k_1 \Delta C_A^* \cdot C_A^0 - \left(k_2 + \frac{F^\circ}{V}\right) \Delta C_B^* \cdot C_A^0 - \frac{C_B^0}{V} \Delta F^* \cdot F^0 \quad (75)$$

$$\frac{d\Delta C_C^* \cdot C_A^0}{dt} = k_2 \Delta C_B^* \cdot C_A^0 - \left(k_3 + \frac{F^\circ}{V}\right) \Delta C_C^* \cdot C_A^0 - \frac{C_C^0}{V} \Delta F^* \cdot F^0 \quad (76)$$

$$\frac{d\Delta C_D^* \cdot C_A^0}{dt} = k_3 \Delta C_C^* \cdot C_A^0 - \frac{F^\circ}{V} \Delta C_D^* \cdot C_A^0 - \frac{C_D^0}{V} \Delta F^* \cdot F^0 \quad (77)$$

Multiplying the previous equations (74 - 77) by  $V/F^\circ C_A^0$ , result in:

$$\frac{d\Delta C_A^*}{dt^*} = -\left(\frac{V}{F^\circ} k_1 + 1\right) \Delta C_A^* + \frac{\Delta F^*}{C_A^0} (C_{A0} - C_A^0) + \Delta C_{A0}^* \quad (78)$$

$$\frac{d\Delta C_B^*}{dt^*} = \frac{V}{F^\circ} k_1 \Delta C_A^* - \left(\frac{V}{F^\circ} k_2 + 1\right) \Delta C_B^* - \frac{C_B^0}{C_A^0} \Delta F^* \quad (79)$$

$$\frac{d\Delta C_C^*}{dt^*} = \frac{V}{F^\circ} k_2 \Delta C_B^* - \left(\frac{V}{F^\circ} k_3 + 1\right) \Delta C_C^* - \frac{C_C^0}{C_A^0} \Delta F^* \quad (80)$$

$$\frac{d\Delta C_D^*}{dt^*} = \frac{V}{F^\circ} k_3 \Delta C_C^* - \Delta C_D^* - \frac{C_D^0}{C_A^0} \Delta F^* \quad (81)$$

where the term  $t^* = (F^\circ \cdot t/V)$  implies a dimensionless parameter (dimensionless time). Following, the representation is in the matrix form

$$\begin{pmatrix} \frac{d\Delta C_A^*}{dt^*} \\ \frac{d\Delta C_B^*}{dt^*} \\ \frac{d\Delta C_C^*}{dt^*} \\ \frac{d\Delta C_D^*}{dt^*} \end{pmatrix} = \begin{pmatrix} -\left(\frac{V}{F^\circ} k_1 + 1\right) & 0 & 0 & 0 \\ \frac{V}{F^\circ} k_1 & -\left(\frac{V}{F^\circ} k_2 + 1\right) & 0 & 0 \\ 0 & \frac{V}{F^\circ} k_2 & -\left(\frac{V}{F^\circ} k_3 + 1\right) & 0 \\ 0 & 0 & \frac{V}{F^\circ} k_3 & -1 \end{pmatrix} \begin{pmatrix} \Delta C_A^* \\ \Delta C_B^* \\ \Delta C_C^* \\ \Delta C_D^* \end{pmatrix} + \begin{pmatrix} \frac{1}{C_A^0} (C_{A0} - C_A^0) & 1 \\ -\frac{C_B^0}{C_A^0} & 0 \\ -\frac{C_C^0}{C_A^0} & 0 \\ -\frac{C_D^0}{C_A^0} & 0 \end{pmatrix} \begin{pmatrix} \Delta F^* \\ \Delta C_{A0}^* \end{pmatrix} \quad (82)$$

Furthermore, as the transfer function  $G(s)$  is given by:

$$G(s) = (sI - A)^{-1} B \quad (83)$$

The outputs are defined as:

$$\begin{aligned} \Delta y_1^* &= \Delta C_A^* \\ \Delta y_2^* &= \Delta C_B^* \\ \Delta y_3^* &= \Delta C_C^* \\ \Delta y_4^* &= \Delta C_D^* \end{aligned} \quad (84)$$

Therefore, it is necessary to determine the matrix  $(sI-A)$  and the respective inverse matrix:

$$(sI - A) = \left[ \begin{pmatrix} s & 0 & 0 & 0 \\ 0 & s & 0 & 0 \\ 0 & 0 & s & 0 \\ 0 & 0 & 0 & s \end{pmatrix} - \begin{pmatrix} -\left(\frac{V}{F^\circ}k_1 + 1\right) & 0 & 0 & 0 \\ \frac{V}{F^\circ}k_1 & -\left(\frac{V}{F^\circ}k_2 + 1\right) & 0 & 0 \\ 0 & \frac{V}{F^\circ}k_2 & -\left(\frac{V}{F^\circ}k_3 + 1\right) & 0 \\ 0 & 0 & \frac{V}{F^\circ}k_3 & -1 \end{pmatrix} \right] \quad (85)$$

$$(sI - A) = \begin{pmatrix} s + \left(\frac{V}{F^\circ}k_1 + 1\right) & 0 & 0 & 0 \\ -\frac{V}{F^\circ}k_1 & s + \left(\frac{V}{F^\circ}k_2 + 1\right) & 0 & 0 \\ 0 & -\frac{V}{F^\circ}k_2 & s + \left(\frac{V}{F^\circ}k_3 + 1\right) & 0 \\ 0 & 0 & -\frac{V}{F^\circ}k_3 & s + 1 \end{pmatrix} \quad (86)$$

$$(sI - A)^{-1} = \begin{bmatrix} \frac{F^\circ}{(F^\circ + F^\circ s + V k_1)} & 0 & 0 & 0 \\ \frac{F^\circ V k_1}{(F^\circ + F^\circ s + V k_1)(F^\circ + F^\circ s + V k_2)} & \frac{F^\circ}{(F^\circ + F^\circ s + V k_2)} & 0 & 0 \\ \frac{F^\circ V^2 k_1 k_2}{(F^\circ + F^\circ s + V k_1)(F^\circ + F^\circ s + V k_2)(F^\circ + F^\circ s + V k_3)} & \frac{F^\circ V k_2}{(F^\circ + F^\circ s + V k_2)(F^\circ + F^\circ s + V k_3)} & \frac{F^\circ}{(F^\circ + F^\circ s + V k_3)} & 0 \\ \frac{V^3 k_1 k_2 k_3}{(s+1)(F^\circ + F^\circ s + V k_1)(F^\circ + F^\circ s + V k_2)(F^\circ + F^\circ s + V k_3)} & \frac{V^2 k_2 k_3}{(s+1)(F^\circ + F^\circ s + V k_2)(F^\circ + F^\circ s + V k_3)} & \frac{V k_3}{(s+1)(F^\circ + F^\circ s + V k_3)} & \frac{1}{s+1} \end{bmatrix} \quad (87)$$

As a result, the transfer function is calculated as:

$$G(s) = \begin{pmatrix} \frac{F^\circ}{(F^\circ + F^\circ s + V k_1)} & 0 \\ \frac{F^\circ V k_1}{(F^\circ + F^\circ s + V k_1)(F^\circ + F^\circ s + V k_2)} & \frac{F^\circ}{(F^\circ + F^\circ s + V k_2)} \\ \frac{F^\circ V^2 k_1 k_2}{(F^\circ + F^\circ s + V k_1)(F^\circ + F^\circ s + V k_2)(F^\circ + F^\circ s + V k_3)} & \frac{F^\circ V k_2}{(F^\circ + F^\circ s + V k_2)(F^\circ + F^\circ s + V k_3)} \\ \frac{V^3 k_1 k_2 k_3}{(s+1)(F^\circ + F^\circ s + V k_1)(F^\circ + F^\circ s + V k_2)(F^\circ + F^\circ s + V k_3)} & \frac{V^2 k_2 k_3}{(s+1)(F^\circ + F^\circ s + V k_2)(F^\circ + F^\circ s + V k_3)} \end{pmatrix} \begin{pmatrix} \frac{1}{C_A^0} (C_{A0} - C_A^0) & 1 \\ -\frac{C_B^0}{C_A^0} & 0 \\ -\frac{C_C^0}{C_A^0} & 0 \\ -\frac{C_D^0}{C_A^0} & 0 \end{pmatrix} \quad (88)$$

The previous equation can be expressed as in (89)

$$G(s) = \begin{bmatrix} g_{11} & g_{12} \\ g_{21} & g_{22} \\ g_{31} & g_{32} \\ g_{41} & g_{42} \end{bmatrix} \quad (89)$$

where the elements of the matrix are represented in (90) to (97):

$$g_{11} = -\frac{F^\circ(C_A^0 - C_{A0})}{C_A^0(F^\circ + F^\circ s + V k_1)}; \quad (90)$$

$$g_{12} = \frac{F^\circ}{(F^\circ + F^\circ s + V k_1)}; \quad (91)$$

$$g_{21} = -\left( \frac{F^\circ C_B^0}{C_A^0(F^\circ + F^\circ s + V k_2)} - \frac{F^\circ V k_1 (C_A^0 - C_{A0})}{(C_A^0(F^\circ + F^\circ s + V k_1) g_3)} \right); \quad (92)$$

$$g_{22} = \frac{F^\circ V k_1}{(F^\circ + F^\circ s + V k_1)(F^\circ + F^\circ s + V k_2)}; \quad (93)$$

$$g_{31} = -\frac{F^\circ C_C^0}{C_A^0(F^\circ + F^\circ s + V k_3)} - \frac{F^\circ V C_B^0 k_2}{C_A^0(F^\circ + F^\circ s + V k_2)(F^\circ + F^\circ s + V k_3)} - \frac{F^\circ V^2 k_1 k_2 (C_A^0 - C_{A0})}{(C_A^0(F^\circ + F^\circ s + V k_1)(F^\circ + F^\circ s + V k_2) g_4)}; \quad (94)$$

$$g_{32} = \frac{F^\circ V^2 k_1 k_2}{(F^\circ + F^\circ s + V k_1)(F^\circ + F^\circ s + V k_2) g_4}; \quad (95)$$

$$g_{41} = -\frac{C_D^0}{C_A^0(s+1)} - \frac{V C_C^0 k_3}{C_A^0(s+1)(F^\circ + F^\circ s + V k_3)} - \frac{V^2 C_B^0 k_2 k_3}{C_A^0(s+1)(F^\circ + F^\circ s + V k_2)(F^\circ + F^\circ s + V k_3)} - \frac{V^3 k_1 k_2 k_3 (C_A^0 - C_{A0})}{C_A^0(s+1)(F^\circ + F^\circ s + V k_1)(F^\circ + F^\circ s + V k_2) g_4}; \quad (96)$$

$$g_{42} = \frac{V^3 k_1 k_2 k_3}{(s+1)(F^\circ + F^\circ s + V k_1)(F^\circ + F^\circ s + V k_2) g_4} \quad (97)$$

## 6 DETERMINATION OF TRANSFER FUNCTION FOR ISOTHERMAL CASE – OXIDATION USING NO<sub>2</sub>

The oxidation of glycerol ( $G$ ) with nitrous oxide ( $R$ ) for the production of glyceraldehyde ( $A$ ), and overoxidation to glyceric acid ( $K$ ) in isothermal conditions is discussed next. The diagram of the system is presented in Fig. 12 having three inputs ( $F$ ,  $C_{R0}$ , and  $C_{G0}$ ), four state variables ( $A$ ,  $R$ ,  $G$  and  $K$ ) and four output variables ( $A$ ,  $R$ ,  $G$ , and  $K$ ).

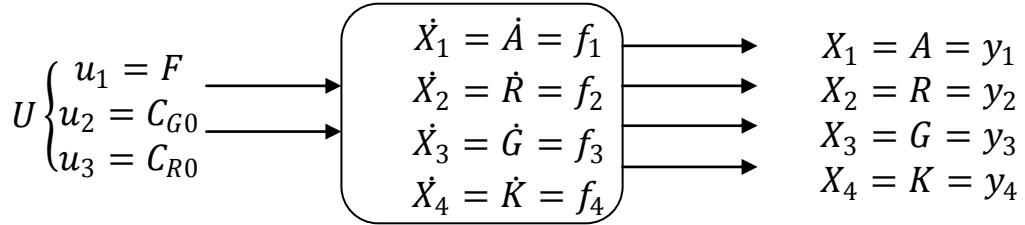


**Fig. 12:** Scheme of the oxidation of glycerol with NO<sub>2</sub> describing the input, state variable and output.

The set of equations that describe the mass balance, including of chemical reactions in which are supposed to be of the first order mechanism, of the components is presented in (98) to (101)

$$\frac{dA}{dt} = k_1 \cdot G \cdot R - k_2 \cdot A \cdot R - \frac{F}{V}A \quad (98)$$

$$\frac{dR}{dt} = -k_1 \cdot G \cdot R - k_2 \cdot A \cdot R + \frac{F}{V}C_{R0} - \frac{F}{V}R \quad (99)$$

$$\frac{dG}{dt} = -k_1 \cdot G \cdot R + \frac{F}{V}C_{G0} - \frac{F}{V}G \quad (100)$$

$$\frac{dK}{dt} = k_2 \cdot A \cdot R - \frac{F}{V}K \quad (101)$$

Again, the described system is non-linear. Therefore, we solved it in the same way as shown in chapter 4. The elements of matrix A, B, are the following:

$$a_{11} = \frac{\partial f_1^0}{\partial A} = -k_2 R^0 - \frac{F^0}{V}; a_{12} = \frac{\partial f_1^0}{\partial R} = k_1 G^0 - k_2 A^0; a_{13} = \frac{\partial f_1^0}{\partial G} = k_1 R^0; a_{14} = \frac{\partial f_1^0}{\partial K} = 0 \quad (102)$$

$$a_{21} = \frac{\partial f_2^0}{\partial A} = -k_2 R^0; a_{22} = \frac{\partial f_2^0}{\partial R} = -k_1 G^0 - k_2 A^0 - \frac{F^0}{V}; a_{23} = \frac{\partial f_2^0}{\partial G} = -k_1 R^0; a_{24} = \frac{\partial f_2^0}{\partial K} = 0 \quad (103)$$

$$\begin{aligned}
a_{31} &= \frac{\partial f_3^0}{\partial A} = 0; a_{32} = \frac{\partial f_3^0}{\partial R} = -k_1 G^0; a_{33} = \frac{\partial f_3^0}{\partial G} = -k_1 R^0 - \frac{F^0}{V}; \\
a_{34} &= \frac{\partial f_3^0}{\partial K} = 0
\end{aligned} \tag{104}$$

$$\begin{aligned}
a_{41} &= \frac{\partial f_4^0}{\partial A} = k_2 R^0; a_{42} = \frac{\partial f_4^0}{\partial R} = k_2 A^0; a_{43} = \frac{\partial f_4^0}{\partial G} = 0; a_{44} = \\
\frac{\partial f_4^0}{\partial K} &= -\frac{F^0}{V}
\end{aligned} \tag{105}$$

Considering the control variables, equations (106) to (109) are obtained:

$$b_{11} = \frac{\partial f_1^0}{\partial F} = -\frac{A^0}{V}; b_{12} = \frac{\partial f_1^0}{\partial C_{G0}} = 0; b_{13} = \frac{\partial f_1^0}{\partial C_{R0}} = 0 \tag{106}$$

$$b_{21} = \frac{\partial f_2^0}{\partial F} = \frac{(C_{R0}-R^0)}{V}; b_{22} = \frac{\partial f_2^0}{\partial C_{G0}} = 0; b_{23} = \frac{\partial f_2^0}{\partial C_{R0}} = \frac{F^0}{V} \tag{107}$$

$$b_{31} = \frac{\partial f_3^0}{\partial F} = \frac{(C_{G0}-G^0)}{V}; b_{32} = \frac{\partial f_3^0}{\partial C_{G0}} = \frac{F^0}{V}; b_{33} = \frac{\partial f_3^0}{\partial C_{R0}} = 0 \tag{108}$$

$$b_{41} = \frac{\partial f_4^0}{\partial F} = -\frac{K^0}{V}; b_{42} = \frac{\partial f_4^0}{\partial C_{G0}} = 0; b_{43} = \frac{\partial f_4^0}{\partial C_{R0}} = 0 \tag{109}$$

Therefore, the representation of the state vector is given by:

$$\begin{aligned}
\begin{pmatrix} \frac{dA}{dt} \\ \frac{dR}{dt} \\ \frac{dG}{dt} \\ \frac{dK}{dt} \end{pmatrix} &= \begin{pmatrix} -\left(k_2 R^0 + \frac{F^0}{V}\right) & k_1 G^0 - k_2 A^0 & k_1 R^0 & 0 \\ -k_2 R^0 & -\left(k_1 G^0 + k_2 A^0 + \frac{F^0}{V}\right) & k_1 R^0 & 0 \\ 0 & -k_1 G^0 & -\left(k_1 R^0 + \frac{F^0}{V}\right) & 0 \\ k_2 R^0 & k_2 A^0 & 0 & -\frac{F^0}{V} \end{pmatrix} \begin{pmatrix} \Delta A \\ \Delta R \\ \Delta G \\ \Delta K \end{pmatrix} + \\
\begin{pmatrix} -\frac{A^0}{V} & 0 & 0 \\ \frac{(C_{R0}-R^0)}{V} & 0 & \frac{F^0}{V} \\ \frac{(C_{G0}-G^0)}{V} & \frac{F^0}{V} & 0 \\ -\frac{K^0}{V} & 0 & 0 \end{pmatrix} \begin{pmatrix} \Delta F \\ \Delta C_{G0} \\ \Delta C_{R0} \end{pmatrix}
\end{aligned} \tag{110}$$

The multiplication procedure leads to the next group of equations:

$$\frac{d\Delta A}{dt} = -\left(k_2 R^0 + \frac{F^0}{V}\right) \Delta A + (k_1 G^0 - k_2 A^0) \Delta R + (k_1 R^0) \Delta G - \frac{A^0}{V} \Delta F \tag{111}$$

$$\frac{d\Delta R}{dt} = -(k_2 R^0) \Delta A - \left(k_1 G^0 + k_2 A^0 + \frac{F^0}{V}\right) \Delta R + (k_1 R^0) \Delta G + \frac{(C_{R0}-R^0)}{V} \Delta F + \frac{F^0}{V} \Delta C_{R0} \tag{112}$$

$$\frac{d\Delta G}{dt} = -(k_1 G^0) \Delta A - \left(k_1 R^0 + \frac{F^0}{V}\right) \Delta G + \frac{1}{V} (C_{G0} - G^0) \Delta F + \frac{F^0}{V} \Delta C_{G0} \tag{113}$$

$$\frac{d\Delta K}{dt} = (k_2 R^0)\Delta A + (k_2 A^0)\Delta R - \left(\frac{F^\circ}{V}\right)\Delta K - \left(\frac{K^0}{V}\right)\Delta F \quad (114)$$

For the purpose of control, it is necessary to introduce the following dimensionless parameters

$$A^* = \frac{A}{G^0} \therefore A = A^* \cdot G^0 \quad (115)$$

$$R^* = \frac{R}{R^0} \therefore R = R^* \cdot R^0 \quad (116)$$

$$G^* = \frac{G}{G^0} \therefore G = G^* \cdot G^0 \quad (117)$$

$$K^* = \frac{K}{G^0} \therefore K = K^* \cdot G^0 \quad (118)$$

$$F^* = \frac{F}{F^0} \therefore F = F^* \cdot F^0$$

$$C_{G0}^* = \frac{C_{G0}}{G^0} \therefore C_{G0} = C_{G0}^* \cdot G^0 \quad (119)$$

$$C_{R0}^* = \frac{C_{R0}}{R^0} \therefore C_{R0} = C_{R0}^* \cdot R^0$$

After substitution of dimensionless dependencies, equations (120) to (123) are obtained:

$$\begin{aligned} \frac{d\Delta A^* \cdot G^0}{dt} = & - \left(k_2 R^0 + \frac{F^\circ}{V}\right) \Delta A^* \cdot G^0 + (k_1 G^0 - k_2 A^0) \Delta R^* \cdot R^0 + \\ & (k_1 R^0) \Delta G^* \cdot G^0 - \frac{A^0}{V} \Delta F^* \cdot F^0 \end{aligned} \quad (120)$$

$$\begin{aligned} \frac{d\Delta R^* \cdot R^0}{dt} = & -(k_2 R^0) \Delta A^* \cdot G^0 - \left(k_1 G^0 + k_2 A^0 + \frac{F^\circ}{V}\right) \Delta R^* \cdot R^0 + \\ & (k_1 R^0) \Delta G^* \cdot G^0 + \frac{(C_{R0} - R^0)}{V} \Delta F^* \cdot F^0 + \frac{F^\circ}{V} \Delta C_{R0}^* \cdot R^0 \end{aligned} \quad (121)$$

$$\begin{aligned} \frac{d\Delta G^* \cdot G^0}{dt} = & -(k_1 G^0) \Delta A^* \cdot G^0 - \left(k_1 R^0 + \frac{F^\circ}{V}\right) \Delta G^* \cdot G^0 + \\ & \frac{1}{V} (C_{G0} - G^0) \Delta F^* \cdot F^0 + \frac{F^\circ}{V} \Delta C_{G0}^* \cdot G^0 \end{aligned} \quad (122)$$

$$\begin{aligned} \frac{d\Delta K^* \cdot G^0}{dt} = & (k_2 R^0) \Delta A^* \cdot G^0 + (k_2 A^0) \Delta R^* \cdot R^0 - \left(\frac{F^\circ}{V}\right) \Delta K^* \cdot G^0 - \\ & \left(\frac{K^0}{V}\right) \Delta F^* \cdot F^0 \end{aligned} \quad (123)$$

Multiplying (120), (122) and (123) by  $V/F^0 G^0$  and (121) by  $V/F^0 R^0$ , the next sets of equations are obtained:

$$\begin{aligned} \frac{d\Delta A^*}{dt^*} = & - \left(\frac{k_2 R^0 V}{F^0} + 1\right) \Delta A^* + \left(\frac{V k_1 R^0}{F^0} - \frac{V k_2 A^0 R^0}{F^0 G^0}\right) \Delta R^* + \frac{V k_1 R^0}{F^0} \Delta G^* - \\ & \frac{A^0}{G^0} \Delta F^* \end{aligned} \quad (124)$$

$$\frac{d\Delta R^*}{dt^*} = -\frac{Vk_2G^0}{F^0}\Delta A^* - \left(\frac{Vk_1G^0}{F^0} + \frac{Vk_2A^0}{F^0} + 1\right)\Delta R^* + \frac{Vk_1G^0}{F^0}\Delta G^* + \frac{(C_{R0}-R^0)}{R^0}\Delta F^* + \Delta C_{R0}^* \quad (125)$$

$$\frac{d\Delta G^*}{dt^*} = -\frac{Vk_1G^0}{F^0}\Delta A^* - \left(\frac{Vk_1R^0}{F^0} + 1\right)\Delta G^* + \frac{(C_{G0}-G^0)}{G^0}\Delta F^* + \Delta C_{G0}^* \quad (126)$$

$$\frac{d\Delta K^*}{dt^*} = \frac{Vk_2R^0}{F^0}\Delta A^* + \frac{Vk_2A^0R^0}{F^0G^0}\Delta R^* - \Delta K^* - \frac{K^0}{G^0}\Delta F^* \quad (127)$$

where the term  $t^* = (F^0 \cdot t/V)$  implies a dimensionless parameter (dimensionless time). As a result, the system represented in (110) transforms into (128)

$$\begin{pmatrix} \frac{d\Delta A^*}{dt^*} \\ \frac{d\Delta R^*}{dt^*} \\ \frac{d\Delta G^*}{dt^*} \\ \frac{d\Delta K^*}{dt^*} \end{pmatrix} = \begin{pmatrix} -\left(\frac{Vk_2R^0}{F^0} + 1\right) & \frac{Vk_1R^0}{F^0} - \frac{Vk_2A^0R^0}{F^0G^0} & \frac{Vk_1R^0}{F^0} & 0 \\ -\left(\frac{Vk_2G^0}{F^0}\right) & -\left(\frac{Vk_1G^0 + Vk_2A^0 + F^0}{F^0}\right) & \left(\frac{Vk_1G^0}{F^0}\right) & 0 \\ -\left(\frac{Vk_1G^0}{F^0}\right) & -\left(\frac{Vk_1R^0}{F^0} + 1\right) & 0 & 0 \\ \left(\frac{Vk_2R^0}{F^0}\right) & \left(\frac{Vk_2A^0R^0}{F^0G^0}\right) & 0 & -1 \end{pmatrix} \begin{pmatrix} \Delta A^* \\ \Delta R^* \\ \Delta G^* \\ \Delta K^* \end{pmatrix} + \begin{pmatrix} -\frac{A^0}{G^0} & 0 & 0 \\ \frac{(C_{R0}-R^0)}{R^0} & 0 & 1 \\ \frac{(C_{G0}-G^0)}{G^0} & 1 & 0 \\ -\left(\frac{K^0}{G^0}\right) & 0 & 0 \end{pmatrix} \begin{pmatrix} \Delta F^* \\ \Delta C_{G0} \\ \Delta C_{R0} \end{pmatrix} \quad (128)$$

Furthermore, as the transfer function  $G(s)$  is given by  $G(s) = (sI - A)^{-1}B$ , firstly it is necessary to calculate:

$$(sI - A) = \begin{pmatrix} s & 0 & 0 & 0 \\ 0 & s & 0 & 0 \\ 0 & 0 & s & 0 \\ 0 & 0 & 0 & s \end{pmatrix} - \begin{pmatrix} -\left(\frac{Vk_2R^0}{F^0} + 1\right) & \frac{Vk_1R^0}{F^0} - \frac{Vk_2A^0R^0}{F^0G^0} & \frac{Vk_1R^0}{F^0} & 0 \\ -\left(\frac{Vk_2G^0}{F^0}\right) & -\left(\frac{Vk_1G^0 + Vk_2A^0 + F^0}{F^0}\right) & \left(\frac{Vk_1G^0}{F^0}\right) & 0 \\ -\left(\frac{Vk_1G^0}{F^0}\right) & -\left(\frac{Vk_1R^0}{F^0} + 1\right) & 0 & 0 \\ \left(\frac{Vk_2R^0}{F^0}\right) & \left(\frac{Vk_2A^0R^0}{F^0G^0}\right) & 0 & -1 \end{pmatrix} \quad (129)$$

Defining the next elements of matrix  $A$ :

$$a_{11} = \left(\frac{Vk_2R^0}{F^0} + 1\right); a_{12} = \frac{Vk_1R^0}{F^0} - \frac{Vk_2A^0R^0}{F^0G^0}; a_{13} = \frac{Vk_1R^0}{F^0} \quad (130)$$

$$a_{21} = \left(\frac{Vk_2G^0}{F^0}\right); a_{22} = \left(\frac{Vk_1G^0 + Vk_2A^0 + F^0}{F^0}\right); a_{23} = \left(\frac{Vk_1G^0}{F^0}\right) \quad (131)$$

$$a_{31} = \left(\frac{Vk_1G^0}{F^0}\right); a_{32} = \left(\frac{Vk_1R^0}{F^0} + 1\right) \quad (132)$$

$$a_{41} = \left(\frac{Vk_2R^0}{F^0}\right); a_{42} = \left(\frac{Vk_2A^0R^0}{F^0G^0}\right) \quad (133)$$

$$(sI - A) = \begin{pmatrix} s + a_{11} & -a_{12} & -a_{13} & 0 \\ a_{21} & s + a_{22} & -a_{23} & 0 \\ a_{31} & a_{32} & s & 0 \\ -a_{41} & -a_{42} & 0 & s + 1 \end{pmatrix} \quad (134)$$

$$(sI - A)^{-1} = \begin{bmatrix} \frac{(s^2 + a_{22}s + a_{23}a_{32})}{D} & \frac{-(a_{13}a_{32} - a_{12}s)}{D} \\ \frac{-(a_{23}a_{31} + a_{21}s)}{D} & \frac{(s^2 + a_{11}s + a_{13}a_{31})}{D} \\ \frac{-(a_{23}a_{31} - a_{21}a_{32} + a_{31}s)}{D} & \frac{-(a_{11}a_{32} + a_{12}a_{31} + a_{32}s)}{D} \\ \frac{a_{41}s^2 - a_{23}a_{31}a_{42} + a_{23}a_{32}a_{41} - a_{21}a_{42}s + a_{22}a_{41}s}{(s+1)D} & \frac{a_{42}s^2 + a_{13}a_{31}a_{42} - a_{13}a_{32}a_{41} + a_{11}a_{42}s + a_{12}a_{41}s}{(s+1)D} \\ \frac{(a_{12}a_{23} + a_{13}a_{22} + a_{13}s)}{D} & 0 \\ \frac{(a_{11}a_{23} - a_{13}a_{21} + a_{23}s)}{D} & 0 \\ \frac{(a_{11}a_{22} + a_{12}a_{21} + a_{11}s + a_{22}s + s^2)}{D} & 0 \\ \frac{a_{11}a_{23}a_{42} + a_{12}a_{23}a_{41} - a_{13}a_{21}a_{42} + a_{13}a_{22}a_{41} + a_{13}a_{41}s + a_{23}a_{42}s}{(s+1)D} & \frac{1}{(s+1)} \end{bmatrix} \quad (135)$$

where:

$$D = s^3 + a_{11}s^2 + a_{22}s^2 + a_{11}a_{22}s + a_{12}a_{21}s + a_{13}a_{31}s + a_{23}a_{32}s + a_{11}a_{23}a_{32} + a_{12}a_{23}a_{31} - a_{13}a_{21}a_{32} + a_{13}a_{22}a_{31} \quad (136)$$

In order to calculate the transfer function  $G(s)$ :

$$G(s) = \begin{bmatrix} \frac{(s^2 + a_{22}s + a_{23}a_{32})}{D} & \frac{-(a_{13}a_{32} - a_{12}s)}{D} \\ \frac{-(a_{23}a_{31} + a_{21}s)}{D} & \frac{(s^2 + a_{11}s + a_{13}a_{31})}{D} \\ \frac{-(a_{23}a_{31} - a_{21}a_{32} + a_{31}s)}{D} & \frac{-(a_{11}a_{32} + a_{12}a_{31} + a_{32}s)}{D} \\ \frac{a_{41}s^2 - a_{23}a_{31}a_{42} + a_{23}a_{32}a_{41} - a_{21}a_{42}s + a_{22}a_{41}s}{(s+1)D} & \frac{a_{42}s^2 + a_{13}a_{31}a_{42} - a_{13}a_{32}a_{41} + a_{11}a_{42}s + a_{12}a_{41}s}{(s+1)D} \\ \frac{(a_{12}a_{23} + a_{13}a_{22} + a_{13}s)}{D} & 0 \\ \frac{(a_{11}a_{23} - a_{13}a_{21} + a_{23}s)}{D} & 0 \\ \frac{(a_{11}a_{22} + a_{12}a_{21} + a_{11}s + a_{22}s + s^2)}{D} & 0 \\ \frac{a_{11}a_{23}a_{42} + a_{12}a_{23}a_{41} - a_{13}a_{21}a_{42} + a_{13}a_{22}a_{41} + a_{13}a_{41}s + a_{23}a_{42}s}{(s+1)D} & \frac{1}{(s+1)} \end{bmatrix} \begin{bmatrix} b_{11} & 0 & 0 \\ b_{21} & 0 & b_{23} \\ b_{31} & b_{32} & 0 \\ b_{41} & 0 & 0 \end{bmatrix} \quad (137)$$

where:

$$b_{11} = -\frac{A^0}{G^0}; \quad b_{21} = \frac{(C_R R^0 - R^0)}{R^0}; \quad b_{23} = 1; \quad b_{31} = \frac{(C_G R^0 - G^0)}{G^0}; \quad b_{32} = 1; \quad b_{41} = -\left(\frac{K^0}{G^0}\right) \quad (138)$$

$$\begin{aligned}
G(s) = & \left[ \begin{array}{l} \frac{b_{11}(s^2 + a_{22}s + a_{23}a_{32})}{D} - \frac{b_{21}(a_{13}a_{32} - a_{12}s)}{D} + \frac{b_{31}(a_{12}a_{23} + a_{13}a_{22} + a_{13}s)}{D} \\ -\frac{b_{11}(a_{23}a_{31} + a_{21}s)}{D} + \frac{b_{21}(s^2 + a_{11}s + a_{13}a_{31})}{D} + \frac{b_{31}(a_{11}a_{23} - a_{13}a_{21} + a_{23}s)}{D} \\ \frac{g_{31}}{D} \\ \frac{g_{41}}{D} \\ \frac{b_{32}(a_{12}a_{23} + a_{13}a_{22} + a_{13}s)}{D} \\ \frac{b_{32}(a_{11}a_{23} - a_{13}a_{21} + a_{23}s)}{D} \\ \frac{b_{32}(a_{11}a_{22} + a_{12}a_{21} + a_{11}s + a_{22}s + s^2)}{D} \\ \frac{b_{32}(a_{11}a_{23}a_{42} + a_{12}a_{23}a_{41} - a_{13}a_{21}a_{42} + a_{13}a_{22}a_{41} + a_{13}a_{41}s + a_{23}a_{42}s)}{(s+1)D} \end{array} \right. \\
& \left. \begin{array}{l} \frac{-b_{23}(a_{13}a_{32} - a_{12}s)}{D} \\ \frac{b_{23}(s^2 + a_{11}s + a_{13}a_{31})}{D} \\ \frac{-b_{23}(a_{11}a_{32} + a_{12}a_{31} + a_{32}s)}{D} \\ \frac{b_{23}(a_{42}s^2 + a_{13}a_{31}a_{42} - a_{13}a_{32}a_{41} + a_{11}a_{42}s + a_{12}a_{41}s)}{(s+1)D} \end{array} \right] \quad (139)
\end{aligned}$$

Defining  $g_{31}$  and  $g_{41}$  as described in (140):

$$\begin{aligned}
g_{31} &= \frac{-b_{11}(a_{23}a_{31} - a_{21}a_{32} + a_{31}s)}{D} - \frac{b_{21}(a_{11}a_{32} - a_{12}a_{31} + a_{32}s)}{D} + \\
& \frac{b_{31}(a_{11}a_{22} + a_{12}a_{21} + a_{11}s + a_{22}s + s^2)}{D} \\
g_{41} &= \frac{b_{11}(a_{41}s^2 - a_{23}a_{31}a_{42} + a_{23}a_{32}a_{41} - a_{21}a_{42}s + a_{22}a_{41}s)}{(s+1)D} + \\
& \frac{b_{21}(a_{42}s^2 + a_{13}a_{31}a_{42} - a_{13}a_{32}a_{41} + a_{11}a_{42}s + a_{12}a_{41}s)}{(s+1)D} + \\
& \frac{b_{31}(a_{11}a_{23}a_{42} + a_{12}a_{23}a_{41} - a_{13}a_{21}a_{42} + a_{13}a_{22}a_{41} + a_{13}a_{41}s + a_{23}a_{42}s)}{(s+1)D} + \frac{b_{41}}{(s+1)} \quad (140)
\end{aligned}$$

In order to simulate the process, the next input parameter values are taken into account:  $F=0.1 \text{ m}^3 \cdot \text{s}^{-1}$ ,  $C_{G0}=1 \text{ mol} \cdot \text{m}^{-3}$ ,  $C_{R0}=1 \text{ mol} \cdot \text{m}^{-3}$ ,  $k_I=0.32 \text{ h}^{-1}$ ,  $k_2=0.49 \text{ h}^{-1}$ ,  $k_3=0.27 \text{ h}^{-1}$ ,  $V=1 \text{ m}^3$ ,  $R=0.2 \text{ mol} \cdot \text{m}^{-3}$ ,  $G=0.3 \text{ mol} \cdot \text{m}^{-3}$ ,  $A=0.5 \text{ mol} \cdot \text{m}^{-3}$ ,  $K=0.2 \text{ mol} \cdot \text{m}^{-3}$ . As a result, the respective transfer functions are given by the following set of equations:

From input  $u_1=F$  to output

$$y_1=A : G(s) = \frac{-1.6667s^3 - 11.49s^2 - 12.2919s - 2.4619}{s^4 + 7.39s^3 + 15.8504s^2 + 12.8288s + 3.3684} \quad (141)$$

$$y_2=R : G(s) = \frac{4s^3 + 16.61s^2 + 18.8436s + 6.2336}{s^4 + 7.39s^3 + 15.8504s^2 + 12.8288s + 3.3684} \quad (142)$$

$$y_3=G : G(s) = \frac{2.3333s^3 + 12.2833s^2 + 20.7807s + 10.8307}{s^4 + 7.39s^3 + 15.8504s^2 + 12.8288s + 3.3684} \quad (143)$$

$$y_4=K : G(s) = \frac{-0.6667s^3 + 0.64s^2 + 4.656s + 5.2533}{s^4 + 7.39s^3 + 15.8504s^2 + 12.8288s + 3.3684} \quad (144)$$

from input  $u_2=C_{G0}$  to output

$$y_1=A : G(s) = \frac{0.6400s^2 + 2.5088s + 1.8688}{s^4 + 7.39s^3 + 15.8504s^2 + 12.8288s + 3.3684} \quad (145)$$

$$y_2=R :G(s) = \frac{0.9600s^2+1.9200s+0.96}{s^4+7.39s^3+15.8504s^2+12.8288s+3.3684} \quad (146)$$

$$y_3=G :G(s) = \frac{1s^3+7.39s^2+13.6616s+7.2716}{s^4+7.39s^3+15.8504s^2+12.8288s+3.3684} \quad (147)$$

$$y_4=K :G(s) = \frac{2.1952s+3.3994}{s^4+7.39s^3+15.8504s^2+12.8288s+3.3684} \quad (148)$$

from input  $u_3=C_{R0}$  to output

$$y_1=A :G(s) = \frac{-0.9933s^2-2.0429s-1.0496}{s^4+7.39s^3+15.8504s^2+12.8288s+3.3684} \quad (149)$$

$$y_2=R :G(s) = \frac{s^3+2.98s^2+2.5944s+0.6144}{s^4+7.39s^3+15.8504s^2+12.8288s+3.3684} \quad (150)$$

$$y_3=G :G(s) = \frac{-1.64s^2-3.9336s-2.2936}{s^4+7.39s^3+15.8504s^2+12.8288s+3.3684} \quad (151)$$

$$y_4=K :G(s) = \frac{1.6333s^2+2.2605s-0.0251}{s^4+7.39s^3+15.8504s^2+12.8288s+3.3684} \quad (152)$$

In order to express equations (141) to (152) in the time domain we perform partial fraction expansion followed by the application of inverse Laplace Transform. Firstly, the partial fraction expansion leads to:

input  $u_1=F$

$$Y_1(s) = \frac{0.723}{s+4.4235} - \frac{3.0361}{s+1.4364} + \frac{0.6464}{s+0.5301} \quad (153)$$

$$Y_2(s) = \frac{2.4697}{s+4.4235} + \frac{1.3396}{s+1.4364} + \frac{0.1907}{s+0.5301} \quad (154)$$

$$Y_3(s) = \frac{1.0725}{s+4.4235} - \frac{0.4997}{s+1.4364} + \frac{1.7604}{s+0.5301} \quad (155)$$

$$Y_4(s) = -\frac{1.3854}{s+4.4235} + \frac{1.8044}{s+1.4364} - \frac{3.0969}{s+1} + \frac{2.0111}{s+0.5301} \quad (156)$$

input  $u_2=C_{G0}$

$$Y_1(s) = -\frac{0.0827}{s+4.4235} - \frac{0.3507}{s+1.4364} + \frac{0.4335}{s+0.5301} \quad (157)$$

$$Y_2(s) = -\frac{0.2826}{s+4.4235} + \frac{0.1548}{s+1.4364} + \frac{0.1278}{s+0.5301} \quad (158)$$

$$Y_3(s) = -\frac{0.1227}{s+4.4235} - \frac{0.0577}{s+1.4364} + \frac{1.1804}{s+0.5301} \quad (159)$$

$$Y_4(s) = \frac{0.1585}{s+4.4235} + \frac{0.2084}{s+1.4364} - \frac{1.7154}{s+1} + \frac{1.3485}{s+0.5301} \quad (160)$$

input  $u_3=C_{R0}$

$$Y_1(s) = \frac{0.2876}{s+4.4235} - \frac{0.1393}{s+1.4364} - \frac{0.1482}{s+0.5301} \quad (161)$$

$$Y_2(s) = \frac{0.9822}{s+4.4235} + \frac{0.0615}{s+1.4364} - \frac{0.0437}{s+0.5301} \quad (162)$$

$$Y_3(s) = \frac{0.4266}{s+4.4235} - \frac{0.0229}{s+1.4364} - \frac{0.4036}{s+0.5301} \quad (163)$$

$$Y_4(s) = -\frac{0.5509}{s+4.4235} + \frac{0.0828}{s+1.4364} + \frac{0.9292}{s+1} - \frac{0.4611}{s+0.5301} \quad (164)$$

Finally, the inverse Laplace transformation leads to equations (165) to (176)

input  $u_1=F$

$$y_1(t) = 0.723e^{-4.4235t} - 3.0361e^{-1.4364t} + 0.6464e^{-0.5301t} \quad (165)$$

$$y_2(t) = 2.4697e^{-4.4235t} + 1.3396e^{-1.4364t} + 0.1907e^{-0.5301t} \quad (166)$$

$$y_3(t) = 1.0725e^{-4.4235t} - 0.4997e^{-1.4364t} + 1.7604e^{-0.5301t} \quad (167)$$

$$y_4(t) = -1.3854e^{-4.423t} + 1.8044e^{-1.436t} - 3.0969e^{-t} + 2.0111e^{-0.53t} \quad (168)$$

input  $u_2=C_{G0}$ :

$$y_1(t) = 0.0827e^{-4.4235t} - 0.3507e^{-1.4364t} + 0.4335e^{-0.5301t} \quad (169)$$

$$y_2(t) = -0.2826e^{-4.4235t} + 0.1548e^{-1.4364t} + 0.1278e^{-0.5301t} \quad (170)$$

$$y_3(t) = -0.1227e^{-4.4235t} - 0.0577e^{-1.4364t} + 1.1804e^{-0.5301t} \quad (171)$$

$$y_4(t) = 0.1585e^{-4.423t} + 0.2084e^{-1.436t} - 1.7154e^{-t} + 1.3485e^{-0.5301t} \quad (172)$$

input  $u_3=C_{R0}$ :

$$y_1(t) = 0.2876e^{-4.4235t} - 0.1393e^{-1.4364t} - 0.1482e^{-0.5301t} \quad (173)$$

$$y_2(t) = 0.98226e^{-4.4235t} + 0.0615e^{-1.4364t} - 0.0437e^{-0.5301t} \quad (174)$$

$$y_3(t) = 0.4266e^{-4.4235t} - 0.0229e^{-1.4364t} - 0.4036e^{-0.5301t} \quad (175)$$

$$y_4(t) = -0.550e^{-4.4235t} + 0.082e^{-1.4364t} + 0.929e^{-t} - 0.461e^{-0.5301t} \quad (176)$$

The response to a step function for the inputs  $u_1$ ,  $u_2$  and  $u_3$  is presented as an example in Fig. 13, 14 and 15 respectively.

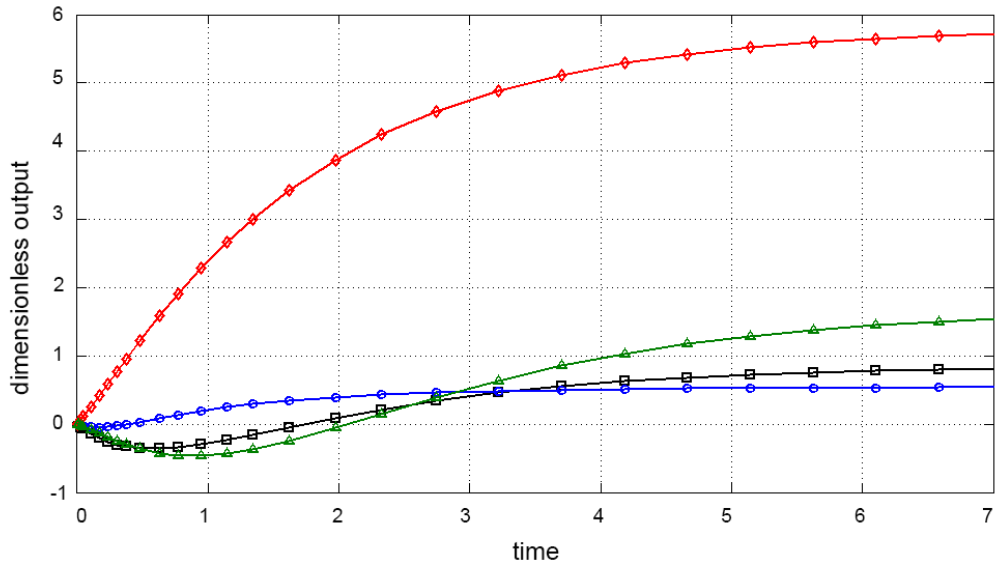


**Fig. 13:** Step response for the system of glycerol oxidation with NO<sub>2</sub>. Input  $u_1=F$  to respective outputs  $y_1=A$  □;  $y_2=R$  ○;  $y_3=G$  ◇;  $y_4=K$  △

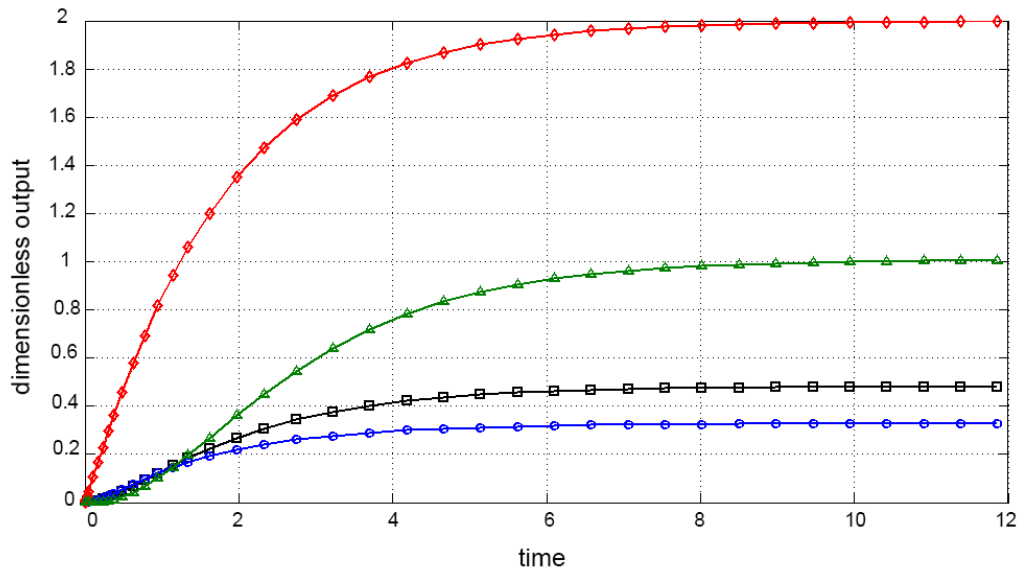


**Fig. 14:** Step response for the system of glycerol oxidation with NO<sub>2</sub>. Input  $u_2=C_{G0}$  to respective outputs  $y_1=A$  □;  $y_2=R$  ○;  $y_3=G$  ◇;  $y_4=K$  △

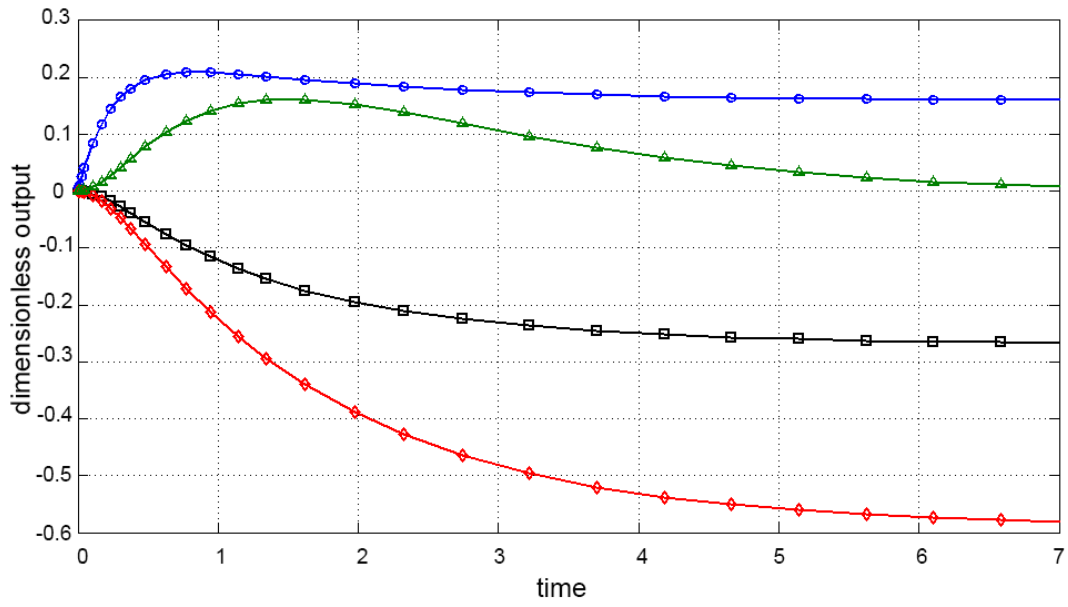


**Fig. 15:** Step response for the system of glycerol oxidation with  $\text{NO}_2$ . Input  $u_3=C_{R0}$  to respective outputs  $y_1=A$  □;  $y_2=R$  ○;  $y_3=G$  ◇;  $y_4=K$  △

## 7 NON-ISOTHERMAL REACTION SYSTEMS

The scheme of a non-isothermal flow reactor depicted in Fig. 16 represents the system under study.

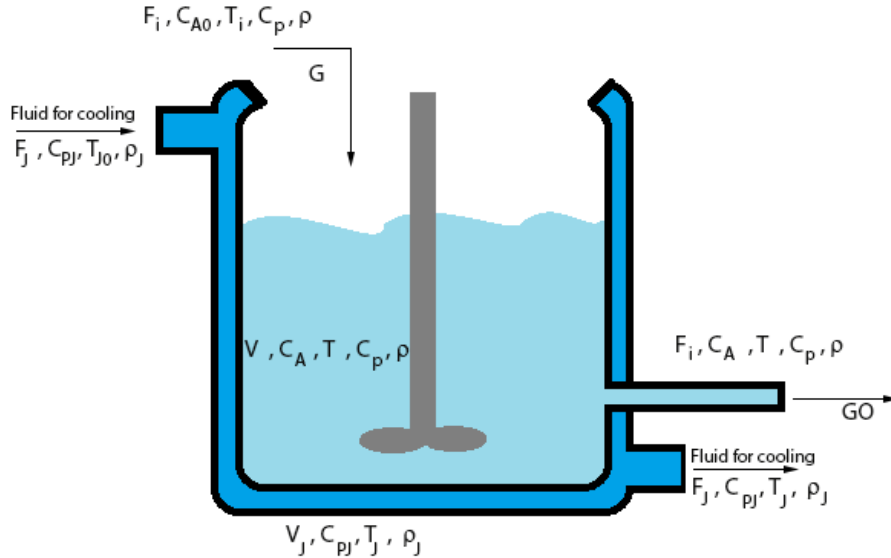


**Fig. 16:** Non-isothermal reaction system for the conversion of glycerol (G) into glycerol oxidation products (GO).

In order to understand the system, it is necessary to perform a material balance in the reactor and an energy balance between the reactor and the heat exchanger. This situation is shown in Fig. 17:

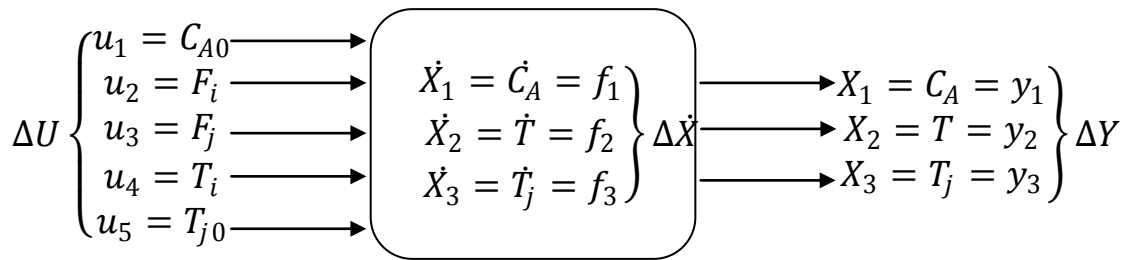


**Fig. 17:** Scheme of the system describing the input, state variable and output.

The concentration of glycerol depends on the conversion into final products as expressed in (177). This means that glycerol concentration changes according to its rate of flow into the system and the conversion into final products

$$V \frac{dC_A}{dt} = F_i(C_{A0} - C_A) - V \cdot k C_A \quad (177)$$

where  $V$  is the volume of the reactor,  $C_A$  is the concentration of glycerol in the reactor and in the output flow (supposing ideal mixing of the reaction blend),  $C_{A0}$  is the initial concentration of glycerol,  $F_i$  is the input flow of glycerol,  $t$  is the reaction time, and  $k$  is the rate constant of disappearance of glycerol. Equation (177) can be also represented as shown in (178)

$$\frac{dC_A}{dt} = \frac{F_i}{V} (C_{A0} - C_A) - kC_A = f_1 \quad (178)$$

Performing an energy balance in the reactor leads to (179)

$$\begin{aligned} & \text{heat accummulated} = \text{input heat} + \text{heat of reaction} - \\ & \text{output heat} - \text{transfer of heat} \end{aligned} \quad (179)$$

For the estimation of the transfer of heat across the boundary of reactor and the heat exchanger, is based on equation (180),

$$V\rho C_p \frac{dT}{dt} = F_i \rho C_p T_i + V \cdot k C_A \Delta H - F_i \rho C_p T - UA(T - T_j) \quad (180)$$

where  $T$  is the temperature of reaction blend in the reactor,  $T_i$  is the inlet temperature of glycerol,  $T_j$  is the mean temperature in the jacket,  $\rho$  is the density,  $C_p$  the specific heat at the reactor temperature, the coolant enters to the heat exchanger at a temperature  $T_{j0}$  and leaves at temperature  $T_j$ .  $U$  is the overall heat transfer coefficient,  $A$  is the area available for heat transfer, and  $\Delta H$  is the heat of reaction

$$\frac{dT}{dt} = \frac{F_i}{V} (T_i - T) + \frac{k}{\rho C_p} C_A \Delta H - \frac{UA}{V\rho C_p} (T - T_j) = f_2 \quad (181)$$

The heat balance for the jacket is based on the equation (154) as expressed in (183) and (184)

$$\begin{aligned} & \text{accumulated heat} = \\ & \text{input heat} - \text{output heat} + \text{transfer of heat} \end{aligned} \quad (182)$$

$$V_j \rho_j C_{p_j} \frac{dT_j}{dt} = F_j \rho_j C_{p_j} T_{j0} - F_j \rho_j C_{p_j} T_j + UA(T - T_j) \quad (183)$$

$$\frac{dT_j}{dt} = \frac{F_j}{V_j} (T_{j0} - T_j) + \frac{UA}{V_j \rho_j C_{p_j}} (T - T_j) = f_3 \quad (184)$$

Considering the state vector as

$$\Delta \dot{X} = \begin{bmatrix} \dot{X}_1 = \dot{C}_A = f_1 \\ \dot{X}_2 = \dot{T} = f_2 \\ \dot{X}_3 = \dot{T}_j = f_3 \end{bmatrix} \quad (185)$$

The system can be represented by the next state space model

$$\begin{aligned} \Delta \dot{X}_{3 \times 1} &= A_{3 \times 3} \Delta X_{3 \times 1} + B_{3 \times 5} \Delta U_{5 \times 1} \\ \Delta Y &= \Delta X \end{aligned} \quad (186)$$

where A is the state matrix of dimension  $3 \times 3$  and B is the control matrix of dimension  $3 \times 5$ . The elements of matrices A are following:

$$a_{11} = \frac{\partial f_1^0}{\partial C_A} = -\left(\frac{F_i^\circ}{V} + k\right); a_{12} = \frac{\partial f_1^0}{\partial T} = 0; a_{13} = \frac{\partial f_1^0}{\partial T_j} = 0 \quad (187)$$

$$a_{21} = \frac{\partial f_2^0}{\partial C_A} = \frac{k\Delta H}{\rho C_p}; a_{22} = \frac{\partial f_2^0}{\partial T} = -\left(\frac{UA}{V\rho C_p} + \frac{F_i^\circ}{V}\right); a_{23} = \frac{\partial f_2^0}{\partial T_j} = \frac{UA}{V\rho C_p}; \quad (188)$$

$$a_{31} = \frac{\partial f_3^0}{\partial C_A} = 0; a_{32} = \frac{\partial f_3^0}{\partial T} = \frac{UA}{V_j\rho_j C_{p_j}}; a_{33} = \frac{\partial f_3^0}{\partial T_j} = -\left(\frac{UA}{V_j\rho_j C_{p_j}} + \frac{F_j^\circ}{V_j}\right) \quad (189)$$

The elements of matrices B are:

$$b_{11} = \frac{\partial f_1^0}{\partial C_{A0}} = \frac{F_i^\circ}{V}; b_{12} = \frac{\partial f_1^0}{\partial F_i} = \frac{C_{A0}^0 - C_A^0}{V}; b_{13} = b_{14} = b_{15} = 0 \quad (190)$$

$$b_{21} = \frac{\partial f_2^0}{\partial C_{A0}} = 0; b_{22} = \frac{\partial f_2^0}{\partial F_i} = \frac{T_i^0 - T^0}{V}; b_{23} = \frac{\partial f_2^0}{\partial F_j} = 0; b_{24} = \frac{\partial f_2^0}{\partial T_i} = \frac{F_i^\circ}{V}; b_{25} = 0 \quad (191)$$

$$b_{31} = \frac{\partial f_3^0}{\partial C_{A0}} = 0; b_{32} = \frac{\partial f_3^0}{\partial F_i} = 0; b_{33} = \frac{\partial f_3^0}{\partial F_j} = \frac{T_{j0}^0 - T_j^0}{V_j}; b_{34} = 0; b_{35} = \frac{\partial f_3^0}{\partial T_{j0}} = \frac{F_j^0}{V_j} \quad (192)$$

Taking into consideration the elements of the previous equations, it follows that:

$$\begin{pmatrix} \frac{d\Delta C_A}{dt} \\ \frac{d\Delta T}{dt} \\ \frac{d\Delta T_j}{dt} \end{pmatrix} = \begin{pmatrix} -\left(\frac{F_i^\circ}{V} + k\right) & 0 & 0 \\ \frac{k\Delta H}{\rho C_p} & -\left(\frac{UA}{V\rho C_p} + \frac{F_i^\circ}{V}\right) & \frac{UA}{V\rho C_p} \\ 0 & \frac{UA}{V_j\rho_j C_{p_j}} & -\left(\frac{UA}{V_j\rho_j C_{p_j}} + \frac{F_j^\circ}{V_j}\right) \end{pmatrix} \begin{pmatrix} \Delta C_A \\ \Delta T \\ \Delta T_j \end{pmatrix} + \begin{pmatrix} \frac{F_i^\circ}{V} & \frac{C_{A0}^0 - C_A^0}{V} & 0 & 0 & 0 \\ 0 & \frac{T_i^0 - T^0}{V} & 0 & \frac{F_i^\circ}{V} & 0 \\ 0 & 0 & \frac{T_{j0}^0 - T_j^0}{V_j} & 0 & \frac{F_j^0}{V_j} \end{pmatrix} \begin{pmatrix} \Delta C_{A0} \\ \Delta F_i \\ \Delta F_j \\ \Delta T_i \\ \Delta T_{j0} \end{pmatrix} \quad (193)$$

Similarly, performing the multiplication, it can be expressed as the next set of equations:

$$\frac{d\Delta C_A}{dt} = -\left(\frac{F_i^\circ}{V} + k\right)\Delta C_A + \frac{F_i^\circ}{V}\Delta C_{A0} + \frac{C_{A0}^0 - C_A^0}{V}\Delta F_i \quad (194)$$

$$\frac{d\Delta T}{dt} = \frac{k\Delta H}{\rho C_p}\Delta C_A - \left(\frac{UA}{V\rho C_p} + \frac{F_i^\circ}{V}\right)\Delta T + \frac{UA}{V\rho C_p}\Delta T_j + \frac{T_i^0 - T^0}{V}\Delta F_i + \frac{F_i^\circ}{V}\Delta T_i \quad (195)$$

$$\frac{d\Delta T_j}{dt} = \frac{UA}{V_j \rho_j c_{pj}} \Delta T - \left( \frac{UA}{V_j \rho_j c_{pj}} + \frac{F_j^\circ}{V_j} \right) \Delta T_j + \frac{T_{j0}^0 - T_j^0}{V_j} \Delta F_j + \frac{F_j^0}{V_j} \Delta T_{j0} \quad (196)$$

For control purpose, it is necessary to introduce the following dimensionless dependences, represented with [\*]:

$$\begin{aligned} \Delta C_A^* &= \frac{\Delta C_A}{C_A^0}; \quad \Delta C_{A0}^* = \frac{\Delta C_{A0}}{C_A^0}; \quad \Delta F_i^* = \frac{\Delta F_i}{F_i^0}; \quad \Delta F_j^* = \frac{\Delta F_j}{F_i^0}; \quad \Delta T^* = \frac{\Delta T}{T^0}; \quad \Delta T_i^* = \frac{\Delta T_i}{T^0}; \\ \Delta T_j^* &= \frac{\Delta T_j}{T^0}; \quad \Delta T_{j0}^* = \frac{\Delta T_{j0}}{T^0} \end{aligned} \quad (197)$$

The implementation of the above dimensionless relations, followed by proper arrangement gives:

$$\frac{d\Delta C_A^* C_A^0}{dt} = - \left( \frac{F_i^\circ}{V} + k \right) \Delta C_A^* C_A^0 + \frac{F_i^\circ}{V} \Delta C_{A0}^* C_A^0 + \frac{C_{A0}^0 - C_A^0}{V} \Delta F_i^* F_i^0 \quad (198)$$

$$\begin{aligned} \frac{d\Delta T^* T^0}{dt} &= \frac{k\Delta H}{\rho c_p} \Delta C_A^* C_A^0 - \left( \frac{UA}{V \rho c_p} + \frac{F_i^\circ}{V} \right) \Delta T^* T^0 + \frac{UA}{V \rho c_p} \Delta T_j^* T^0 + \\ &\frac{T_i^0 - T^0}{V} \Delta F_i^* F_i^0 + \frac{F_i^\circ}{V} \Delta T_i^* T^0 \end{aligned} \quad (199)$$

$$\begin{aligned} \frac{d\Delta T_j^* T^0}{dt} &= \frac{UA}{V_j \rho_j c_{pj}} \Delta T^* T^0 - \left( \frac{UA}{V_j \rho_j c_{pj}} + \frac{F_j^\circ}{V_j} \right) \Delta T_j^* T^0 + \frac{T_{j0}^0 - T_j^0}{V_j} \Delta F_j^* F_i^0 + \\ &\frac{F_j^0}{V_j} \Delta T_{j0}^* T^0 \end{aligned} \quad (200)$$

Multiplying equation (198) by  $V/F_i^0 C_A^0$

$$\frac{d\Delta C_A^*}{dt^*} = - \left( \frac{F_i^\circ}{V} + k \right) \Delta C_A^* \frac{V}{F_i^0} + \Delta C_{A0}^* + \frac{C_{A0}^0 - C_A^0}{C_A^0} \Delta F_i^* \quad (201)$$

$$\frac{d\Delta C_A^*}{dt^*} = - \left( 1 + k \frac{V}{F_i^0} \right) \Delta C_A^* + \Delta C_{A0}^* + \frac{C_{A0}^0 - C_A^0}{C_A^0} \Delta F_i^* \quad (202)$$

Multiplying equations (199) and (200) by  $V/F_i^0 T^0$

$$\begin{aligned} \frac{d\Delta T^*}{dt^*} &= \frac{k\Delta H C_A^0 V}{\rho c_p F_i^0 T^0} \Delta C_A^* - \left( \frac{UA}{\rho c_p F_i^0} + 1 \right) \Delta T^* + \frac{UA}{F_i^0 \rho c_p} \Delta T_j^* + \frac{(T_i^0 - T^0)}{T^0} \Delta F_i^* + \\ &\Delta T_i^* \end{aligned} \quad (203)$$

$$\begin{aligned} \frac{d\Delta T_j^*}{dt} &= \frac{UAV}{V_j \rho_j c_{pj} F_i^0} \Delta T^* - \left( \frac{UAV}{V_j \rho_j c_{pj} F_i^0} + \frac{F_j^\circ V}{V_j F_i^0} \right) \Delta T_j^* + \frac{V(T_{j0}^0 - T_j^0)}{T^0 V_j} \Delta F_j^* + \\ &\frac{V F_j^0}{F_i^0 V_j} \Delta T_{j0}^* \end{aligned} \quad (204)$$

where the term  $t^* = (t F_i^0 / V)$  implies a dimensionless parameter (dimensionless time). As a result, the system represented in (193) transforms into (205)

$$\begin{pmatrix} \dot{C}_A^* \\ \Delta \dot{T}^* \\ \Delta \dot{T}_j^* \end{pmatrix} = \begin{pmatrix} -\left(1 + k \frac{V}{F_i^0}\right) & 0 & 0 \\ \frac{k\Delta H C_A^0 V}{\rho C_p F_i^0 T^0} & -\left(\frac{UA}{\rho C_p F_i^0} + 1\right) & \frac{UA}{F_i^0 \rho C_p} \\ 0 & \frac{UAV}{V_j \rho_j C_{p_j} F_i^0} & -\left(\frac{UAV}{V_j \rho_j C_{p_j} F_i^0} + \frac{F_j^0 V}{V_j F_i^0}\right) \end{pmatrix} \begin{pmatrix} \Delta C_A^* \\ \Delta T^* \\ \Delta T_j^* \end{pmatrix} + \begin{pmatrix} 1 & \frac{C_{A0}^0 - C_A^0}{C_A^0} & 0 & 0 \\ 0 & \frac{(T_i^0 - T^0)}{T^0} & 0 & 1 \\ 0 & 0 & \frac{V(T_{j0}^0 - T_j^0)}{T^0 V_j} & 0 \end{pmatrix} \begin{pmatrix} \Delta C_{A0}^* \\ \Delta F_i^* \\ \Delta F_j^* \\ \Delta T_i^* \\ \Delta T_{j0}^* \end{pmatrix} \quad (205)$$

In order to obtain the transfer function, it is necessary to consider that  $G(s) = (sI - A)^{-1}B$ ,

$$(sI - A) = \begin{bmatrix} s + \left(1 + k \frac{V}{F_i^0}\right) & 0 & 0 \\ -\frac{k\Delta H C_A^0 V}{\rho C_p F_i^0 T^0} & s + \left(\frac{UA}{\rho C_p F_i^0} + 1\right) & -\frac{UA}{F_i^0 \rho C_p} \\ 0 & -\frac{UAV}{V_j \rho_j C_{p_j} F_i^0} & s + \left(\frac{UAV}{V_j \rho_j C_{p_j} F_i^0} + \frac{F_j^0 V}{V_j F_i^0}\right) \end{bmatrix} \quad (206)$$

Defining the next elements of the matrix  $A$

$$a_{11}^* = \left(1 + k \frac{V}{F_i^0}\right) \quad (207)$$

$$a_{21}^* = \frac{k\Delta H C_A^0 V}{\rho C_p F_i^0 T^0}; \quad a_{22}^* = \left(\frac{UA}{\rho C_p F_i^0} + 1\right); \quad a_{23}^* = a_{22} - 1 \quad (208)$$

$$a_{32}^* = \frac{UAV}{V_j \rho_j C_{p_j} F_i^0}; \quad a_{33}^* = \left(\frac{UAV}{V_j \rho_j C_{p_j} F_i^0} + \frac{F_j^0 V}{V_j F_i^0}\right) \quad (209)$$

$$b_{12}^* = \frac{C_{A0}^0 - C_A^0}{C_A^0} \quad (210)$$

$$b_{22}^* = \frac{(T_i^0 - T^0)}{T^0} \quad (211)$$

$$b_{33}^* = \frac{V(T_{j0}^0 - T_j^0)}{T^0 V_j}; \quad b_{35}^* = \frac{V F_j^0}{F_i^0 V_j} \quad (212)$$

The value of  $(sI - A)^{-1}$  becomes

$$(sI - A)^{-1} = \begin{bmatrix} \frac{1}{a_{11}^* + s} & 0 & 0 \\ \frac{a_{21}^*(a_{33}^* + s)}{(d)} & \frac{(a_{33}^* + s)}{a_{22}^* a_{33}^* - a_{23}^* a_{32}^* + a_{22}^* s + a_{33}^* s + s^2} & \frac{(a_{23}^*)}{a_{22}^* a_{33}^* - a_{23}^* a_{32}^* + a_{22}^* s + a_{33}^* s + s^2} \\ \frac{a_{21}^* a_{32}^*}{(d)} & \frac{a_{32}^*}{a_{22}^* a_{33}^* - a_{23}^* a_{32}^* + a_{22}^* s + a_{33}^* s + s^2} & \frac{(a_{22}^* + s)}{a_{22}^* a_{33}^* - a_{23}^* a_{32}^* + a_{22}^* s + a_{33}^* s + s^2} \end{bmatrix} \quad (213)$$

where:

$$d = a_{11}^*s^2 + a_{22}^*s^2 + a_{33}^*s^2 + s^3 + a_{11}^*a_{22}^*a_{33}^* - a_{11}^*a_{23}^*a_{32}^* + a_{11}^*a_{22}^*s + a_{11}^*a_{33}^*s + a_{22}^*a_{33}^*s - a_{23}^*a_{32}^*s \quad (214)$$

As a result, in order to calculate the transfer function  $G(s)$ :

$$G(s) = \begin{bmatrix} \frac{1}{a_{11}^*+s} & 0 & 0 \\ \frac{a_{21}^*(a_{33}^*+s)}{(d)} & \frac{(a_{33}^*+s)}{a_{22}^*a_{33}^*-a_{23}^*a_{32}^*+a_{22}^*s+a_{33}^*s+s^2} & \frac{(a_{23}^*)}{a_{22}^*a_{33}^*-a_{23}^*a_{32}^*+a_{22}^*s+a_{33}^*s+s^2} \\ \frac{a_{21}^*a_{32}^*}{(d)} & \frac{a_{32}^*}{a_{22}^*a_{33}^*-a_{23}^*a_{32}^*+a_{22}^*s+a_{33}^*s+s^2} & \frac{(a_{22}^*+s)}{a_{22}^*a_{33}^*-a_{23}^*a_{32}^*+a_{22}^*s+a_{33}^*s+s^2} \end{bmatrix} \begin{pmatrix} 1 & b_{12}^* & 0 & 0 & 0 \\ 0 & b_{22}^* & 0 & 1 & 0 \\ 0 & 0 & b_{33}^* & 0 & b_{35}^* \end{pmatrix} \quad (215)$$

$$G(s) = \begin{bmatrix} g_{11} & g_{12} & 0 & 0 & 0 \\ g_{21} & g_{22} & g_{23} & g_{24} & g_{25} \\ g_{31} & g_{32} & g_{33} & 0 & g_{35} \end{bmatrix} \quad (216)$$

where the elements of the matrix  $G(s)$  are given by:

$$g_{11} = \frac{1}{a_{11}^*+s}; g_{12} = \frac{b_{12}^*}{a_{11}^*+s} \quad (217)$$

$$g_{21} = \frac{a_{21}^*(a_{33}^*+s)}{d}; g_{22} = \frac{b_{22}^*(a_{33}^*+s)}{a_{22}^*a_{33}^*-a_{23}^*a_{32}^*+a_{22}^*s+a_{33}^*s+s^2} + \frac{a_{21}^*b_{12}^*(a_{33}^*+s)}{d}; \quad (218)$$

$$g_{23} = \frac{(a_{23}^*b_{33}^*)}{a_{22}^*a_{33}^*-a_{23}^*a_{32}^*+a_{22}^*s+a_{33}^*s+s^2}; g_{24} = \frac{(a_{33}^*+s)}{a_{22}^*a_{33}^*-a_{23}^*a_{32}^*+a_{22}^*s+a_{33}^*s+s^2}; \quad (219)$$

$$g_{25} = \frac{(a_{23}^*)b_{35}^*}{a_{22}^*a_{33}^*-a_{23}^*a_{32}^*+a_{22}^*s+a_{33}^*s+s^2}$$

$$g_{31} = \frac{a_{21}^*a_{32}^*}{d}; g_{32} = \frac{a_{32}^*b_{22}^*}{a_{22}^*a_{33}^*-a_{23}^*a_{32}^*+a_{22}^*s+a_{33}^*s+s^2} + \frac{a_{21}^*a_{32}^*b_{12}^*}{d}; \quad (220)$$

$$g_{33} = \frac{(a_{22}^*+s)b_{33}^*}{a_{22}^*a_{33}^*-a_{23}^*a_{32}^*+a_{22}^*s+a_{33}^*s+s^2}; g_{34} = \frac{a_{32}^*}{a_{22}^*a_{33}^*-a_{23}^*a_{32}^*+a_{22}^*s+a_{33}^*s+s^2};$$

$$g_{35} = \frac{(a_{22}^*+s)b_{35}^*}{a_{22}^*a_{33}^*-a_{23}^*a_{32}^*+a_{22}^*s+a_{33}^*s+s^2}$$

In order to simulate the process, the next parameter values are considered:  $C_{A0}=1 \text{ mol}\cdot\text{m}^{-3}$ ,  $F_i=0.1 \text{ m}^3\cdot\text{s}^{-1}$ ,  $F_j=0.1 \text{ m}^3\cdot\text{s}^{-1}$ ,  $T_i= 333 \text{ K}$ ,  $T_{j0}= 298 \text{ K}$ ,  $K=0.2 \text{ mol}\cdot\text{m}^{-3}$ .  $V=1 \text{ m}^3$ ,  $\Delta H=2.4 \times 10^6 \text{ J}\cdot\text{kg}^{-1}$ ,  $\rho = 1000 \text{ kg}\cdot\text{m}^{-3}$ ,  $C_p = 4200 \text{ J}\cdot\text{kg}^{-1}\cdot\text{K}^{-1}$ ,  $U= 900 \text{ W}\cdot\text{m}^{-2}\cdot\text{K}^{-1}$ ,  $A = 10 \text{ m}^2$ ,  $V_j = 0.1 \text{ m}^3$ ,  $\rho_j = 1000 \text{ kg}\cdot\text{m}^{-3}$ , and  $C_{pj} = 4200 \text{ J}\cdot\text{kg}^{-1}\cdot\text{K}^{-1}$ ,

The respective transfer functions can be also expressed as the following set of equations:

From input  $u_1=C_{A0}$  to output:

$$y_1=C_A : G(s) = \frac{1s^2-9.7643s-0.2051}{s^3-6.7643s^2-29.498s-0.6153} \quad (221)$$

$$y_2=T : G(s) = \frac{0.0018s-0.0178}{s^3-6.7643s^2-29.498s-0.6153} \quad (222)$$

$$y_3=T_j : G(s) = \frac{-0.0004}{s^3-6.7643s^2-29.498s-0.6153} \quad (223)$$

From input  $u_2=F_i$  to output:

$$y_1=C_A : \quad G(s) = \frac{1s^2-9.7643s-0.2051}{s^3-6.7643s^2-29.498s-0.6153} \quad (224)$$

$$y_2=T : \quad G(s) = \frac{0.0571s^2-0.3859s-1.6953}{s^3-6.7643s^2-29.498s-0.6153} \quad (225)$$

$$y_3=T_j : \quad G(s) = \frac{-0.0122s-0.0371}{s^3-6.7643s^2-29.498s-0.6153} \quad (226)$$

From input  $u_3=F_j$  to output:

$$y_2=T : \quad G(s) = \frac{-0.0048s-0.0143}{s^3-6.7643s^2-29.498s-0.6153} \quad (227)$$

$$y_3=T_j : \quad G(s) = \frac{0.2222s^2-0.6714s-0.0143}{s^3-6.7643s^2-29.498s-0.6153} \quad (228)$$

From input  $u_4=T_i$  to output:

$$y_2=T : \quad G(s) = \frac{1s^2-6.7857s-29.3571}{s^3-6.7643s^2-29.498s-0.6153} \quad (229)$$

$$y_3=T_j : \quad G(s) = \frac{-0.2143s-0.6429}{s^3-6.7643s^2-29.498s-0.6153} \quad (230)$$

From input  $u_5=T_{j0}$  to output:

$$y_2=T : \quad G(s) = \frac{0.2143s+0.6429}{s^3-6.7643s^2-29.498s-0.6153} \quad (231)$$

$$y_3=T_j : \quad G(s) = \frac{10s^2+30.2143s+0.6429}{s^3-6.7643s^2-29.498s-0.6153} \quad (232)$$

## 8 A SIMPLIFIED MODEL FOR THE OXIDATION OF GLYCEROL INTO GLYCERALDEHYDE AND THE DETERMINATION OF TRANSFER FUNCTION

A linear state mathematical model including input, output and inner-state variables for the oxidation of glycerol into glyceraldehyde is proposed next to describe the final stage in the process of glycerol anodic oxidation. In this model, the heat transfer between the coolant and the reactor can be determined using the enthalpy values of the oxidation reaction, the mass flow input of glycerol, the volume flow rate as well as the mass fraction of pure glycerin in the mass flow and the input temperature of coolant as input parameters. The diagram of the system is presented in Fig. 18. The analog nonlinear system is described in equations (233) and (234)

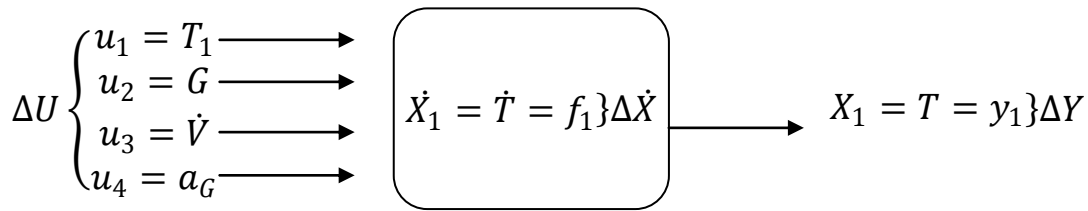


**Fig. 18:** Scheme of the system describing the input, state variable and output.

$$\dot{X} = F(X, U) \quad (233)$$

$$Y = G(X, U) \quad (234)$$

In the previous equations,  $X$  represents the state vector,  $U$  the input vector,  $Y$  the output vector,  $F$  and  $G$  are vectors functions and  $\dot{X}$  is time derivative of state variables as showed in (235)

$$\dot{X} = \frac{dX}{dt} \quad (235)$$

The scheme of the reactor configuration is presented in Fig. 19 and the balance of energy for the oxidation of glycerol into glyceraldehyde is presented in equation (236)

$$G\Delta H_r^0 a_G + \rho_1 \dot{V} T_1 c_p = \dot{V} \rho_2 c_p T + \rho_2 c_p V \frac{dT}{dt} \quad (236)$$

where  $G$  is the mass flow input of dilute glycerin ( $\text{kg}\cdot\text{s}^{-1}$ ),  $\Delta H_r^0$  is the enthalpy of the oxidation reaction of glycerol to glyceraldehyde ( $\text{J}\cdot\text{kg}^{-1}$ ),  $a_G$  the mass fraction of pure glycerin in the mass flow,  $\rho$  is the density ( $\text{kg}\cdot\text{m}^{-3}$ ),  $\dot{V}$  the volume flow rate ( $\text{m}^3\cdot\text{s}^{-1}$ ),  $T_1$  and  $T$  the input and output temperature of the cooling water ( $^\circ\text{C}$ ) respectively,  $C_p$  is the specific heat ( $\text{J}\cdot[^\circ\text{C}\cdot\text{kg}]^{-1}$ ),  $V$  the

volume of reactor ( $\text{m}^3$ ) and  $t$  the time (s). Assuming no variation of density, the equation is solved and presented in equations (237) to (251) for determination of reaction temperature.

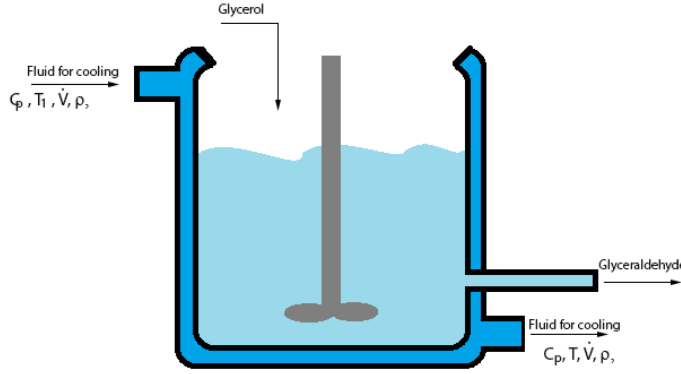


**Fig. 19:** Scheme of chemical reactor for anodic oxidation of glycerol in which glyceraldehyde is the main product.

$$\rho_1 = \rho_2 = \rho \quad (237)$$

$$\frac{dT}{dt} = \frac{a_G(\Delta H)_r^0 G}{\rho c_p V} + \frac{\dot{V}}{V} (T_1 - T) \quad (238)$$

$$\frac{dT}{dt} = \frac{a_G(\Delta H)_r^0 G + \rho c_p \dot{V} (T_1 - T)}{\rho c_p V} \quad (239)$$

$$\int \frac{\rho c_p V dT}{a_G(\Delta H)_r^0 G + \rho c_p \dot{V} (T_1 - T)} = \int dt \quad (240)$$

$$\rho c_p V \int \frac{dT}{a_G(\Delta H)_r^0 G + \rho c_p \dot{V} (T_1 - T)} = t \quad (241)$$

$$-\rho c_p V \cdot \frac{1}{\rho c_p \dot{V}} \ln |a_G(\Delta H)_r^0 G + \rho c_p \dot{V} (T_1 - T)| + C = t \quad (242)$$

$$-V \cdot \frac{1}{\dot{V}} \ln |a_G(\Delta H)_r^0 G + \rho c_p \dot{V} (T_1 - T)| + C = t \quad (243)$$

For calculation of C: @  $t=0, T=T_1$

$$-V \cdot \frac{1}{\dot{V}} \ln |a_G(\Delta H)_r^0 G + \rho c_p \dot{V} (T_1 - T_1)| + C = 0 \quad (244)$$

$$C = \frac{V}{\dot{V}} \ln |a_G(\Delta H)_r^0 G| \quad (245)$$

Substituting the value of C:

$$-V \cdot \frac{1}{\dot{V}} \ln |a_G(\Delta H)_r^0 G + \rho c_p \dot{V} (T_1 - T)| + \frac{V}{\dot{V}} \ln |a_G(\Delta H)_r^0 G| = t \quad (246)$$

$$-\frac{V}{\dot{V}} \left\{ \ln |a_G(\Delta H)_r^0 G| + \ln \left| 1 + \frac{\rho c_p \dot{V} (T_1 - T)}{a_G(\Delta H)_r^0 G} \right| \right\} + \frac{V}{\dot{V}} \ln |a_G(\Delta H)_r^0 G| = t \quad (247)$$

$$-\frac{V}{\dot{V}} \ln \left| 1 + \frac{\rho c_p \dot{V} (T_1 - T)}{a_G(\Delta H)_r^0 G} \right| = t \quad (248)$$

$$-\frac{t\dot{V}}{V} = \ln \left| 1 + \frac{\rho c_p \dot{V}(T_1 - T)}{a_G(\Delta H)_r^0 G} \right| \quad (249)$$

$$e^{-\frac{t\dot{V}}{V}} = 1 + \frac{\rho c_p \dot{V}(T_1 - T)}{a_G(\Delta H)_r^0 G} \quad (250)$$

$$T = \frac{a_G(\Delta H)_r^0 G}{\rho c_p \dot{V}} \left( 1 - e^{-\frac{t\dot{V}}{V}} \right) + T_1 \quad (251)$$

The profile of temperature in function of time for glycerol oxidation to glyceraldehyde is represented by previous equation (251) and in Fig. 20. Fig. 21 and Fig. 22 express the influence of two parameters ( $a_G$  - time and  $a_G$  – mass flow input of dilute glycerin) on temperature respectively.

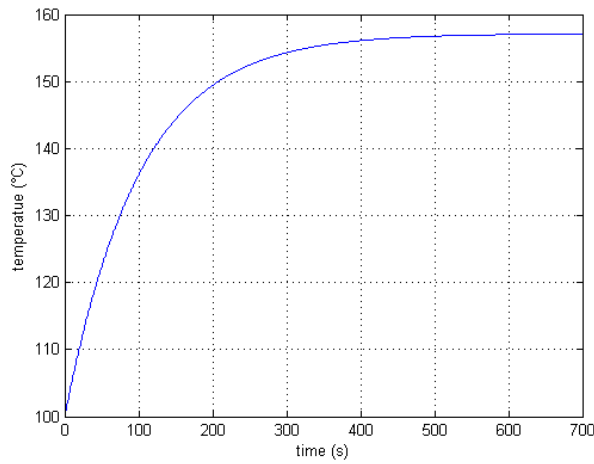


**Fig. 20:** Profile of temperature in function of time for glycerol oxidation to glyceraldehyde.

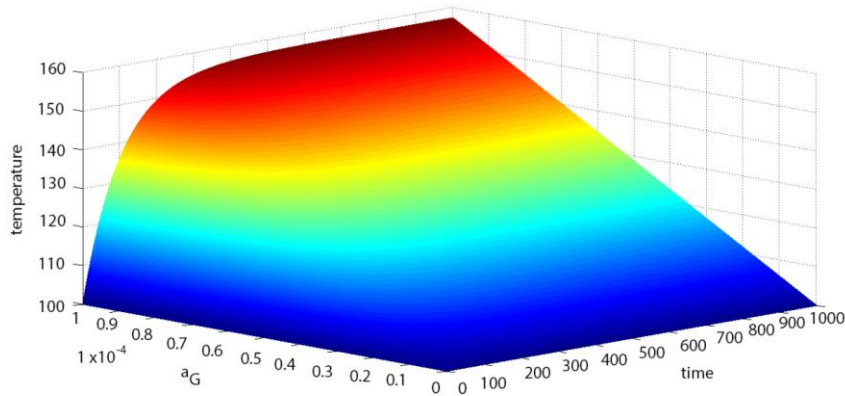


**Fig. 21:** Profile of reaction temperature in function of time and  $a_G$  for glycerol oxidation to glyceraldehyde.

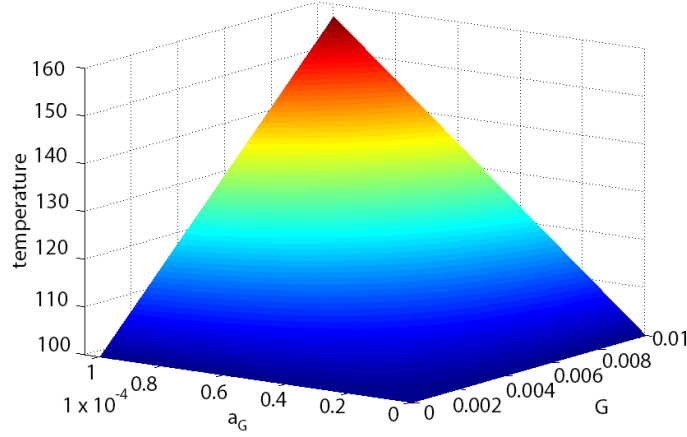


**Fig 22:** Profile of reaction temperature in function of  $a_G$  and mass flow input of glycerol for glycerol oxidation to glyceraldehyde.

This system, as a real system, fulfils the strong physical condition of the feasibility (the outputs are functions only of the state variables). Considering the input variables as  $T_1$ ,  $G$ ,  $\dot{V}$ , and  $a_G$ , and the output variable as  $T$ , the system becomes:

$$\Delta \dot{X}_{1 \times 1} = A \Delta X_{1 \times 1} + B_{1 \times 4} \Delta U_{4 \times 1}, \Delta Y = \Delta X \quad (252)$$

Considering equilibrium:

$$\frac{\partial f^0}{\partial T} = -\frac{\dot{V}^0}{V} = a_{11} \quad (253)$$

$$\frac{\partial f^0}{\partial T_1} = \frac{\dot{V}^0}{V} = b_{11} \quad (254)$$

$$\frac{\partial f^0}{\partial G} = \frac{a_G^0 (\Delta H)_r^0}{\rho c_p V} = b_{12} \quad (255)$$

$$\frac{\partial f^0}{\partial \dot{V}} = \frac{T_1^0 - T^0}{V} = b_{13} \quad (256)$$

$$\frac{\partial f^0}{\partial a_G} = \frac{(\Delta H)_r^0 G^0}{\rho c_p V} = b_{14} \quad (257)$$

$$\Delta T^0 = -\frac{\dot{V}^0}{V} \Delta T + \left[ \frac{\dot{V}^0}{V} \quad \frac{a_G^0 (\Delta H)_r^0}{\rho c_p V} \quad \frac{T_1^0 - T^0}{V} \quad \frac{(\Delta H)_r^0 G^0}{\rho c_p V} \right] \begin{bmatrix} \Delta T_1 \\ \Delta G \\ \Delta \dot{V} \\ \Delta a_G \end{bmatrix} \quad (258)$$

Multiplying we get:

$$\frac{d\Delta T}{dt} = -\frac{\dot{V}^0}{V} \Delta T + \frac{\dot{V}^0}{V} \Delta T_1 + \frac{a_G^0 (\Delta H)_r^0}{\rho c_p V} \Delta G + \frac{T_1^0 - T^0}{V} \Delta \dot{V} + \frac{(\Delta H)_r^0 G^0}{\rho c_p V} \Delta a_G \quad (259)$$

Introducing dimensionless dependencies:

$$\Delta T^* = \frac{\Delta T}{T^0} \quad (260)$$

$$\Delta T_1^* = \frac{\Delta T_1}{T^0} \quad (261)$$

$$\Delta G^* = \frac{\Delta G}{G^0} \quad (262)$$

$$\Delta \dot{V}^* = \frac{\Delta \dot{V}}{\dot{V}^0} \quad (263)$$

$$\Delta a_G^* = \frac{\Delta a_G}{a_G^0} \quad (264)$$

$$\Delta T = \Delta T^* T^0 \quad (265)$$

$$\Delta T_1 = \Delta T_1^* T^0 \quad (266)$$

$$\Delta G = \Delta G^* G^0 \quad (267)$$

$$\Delta \dot{V} = \Delta \dot{V}^* \dot{V}^0 \quad (268)$$

$$\Delta a_G = \Delta a_G^* a_G^0 \quad (269)$$

By substitution of the previous dimensionless dependencies in (259):

$$\begin{aligned} \frac{d(\Delta T^* T^0)}{dt} = & -\frac{V^0}{V} (\Delta T^* T^0) + \frac{V^0}{V} (\Delta T_1^* T^0) + \frac{a_G^0 (\Delta H)_r^0}{\rho c_p V} (\Delta G^* G^0) + \\ & \frac{T_1^0 - T^0}{V} \Delta \dot{V}^* \dot{V}^0 + \frac{(\Delta H)_r^0 G^0}{\rho c_p V} \Delta a_G^* a_G^0 \end{aligned} \quad (270)$$

Multiplying by  $\frac{V}{T^0 \dot{V}^0}$  both sides of the equation

$$\frac{d(\Delta T^*)}{d\left(\frac{t \dot{V}}{V}\right)} = \frac{d(\Delta T^*)}{d(t^*)} = \Delta \dot{T}^* \quad (271)$$

$$\begin{aligned} \Delta \dot{T}^* = & -(\Delta T^*) + (\Delta T_1^*) + \frac{a_G^0 (\Delta H)_r^0}{T^0 \dot{V}^0 \rho c_p} (\Delta G^* G^0) + \frac{T_1^0 - T^0}{T^0} \Delta \dot{V}^* + \\ & \frac{(\Delta H)_r^0 G^0}{T^0 \dot{V}^0 \rho c_p} (\Delta a_G^* a_G^0) \end{aligned} \quad (272)$$

$$\begin{aligned} \Delta \dot{T}^* = & -(\Delta T^*) + (\Delta T_1^*) + \frac{a_G^0 (\Delta H)_r^0}{T^0 \dot{V}^0 \rho c_p} (\Delta G^* G^0) + \frac{T_1^0 - T^0}{T^0} \Delta \dot{V}^* + \\ & \frac{(\Delta H)_r^0 G^0}{T^0 \dot{V}^0 \rho c_p} (\Delta a_G^* a_G^0) \end{aligned} \quad (273)$$

$$\Delta \dot{T}^* = -[\Delta T^*] + \begin{bmatrix} 1 & \frac{a_G^0 (\Delta H)_r^0 G^0}{T^0 \dot{V}^0 \rho c_p} & \frac{T_1^0 - T^0}{T^0} & \frac{(\Delta H)_r^0 G^0 a_G^0}{T^0 \dot{V}^0 \rho c_p} \end{bmatrix} \begin{bmatrix} \Delta T_1^* \\ \Delta G^* \\ \Delta \dot{V}^* \\ \Delta a_G^* \end{bmatrix} \quad (274)$$

$$A^* = [-1] \quad (275)$$

$$B^* = \begin{bmatrix} 1 & \frac{a_G^0 (\Delta H)_r^0 G^0}{T^0 \dot{V}^0 \rho c_p} & \frac{T_1^0 - T^0}{T^0} & \frac{(\Delta H)_r^0 G^0 a_G^0}{T^0 \dot{V}^0 \rho c_p} \end{bmatrix} \quad (276)$$

Taking the Laplace transform:

$$s\Delta X_L = A\Delta X_L + B\Delta U_L \quad (277)$$

$$(s - A)\Delta X_L = B\Delta U_L \quad (278)$$

$$\Delta X_L = \Delta Y_L \quad (279)$$

$$(s - A)\Delta Y_L = B\Delta U_L \quad (280)$$

$$\frac{\Delta Y_L}{\Delta U_L} = (s - A)^{-1}B \quad (281)$$

Equation (281) represents the value of the transfer Function  $G(s)$ . Therefore:

$$\frac{\Delta Y_L}{\Delta U_L} = G(s) = [s + 1]^{-1} \left[ 1 \quad \frac{a_G^0 (\Delta H)_r^0 G^0}{T^0 V^0 \rho c_p} \quad \frac{T_1^0 - T^0}{T^0} \quad \frac{(\Delta H)_r^0 G^0 a_G^0}{T^0 V^0 \rho c_p} \right] \quad (282)$$

$$G(s) = \left( \frac{1}{(s+1)} \quad \frac{a_G^0 (\Delta H)_r^0 G^0}{T^0 V^0 \rho c_p (s+1)} \quad \frac{T_1^0 - T^0}{T^0 (s+1)} \quad \frac{(\Delta H)_r^0 G^0 a_G^0}{T^0 V^0 \rho c_p (s+1)} \right) \quad (283)$$

## 9 ANALYSIS OF THE OXIDATION OF GLYCEROL CONSIDERING CONSECUTIVE REVERSIBLE REACTION

The input-output block diagram of the reaction mechanism represented in Fig. 23, which considers the oxidation of glycerol into five different products considering reversible reactions, is presented in Fig. 24. The input is the initial concentration of glycerol. The state and output variables are considered to be the concentration of glycerol, glyceraldehyde, glyceric acid, glycolic acid, tartronic acid and mesoxalic acid.

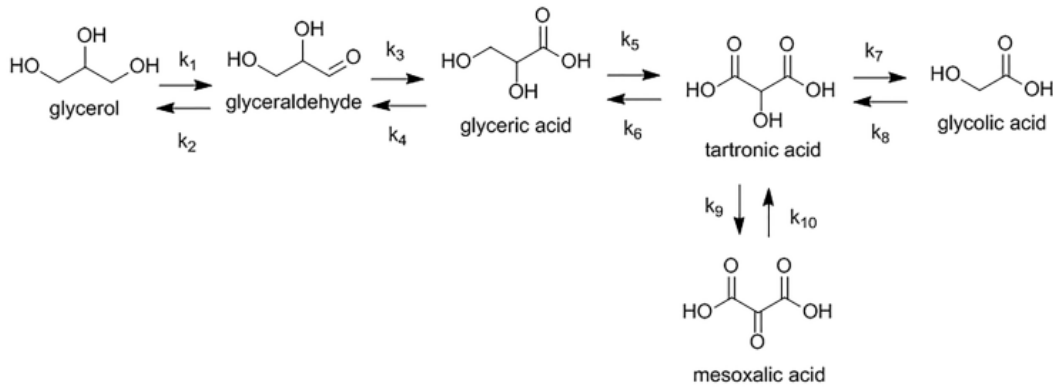


**Fig. 23:** Full mechanism of anodic oxidation with reversible reactions.

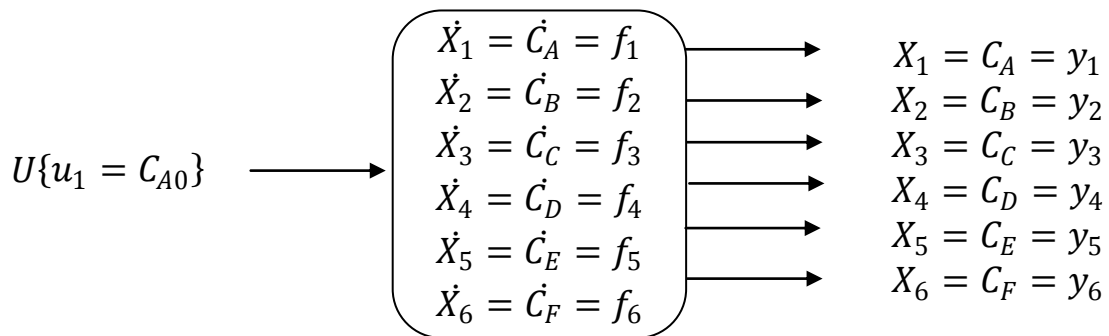


**Fig 24:** Description of the system including the input, state variable and output.

Then, the mechanism can be described by the set of differential equations presented through (284) to (289)

$$dC_A/dt = -k_1C_A + k_2C_B \quad (284)$$

$$dC_B/dt = k_1C_A - k_2C_B - k_3C_B + k_4C_C \quad (285)$$

$$dC_C/dt = k_3C_B - k_4C_C - k_5C_C + k_6C_D \quad (286)$$

$$dC_D/dt = k_5C_C - k_6C_D - k_7C_D + k_8C_E - k_9C_D + k_{10}C_F \quad (287)$$

$$dC_E/dt = k_7C_D - k_8C_E \quad (288)$$

$$dC_F/dt = k_9C_D - k_{10}C_F \quad (289)$$

These equations lead to the vector differential equations shown in (290) to (292). The variables  $C_A$  to  $C_F$  refer to the concentration values for reactant and products (glycerol, glyceraldehyde, glyceric acid, tartronic acid, glycolic acid, and mesoxalic acid respectively). Considering that the input includes a defined initial concentration of glycerol we obtain the system represented in (293):

$$\dot{\mathbf{C}} = \mathbf{A} \cdot \mathbf{C} \quad (290)$$

$$\mathbf{C}(0) = \mathbf{C}_0 \quad (291)$$

$$\begin{pmatrix} \dot{C}_A \\ \dot{C}_B \\ \dot{C}_C \\ \dot{C}_D \\ \dot{C}_E \\ \dot{C}_F \end{pmatrix} = \begin{pmatrix} -k_1 & k_2 & 0 & 0 & 0 & 0 \\ k_1 & -(k_2+k_3) & k_4 & 0 & 0 & 0 \\ 0 & k_3 & -(k_4+k_5) & k_6 & 0 & 0 \\ 0 & 0 & k_5 & -(k_6+k_7+k_9) & k_8 & k_{10} \\ 0 & 0 & 0 & k_7 & -k_8 & 0 \\ 0 & 0 & 0 & k_9 & 0 & -k_{10} \end{pmatrix} \begin{pmatrix} C_A \\ C_B \\ C_C \\ C_D \\ C_E \\ C_F \end{pmatrix} \quad (292)$$

$$\begin{pmatrix} C_A(0) \\ C_B(0) \\ C_C(0) \\ C_D(0) \\ C_E(0) \\ C_F(0) \end{pmatrix} = \begin{pmatrix} C_{A0} \\ 0 \\ 0 \\ 0 \\ 0 \\ 0 \end{pmatrix} \quad (293)$$

Equations (292) and (293) are considered to obtain the system represented in (294)

$$\begin{aligned} \Delta \dot{X}_{6 \times 1} &= A_{6 \times 6} \Delta X_{6 \times 1} + B_{6 \times 1} \Delta U_{1 \times 1} \\ \Delta Y &= \Delta X \end{aligned} \quad (294)$$

where A is the state matrix of dimension  $6 \times 6$  and B is the control matrix of dimension  $6 \times 1$ . The elements of both matrices A and B correspond to the systems presented in (292) and (293) respectively. In order to determine the transfer function  $G(s)$  we need to calculate  $G(s) = (sI - A)^{-1}B$ ,

$$(sI - A) = \begin{pmatrix} s & 0 & 0 & 0 & 0 & 0 \\ 0 & s & 0 & 0 & 0 & 0 \\ 0 & 0 & s & 0 & 0 & 0 \\ 0 & 0 & 0 & s & 0 & 0 \\ 0 & 0 & 0 & 0 & s & 0 \\ 0 & 0 & 0 & 0 & 0 & s \end{pmatrix} - \begin{pmatrix} -k_1 & k_2 & 0 \\ k_1 & -(k_2+k_3) & k_4 \\ 0 & k_3 & -(k_4+k_5) \\ 0 & 0 & k_5 \\ 0 & 0 & 0 \\ 0 & 0 & 0 \end{pmatrix} \begin{pmatrix} 0 \\ 0 \\ 0 \\ k_6 \\ -(k_6+k_7+k_9) \\ k_7 \\ k_9 \end{pmatrix} \begin{pmatrix} 0 \\ 0 \\ 0 \\ k_8 & k_{10} \\ -k_8 & 0 \\ 0 & -k_{10} \end{pmatrix} \quad (295)$$

$$(sI - A) = \begin{pmatrix} s + k_1 & -k_2 & 0 & 0 & 0 & 0 \\ -k_1 & s + (k_2 + k_3) & -k_4 & 0 & 0 & 0 \\ 0 & -k_3 & s + (k_4 + k_5) & -k_6 & 0 & 0 \\ 0 & 0 & -k_5 & s + (k_6 + k_7 + k_9) & -k_8 & -k_{10} \\ 0 & 0 & 0 & -k_7 & s + k_8 & 0 \\ 0 & 0 & 0 & -k_9 & 0 & s + k_{10} \end{pmatrix} \quad (296)$$

Following, we obtain the value of  $(sI - A)^{-1}$  and multiply by matrix B in order to obtain the transfer function. Numerical values for the transfer function can be obtained by defining specific values of  $C_{A0}$  and rate constants ( $k$ ). For example, by defining  $C_{A0} = 1 \text{ mol} \cdot \text{m}^{-3}$ ,  $k_1 = 0.04 \text{ h}^{-1}$ ,  $k_2 = 0.18 \text{ h}^{-1}$ ,  $k_3 = 2 \text{ h}^{-1}$ ,  $k_4 = 1.9 \text{ h}^{-1}$ ,  $k_5 = 3 \text{ h}^{-1}$ , and  $k_6 = 30 \text{ h}^{-1}$ ,  $k_7 = 80 \text{ h}^{-1}$ ,  $k_8 = 18 \text{ h}^{-1}$ ,  $k_9 = 0.1 \text{ h}^{-1}$ ,  $k_{10} = 0.01 \text{ h}^{-1}$  the corresponding transfer functions are:

From input  $u_I = C_{A0}$  to output:

$$y_1 = C_A \rightarrow G(s) = \frac{1s^5 + 135.2s^4 + 1367s^3 + 2915s^2 + 225.9s + 1.8}{1s^6 + 135.2s^5 + 1372.4s^4 + 2968.7s^3 + 334.8s^2 + 3.4s - 8.3272e^{-15}} \quad (297)$$

$$y_2 = C_B \rightarrow G(s) = \frac{5.3s^3 + 43.2s^2 + 41.8s + 0.4}{1s^6 + 135.2s^5 + 1372.4s^4 + 2968.7s^3 + 334.8s^2 + 3.4s - 8.3272e^{-15}} \quad (298)$$

$$y_3 = C_C \rightarrow G(s) = \frac{0.1s^3 + 10.2s^2 + 43.4s + 0.4}{1s^6 + 135.2s^5 + 1372.4s^4 + 2968.7s^3 + 334.8s^2 + 3.4s - 8.3272e^{-15}} \quad (299)$$

$$y_4 = C_D \rightarrow G(s) = \frac{0.2s^2 + 4.34s + 0.0432}{1s^6 + 135.2s^5 + 1372.4s^4 + 2968.7s^3 + 334.8s^2 + 3.4s - 8.3272e^{-15}} \quad (300)$$

$$y_5 = C_E \rightarrow G(s) = \frac{19.2s + 0.2}{1s^6 + 135.2s^5 + 1372.4s^4 + 2968.7s^3 + 334.8s^2 + 3.4s - 8.3272e^{-15}} \quad (301)$$

$$y_6 = C_F \rightarrow G(s) = \frac{0.4}{1s^6 + 135.2s^5 + 1372.4s^4 + 2968.7s^3 + 334.8s^2 + 3.4s - 8.3272e^{-15}} \quad (302)$$

The previous equations in the s-domain can be also expressed in the time domain. Firstly we require to perform partial fraction expansion of equations (297) to (302) followed by the Inverse Laplace transform, as can be seen in equations (303) to (308):

$$y_1(t) = -0.0004e^{-124.35t} + 0.0006e^{-7.85t} + 0.0003e^{-2.876t} + 0.3449e^{-0.1074t} + 0.1251e^{-0.0113t} + 0.5294 \quad (303)$$

$$y_2(t) = 0.0004e^{-124.35t} - 0.0008e^{-7.85t} + 0.0081e^{-2.876t} - 0.1309e^{-0.1074t} + 0.0218e^{-0.0113t} + 0.1176 \quad (304)$$

$$y_3(t) = 0.0009e^{-7.85t} + 0.0031e^{-2.876t} - 0.1507e^{-0.1074t} + 0.0291e^{-0.0113t} + 0.1176 \quad (305)$$

$$y_4(t) = -0.0001e^{-7.85t} + 0.0008e^{-2.876t} - 0.0151e^{-0.1074t} + 0.0017e^{-0.0113t} + 0.0127 \quad (306)$$

$$y_5(t) = -0.0005e^{-7.85t} + 0.0040e^{-2.876t} - 0.0677e^{-0.1074t} + 0.0055e^{-0.0113t} + 0.0588 \quad (307)$$

$$y_6(t) = 0.0146e^{-0.1074t} - 0.1322e^{-0.0113t} + 0.1176 \quad (308)$$

The output of the system using the transfer functions determined in previous equations for concentration of glycerol and oxidation products is presented in Fig. 25 and Fig. 26.

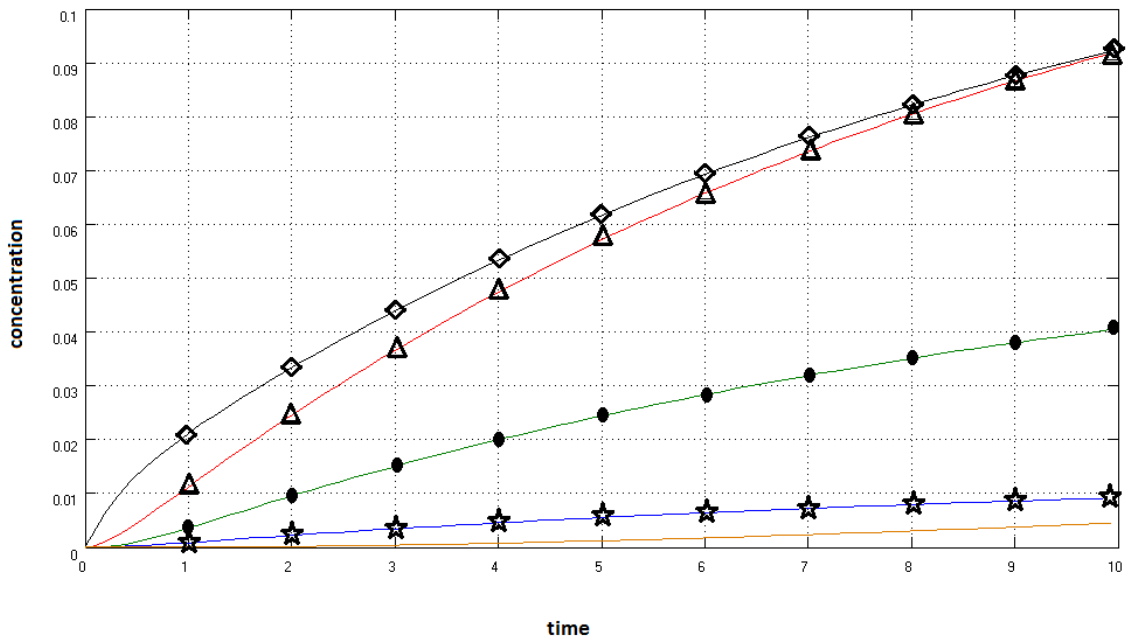


**Fig. 25:** Output of the system for concentration of oxidation products based on the respective transfer functions ( $\diamond C_B$ ;  $\triangle C_C$ ;  $*C_D$ ;  $\bullet C_E$ ;  $—C_F$ ).

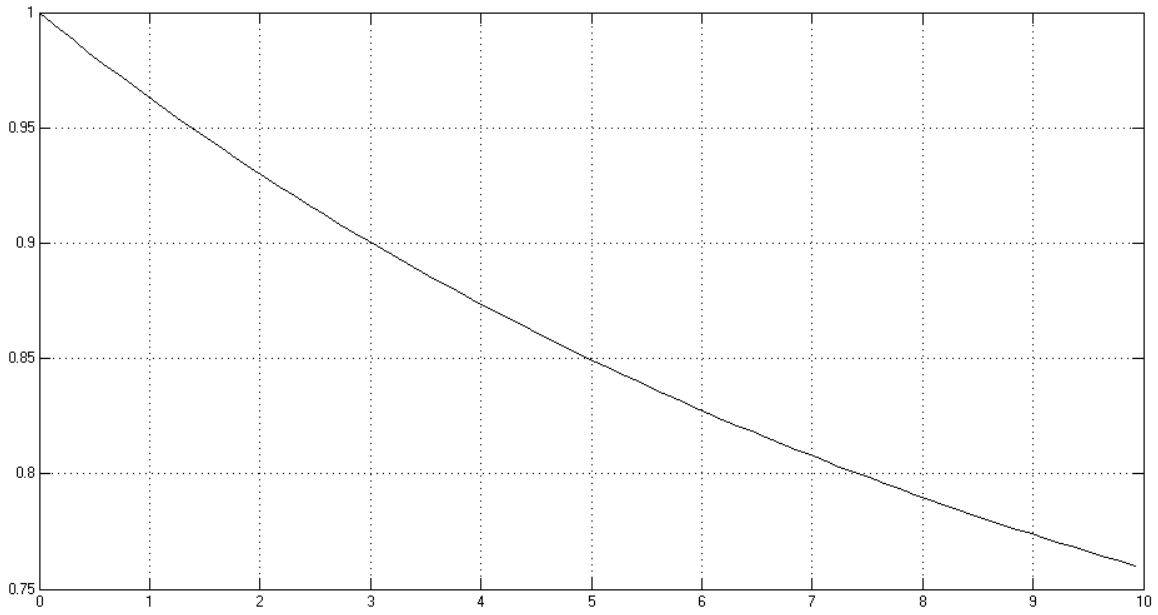


**Fig. 26:** Output of the system for concentration of glycerol.

## **10 EXPERIMENTAL MEASUREMENTS**

### **10.1 Liquid chromatography method**

Partial oxidation of glycerol leads to several glycerol derivatives which in some cases are formed simultaneously, due to the reactivity of primary and secondary hydroxyl groups, *e.g.* [72]. As a result, and according to [72], the selectivity for a specific product is not easy to achieve and still remains as a challenge. For this reason, it is important to have accurate and rapid methods for the analysis, identification and quantification of these compounds. Especially, an analytical method able to simultaneously determine all products of mild oxidation can significantly reduce and simplify the development of new catalysts and oxidation techniques. Such a method is also of value for the characterization of final products because it will in most cases contain also other substances formed during the glycerol oxidation. Techniques such as Thin Layer Chromatography [73] and HPLC have been used for the identification, yield, and quantitative determination of glycerol oxidation products. In particular, HPLC has been broadly employed for this purpose as it provides short elution times and easy sample preparation with no need of derivatization, see *e.g.*, [74]

#### **10.1.1 Instrument**

Analysis of samples for quantification purposes was performed using a Shimadzu HPLC instrument with automatic injection. The system comprised a degassing unit DGU-20A 5R, a pump LC-20AD, an auto sampler SIL-30AC, a column oven CTO—20rA, a Refractive index detector RID-10A, an UV Detector SPD-20A and a communications bus module (control unit) CBM-20A. Data analysis and acquisition was performed with LabSolutions Software. The HPLC column used was a reversed-phase Aminex HPX-87C (300mm x 7,8mm).

#### **10.1.2 Chemicals and reagents**

Deionized water was used in all procedures (Millipore). Glycerol (Propane-1,2,3-triol), glyceraldehyde (2,3-Dihydroxypropanal), dihydroxyacetone (1,3-Dihydroxypropan-2-one), tartronic acid (2-Hydroxypropanedioic acid), glycolic acid (2-Hydroxyethanoic acid), glyceric acid (2,3-Dihydroxypropanoic acid), and mesoxalic acid (Oxopropanedioic acid) standards were obtained from Sigma-Aldrich (Czech Republic).

#### **10.1.3 Sample preparation for development of the HPLC method**

The preparation of the stock solutions was realized by weighting 100 mg of each standard and dissolving with deionized water in a 10 mL volumetric flask and filtering through a nylon Millipore filter (0.22  $\mu\text{m}$ ). Concentrations ranging

from 0.5 to 10 mg mL<sup>-1</sup> were prepared for calibration purposes. A 0.01 M H<sub>2</sub>SO<sub>4</sub> solution was made by weighing 1.024 g of 95 % H<sub>2</sub>SO<sub>4</sub> (0.54 mL), pouring it into a 1 L volumetric flask and dissolving deionized water. From this stock solution, different concentrations of sulfuric acid were prepared to be used as mobile phase.

#### 10.1.4 Chromatographic method development

The analysis of the glycerol oxidation products was performed using an ion exchange Aminex HPX-87C (300 mm x 7,8 mm) column in isocratic mode with aqueous H<sub>2</sub>SO<sub>4</sub> solution as mobile phase and monitored at 210 nm by UV detection of carbonyl compounds from carboxylic acids, ketones and aldehydes. In order to reveal the order of elution and the individual retention time of each of the standards, a first set of experimental conditions including flow: 0.7 ml min<sup>-1</sup>, temperature: 60 °C, and 0.01 M H<sub>2</sub>SO<sub>4</sub> as mobile phase were used. The temperature of the refractometric detector remained constant at 30 °C. After the introductory experiment was conducted, a solution containing a mixture of the standards was analyzed at 30 and 60 °C under the same conditions. In order to optimize the mobile phase composition for the HPLC analysis, different flow rates (0.2, 0.5, 0.7 and 0.8 mL·min<sup>-1</sup>) and mobile phase conditions of aqueous H<sub>2</sub>SO<sub>4</sub> (1, 3, 5, and 10 mM) were tested and the column temperature was increased to 70 °C. The injection volume used was 20 µL and the temperature of the RI detector remained constant at 30 °C.

#### 10.1.5 Chromatographic validation

For the purpose of testing the limit of detection, different concentration of glyceric acid (the compound that showed the less response in RI detector) were analyzed. Dilutions were prepared sequentially from a solution that presented a signal to noise (S/N) ratio of at least 30 until the S/N ratio was approximately 3. The intra-day precision test was performed to know the variability in measurements between experiments in terms of the peak-area ratios at a specific concentration on the same day. For the HPLC Calibration curves, six different concentrations of the standards (0.5, 1, 2, 5, 7, and 10 mg·mL<sup>-1</sup>) were prepared and the suitability was analyzed by means of linear regression. Sensitivity of both detectors was determined by using the variability in the response (mV·s) at six different concentrations (mg·mL<sup>-1</sup>).

Normally, during the development of a chromatographic method, it is recommended to change sequentially conditions that will optimize values for capacity factor (*k*), selectivity ( $\alpha$ ), efficiency (*N*) and resolution (*R<sub>s</sub>*), such as mobile and stationary phase composition and temperature. Optionally it is

possible to vary column conditions (flow rate, columns length or particle size), see *e.g.*, [75]. As showed in equation (309),  $R_s$  is usually expressed as a function of  $k$ ,  $\alpha$ , and  $N$ , therefore this value was used as the variable response for the optimization purpose. Calculation of  $R_s$  value for two adjacent bands (represented as “A” and “B”) was performed according to equation (310), where  $t_B$  and  $t_A$  corresponds to the retention time of both compounds, and  $W$  represents the bandwidths at half height of both peaks. For precise and rugged quantitative analysis, an  $R_s$  value greater than 1.5 is usually required, as reported in [76].

$$R_s = \left(\frac{1}{4}\right) (\alpha - 1) N^{1/2} \left[ \frac{k}{1+k} \right] \quad (309)$$

$$R_s = 1.18 \frac{(t_B - t_A)}{W_{0.5,A} + W_{0.5,B}} \quad (310)$$

## 10.2 Electrochemical experiments

### 10.2.1 Anodic oxidation

The electrochemical oxidation of glycerol was analyzed using a three electrode system. Electrochemical experiments were performed in a three electrode glass cell of 25 mL capacity. The working electrode consisted of a Pt electrode (Radiometer model P101). Silver/silver chloride/saturated KCl electrode (Ag/AgCl/KCl (sat.)) was used as a reference electrode and boron-doped diamond as auxiliary electrode.

### 10.2.2 Instrument

Electrochemical oxidation was carried out using an EmStat Potentiostat (made by PalmSens) with computerized control by PSTrace Software to record the data from and multiple pulse amperometry measurements.

### 10.2.3 Voltammetric measurements

Electrochemical experiments were performed in a three electrode glass cell of 25 mL capacity and a conventional three electrode system was used (Fig. 27). The glycerol electrooxidation reaction was studied in presence of  $\text{MnO}_2$ . Cyclic voltammetry was used systematically in the present work. Two different cyclic voltammogram analyses were performed in the presence of  $\text{MnO}_2$  (0.063 M) and a solution of 0.007 M glycerol and 0.063 M  $\text{MnO}_2$  at the same scan rate (50 mV/s), temperature (25°C) and between -1.5 and 1.5. The potentials reported are all referred to Ag/AgCl electrode

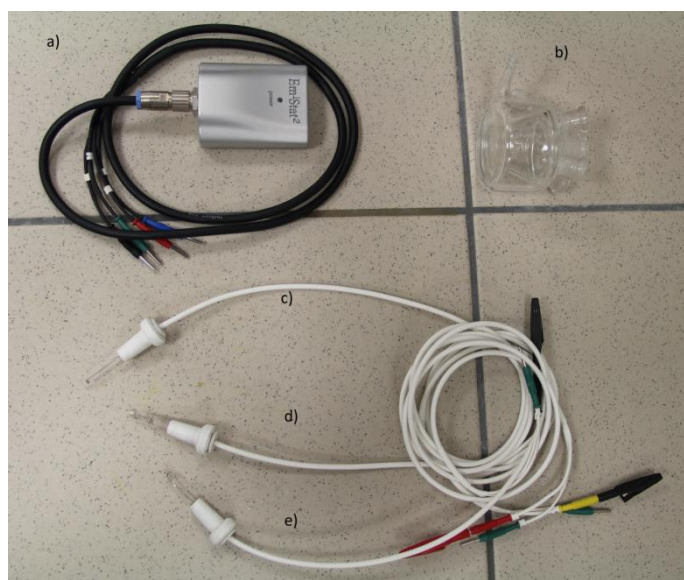


**Fig. 27:** Devices used for electrochemical experiments. a)EmStat Potentiostat. b)electrochemical cell, c)working electrode, d)reference electrode, e)counter electrode.

#### 10.2.4 Effect of varying glycerol and MnO<sub>2</sub> concentration

In order to analyze the reaction order for glycerol and MnO<sub>2</sub>, two different cyclic voltammogram analyses were performed at the same scan rate (50 mV·s<sup>-1</sup>) and temperature (25°C). The first one between -1.5 and 1.5 V vs Ag/AgCl in 62 mM glycerol solutions with MnO<sub>2</sub> concentration between 15 and 124 mM. The second one consisted in 14 mM MnO<sub>2</sub> solutions with a glycerol concentration of 15-124 mM at 50 mV·s<sup>-1</sup>, 25°C and range of -1.5 and 1.5 V vs Ag/AgCl.

#### 10.2.5 Effect of potential scan limits, scan rate and analysis of temperature variation

The effect of the increment of positive and negative potential limit was studied in a range of -1.5 to 1.5 V vs Ag/AgCl for solutions of 0.0625 M glycerol in 0.014 M MnO<sub>2</sub>. Cyclic voltammograms were recorded at a scan rate of 0.05 V·s<sup>-1</sup> and 25 °C. A scan rate of 0.01 to 0.08 V·s<sup>-1</sup> was studied in 0.0625 M glycerol in presence of 0.014 M MnO<sub>2</sub>. For the analysis of temperature effect, similar parameters were employed using a scan rate of 0.03 V·s<sup>-1</sup> in a temperature range of 27 to 60 °C.

## 10.2.6 Oxidation of glycerol using multiple pulse amperometry

Glycerol partial oxidation was studied at a controlled potential by means of Multiple pulse amperometry during prolonged electrolysis, using a potential of 0.5V vs Ag/AgCl (2s) and two cleaning steps at 1.5 (1s) and -1.5 V (1s). The oxidation was performed over a 5 h period. Sample was taken every hour and the concentration of glycerol and oxidation products was determined using a reversed-phase Aminex HPX-87C (300mm x 7,8mm) column at 30°C in isocratic mode with 3mM H<sub>2</sub>SO<sub>4</sub> as a mobile phase, with a flow of 0.5mL/min. The temperature of the RI detector was set to 30°C. Selectivity and conversion to different products was calculated as presented in (311) and (312) respectively.

$$selectivity (\%) = \frac{[P] \cdot V_f}{([G_0] \cdot V_0) - ([G_f] \cdot V_f)} \times 100 \quad (311)$$

$$conversion (\%) = \frac{[P] \cdot V_f}{\frac{([G_0] \cdot V_0) \times MW_P}{MW_G}} \times 100 \quad (312)$$

where [P] represents the concentration of the product (mg·mL<sup>-1</sup>), V<sub>f</sub> the final volume (mL), [G<sub>0</sub>] and [G<sub>f</sub>] the initial and final concentration of glycerol respectively (mg·mL<sup>-1</sup>), V<sub>0</sub> the initial volume (mL), and MW<sub>P</sub> and MW<sub>G</sub> the molecular weight of the product and glycerol respectively (g·mol<sup>-1</sup>). Figures 28 to 30 show the HPLC chromatogram of the reaction blend after 3-5 hours of oxidation at controlled potential, where the evolution of glyceraldehyde (peak at ≈17.5 min) can be also observed.

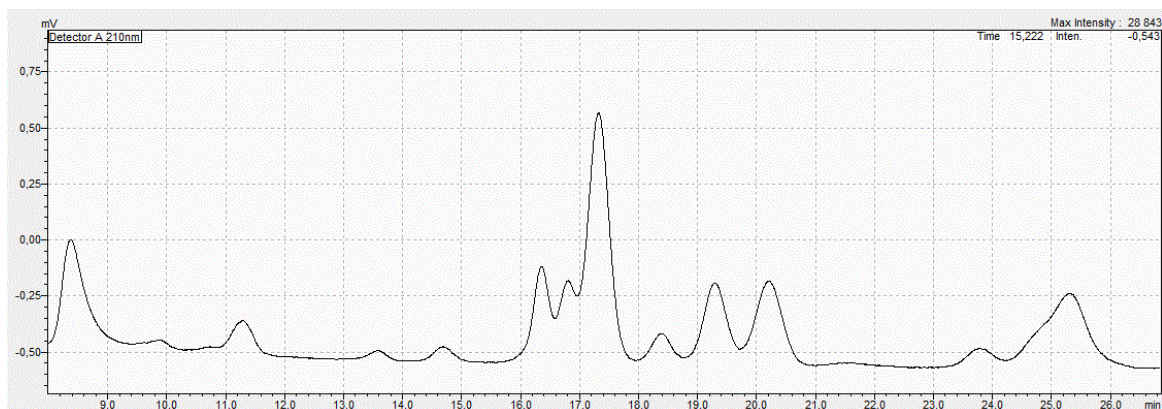


**Fig. 28:** HPLC chromatogram and Cyclic voltammogram after 3 hours of controlled potential.

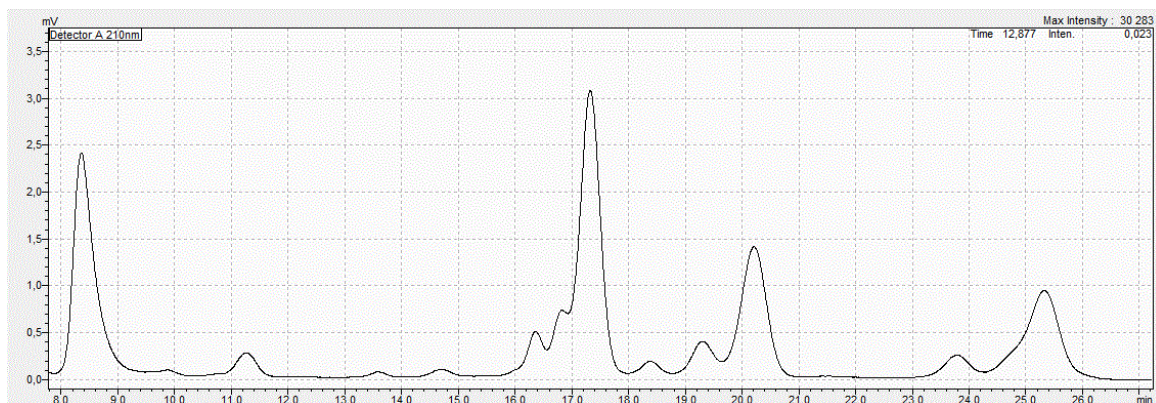


**Fig. 29:** HPLC chromatogram after 4 hours of controlled potential.

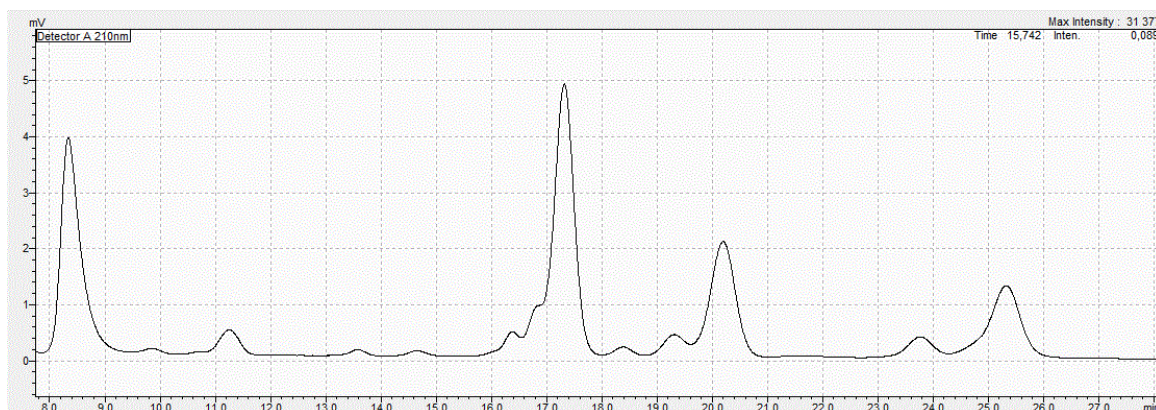


**Fig 30:** HPLC chromatogram after 5 hours of controlled potential.

As an example, the HPLC chromatograms of several experiments can be also appreciated in Appendix A where the main compounds are generally glyceraldehyde, glyceric acid, glycolic acid, or mesoxalic acid. Chromatograms from other experiments share similar characteristics and are not presented here.

### 10.3 Approximate experiments oxidation of glycerol nitrous oxide

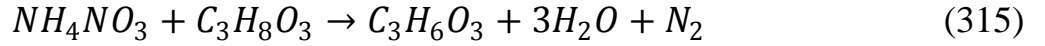
One possibility to perform the controlled partial oxidation of glycerol to glyceraldehyde is using an oxidizing agent in low concentrations, which is suppressed by the subsequent oxidation of glyceraldehyde to glyceric acid, due to the very low residual concentrations of the oxidizing agent. For orientation experiments I chose nitrous oxide generated by thermal decomposition of ammonium nitrate as expressed in next equation



The oxidation of glycerin to glyceraldehyde is presented next:



Taking into account the reactions expressed in (313) and (314), the expression (315) is obtained:



Using the values of the standard formed enthalpy listed on page 24, and published values for ammonium nitrate (-361.1kJ/mol), the calculated reaction enthalpy is -426.272 kJ · mol<sup>-1</sup>.

$$(\Delta H)_r = [-598.312 \text{ kJ} \cdot \text{mol}^{-1} - 3 * 285.83 \text{ kJ} \cdot \text{mol}^{-1}] - [-668.43 \text{ kJ} \cdot \text{mol}^{-1} - 361.1 \text{ kJ} \cdot \text{mol}^{-1}] \quad (316)$$

$$(\Delta H)_r = -1455.8 \text{ kJ} \cdot \text{mol}^{-1} + 1029.53 \text{ kJ} \cdot \text{mol}^{-1} \quad (317)$$

$$(\Delta H)_r = -426.272 \text{ kJ} \cdot \text{mol}^{-1} \quad (318)$$

Adiabatic heating is then estimated by the following equation:

$$\Delta T = \frac{n \cdot [-(\Delta H)_r - 3(\Delta H)_{H_2O}^{vap} - \Delta t c_a - (\Delta H)_m]}{n_r \cdot \bar{C}_{p_{reactionblend}}} \quad (319)$$

where n is the number of moles of ammonium nitrate, n<sub>r</sub> is the number of moles of reaction blend integral, c<sub>p</sub> is the specific heat of the reaction mixture, c<sub>a</sub> is the specific heat of ammonium nitrate, and (ΔH)<sub>m</sub> is the enthalpy of fusion of ammonium nitrate (6.4 kJ · mol<sup>-1</sup>), according to [77]. The value of  $\bar{C}_p$  can be calculated from equation (320)

$$\bar{C}_{p_{reactionblend}} = \frac{1}{4} \bar{C}_{p_{glyceralde\ hyde}} + \frac{3}{4} \bar{C}_{p_{H_2O}} \quad (320)$$

$$\bar{C}_{p_{reactionblend}} = \frac{1}{4} (0.219 \text{ kJ} \cdot \text{mol}^{-1} \text{K}^{-1}) + \frac{3}{4} (0.0752 \text{ kJ} \cdot \text{mol}^{-1} \text{K}^{-1}) \quad (321)$$

$$\bar{C}_{p_{reactionblend}} = 0.11 \text{ kJ} \cdot \text{mol}^{-1} \text{K}^{-1} \quad (322)$$

Practical design experiment was conducted heating pure glycerol at 202 °C temperature. To this heated glycerin is gradually dosed ammonium nitrate or its concentrated solution, while monitoring the reaction temperature. After heating pure glycerol at 202 °C, a defined amount of NH<sub>4</sub>NO<sub>3</sub> was added gradually, recording the minimum and maximum temperature registered after the addition. The overall results are summarized in Table 5

**Table 5.** Record of temperature variation after addition of  $\text{NH}_4\text{NO}_3$

Adding	Mass of sample[g]	$t_{\min}$ after dosing [°C]	$t_{\max}$ after dosing [°C]	Sum [g]	Sum [%]
1	0,62	206	218	0,62	1,4
2	0,52	210	215	1,14	2,6
3	0,53	203	213	1,67	3,84
4	0,55	206	214	2,22	5,1
5	0,53	208	220	2,75	6,32
6	0,51	212	223	3,26	7,49
7	0,51	211	221	3,77	8,67
8	0,49	203	216	4,26	9,79
9	0,50	210	220	4,76	10,94
10	0,51	213	223	5,27	12,12
11	0,48	211	225	5,75	13,24
12	0,51	211	226	6,26	14,14
13	0,48	212	223	6,74	15,52
14	0,53	208	218	7,27	16,74
15	0,50	200	214	7,77	17,89
16	0,52	206	220	8,29	19,08

The following figure represents the record of temperature in the case of gradual dose of aqueous saturated solution of ammonium nitrate

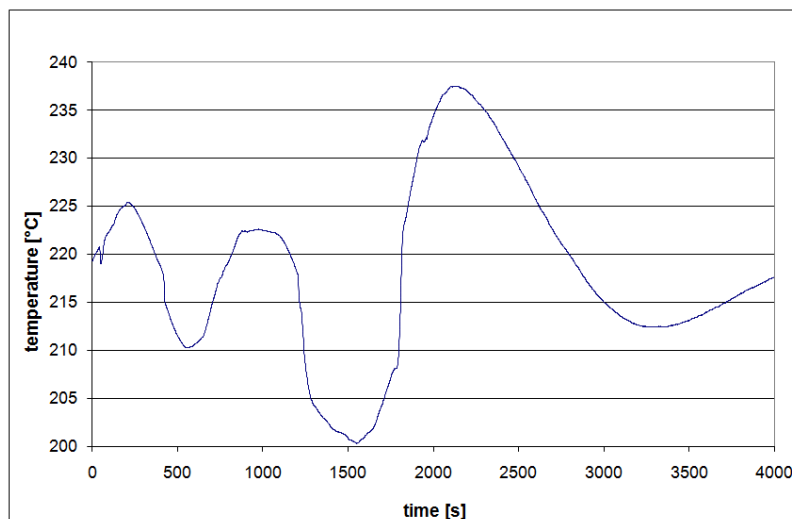


**Fig 31:** Temperature vs time plot for the oxidation of glycerol in ammonium nitrate.

Because of the low conversion during glycerin oxidation, the value of specific heat of glycerol was used for adiabatic heating calculations. Specific heat for of

ammonium nitrate ( $0.139 \text{ kJ}\cdot\text{mol}^{-1}\text{K}^{-1}$ ) was taken from reference [78],  $\Delta t$  is calculated considering an initial temperature of  $20 \text{ }^\circ\text{C}$  and final temperature of  $206 \text{ }^\circ\text{C}$  and  $n_r$  considering the initial mass of glycerol of  $50.16 \text{ g}$  ( $0.545 \text{ mol}$ )

Therefore:

$$\Delta T = \frac{0.00775 \cdot [426.272 - 3(40.72) - 186(0.139) - 6.4] \text{ kJ}\cdot\text{mol}^{-1}}{(0.545)(0.11 \text{ kJ}\cdot\text{mol}^{-1}\text{K}^{-1})} \quad (323)$$

$$\Delta T = 35.14 \text{ K or } 35.14 \text{ }^\circ\text{C} \text{ (Temperature difference)} \quad (324)$$

Lower values of adiabatic heat (i.e.  $17.65 \text{ }^\circ\text{C}$ ) can be calculated if assuming a  $\bar{c}_{p_{\text{reactionblend}}}$  value of  $0.219 \text{ kJ}\cdot\text{mol}^{-1}\text{K}^{-1}$  which would correspond with a lower conversion of glycerol. These values would correspond to an ideal isolation case. Such conditions differed in the experimental case, for example, the average measured value of temperature when dosing  $0.6 \text{ g}$  of ammonium nitrate was  $12 \text{ }^\circ\text{C}$ .

## 11 RESULTS

### 11.1 Chromatographic method development

The analysis of the glycerol oxidation products was performed using an ion exchange Aminex HPX-87C (300 mm x 7.8 mm) column in an isocratic mode with aqueous H<sub>2</sub>SO<sub>4</sub> solution as the mobile phase. Analytes were monitored by UV detection of carbonyl groups from carboxylic acids, ketones, and aldehydes at 210 nm coupled in series with RI detector. In order to reveal the order of elution and the individual retention time of each of the standards, a first set of experimental conditions including mobile phase flow rate: 0.7 mL·min<sup>-1</sup>, temperature: 60 °C, and 0.01 M aqueous H<sub>2</sub>SO<sub>4</sub> was used. The temperature of the refractometric detector remained constant at 30 °C.

The preliminary tests showed that the peaks of glyceraldehyde–glyceric acid–glycerol (first group) and peaks of glycolic acid–DHA (second group) were overlapped as it was indicated in the literature, see *e.g.*, [69] and [70]. The effort was, therefore, focused on the improvement of resolution between substances in these two groups by evaluating the effect of temperature (30, 60, and 70 °C); flow rate (0.2, 0.5, and 0.7 mL·min<sup>-1</sup>); and concentrations of H<sub>2</sub>SO<sub>4</sub> in mobile phase (1, 3, 5, and 10 mM). The experiments showed that resolution between glyceraldehyde and glyceric acid increased with the raise in flow rate and concentration of sulfuric acid in mobile phase as it is presented also in Fig. 32. On the contrary, decreasing the concentration of H<sub>2</sub>SO<sub>4</sub> below 5 mM (2 < pH < 2.7) improved the separation between glyceric acid and glycerol, allowing the qualitative determination of these compounds. Glyceric acid could be identified with good resolution and without overlapping by UV detector, since glycerol does not show absorption at the wavelength applied. Moreover, the decrease of H<sub>2</sub>SO<sub>4</sub> concentration positively influences the *R<sub>s</sub>* value between glycolic acid and dihydroxyacetone, as illustrated in Fig. 33. In summary, the choice of the sulfuric acid concentration presents a compromise between resolution of glyceraldehyde and glyceric acid on the one hand and glyceric acid and glycerol on the other hand. The temperature in the column also influenced the separation of products. At 30 °C, the peaks were highly asymmetric with a notable fronting observed. However, this situation was overcome by increasing the column temperature to 70 °C.

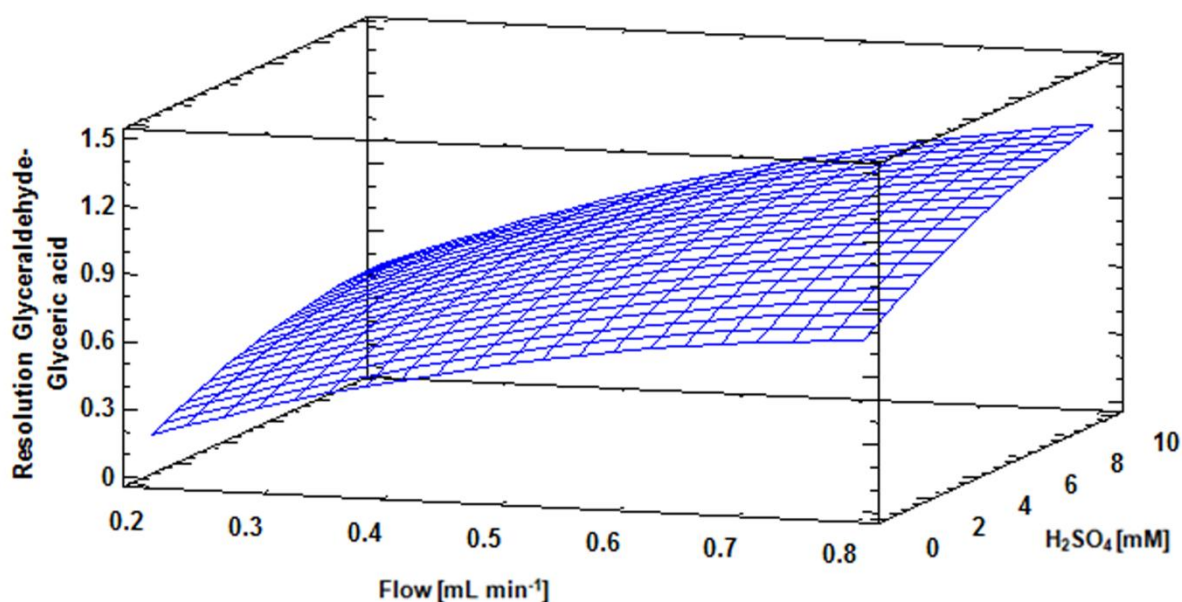


**Fig. 32:** Influence of flow rate and concentration of mobile phase on resolution between glyceric acid and glyceraldehyde

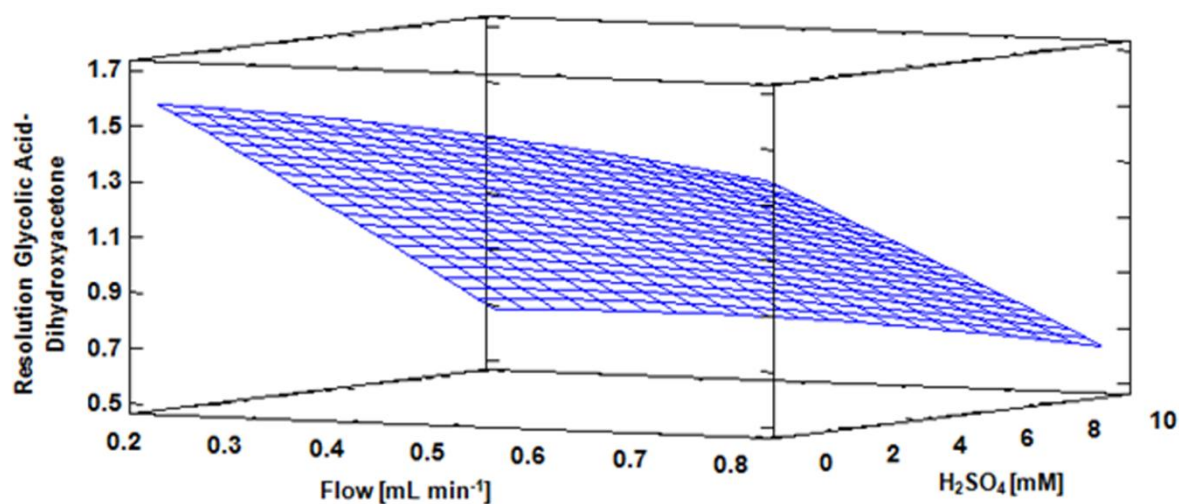


**Fig. 33:** Influence of flow rate and concentration of mobile phase on resolution between glycolic acid and dihydroxyacetone.

Table 6 presents the conditions that allowed the identification of the glycerol derivatives with the respective value of resolution acquired. The final chromatographic conditions were set as follows: column temperature was increased to 70 °C, the injection volume used was 20 mL, flow rate of 0.5 mL·min<sup>-1</sup>, mobile phase with 3 mM H<sub>2</sub>SO<sub>4</sub> and the temperature of the RI detector remained constant at 30 °C.

**Table 6.** Summary of conditions allowing the identification of all the standards analyzed with the respective resolution achieved.

H <sub>2</sub> SO <sub>4</sub> (mM) in mobile phase	pH	Flow rate (mL·min <sup>-1</sup> )	Resolution			
			A*	B*	C*	D*
3	2.2	0.5	3.13	0.73	0.61	1.27
3	2.2	0.7	3.1	0.96	0.51	1.22
2	2.4	0.5	3.0	0.85	0.56	1.35

A\* Mesoxalic-Tartronic acid

B\* Glyceraldehyde-Glyceric acid

C\* Glyceric Acid-Glycerol

D\* Glycolic Acid-Dihydroxyacetone

Fig. 34 shows the RI chromatogram using the developed method from where it is possible to see the elution order and separation of glycerol derivatives.

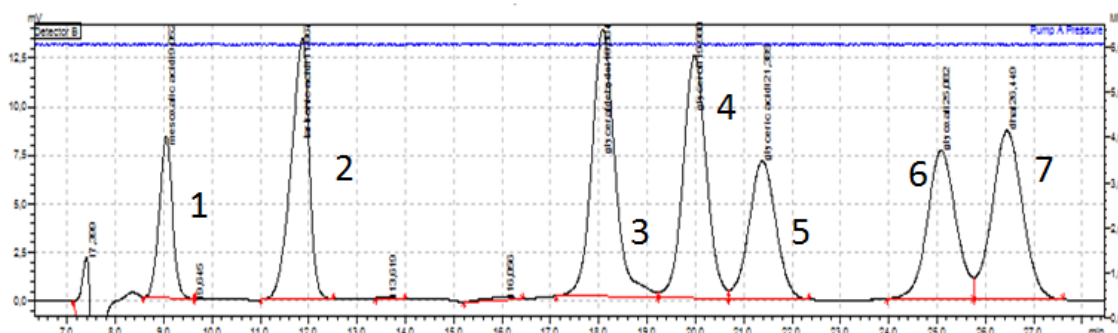


**Fig. 34:** HPLC analysis at optimized conditions: Temperature: 30 °C, mobile phase: 3mM H<sub>2</sub>SO<sub>4</sub> flow rate: 0.5mL/min. The elution order is 1.Mesoxalic acid, 2.Tartronic acid, 3.Glyceraldehyde, 4.glycerol, 5.Glyceric acid, 6.Glycolic acid, 7.Dihydroxyacetone.

## 11.2 Validation parameters

In order to develop the quantitative analysis, it was assumed that the area of the peaks in the chromatogram was proportional to the concentration of the respective compound. The quantification was made by calibration curves based on the UV and RI spectrophotometric response of known amounts of the standards in aqueous solutions. Table 7 presents the analysis in a concentration range of 0.5-10 mg·mL<sup>-1</sup>. A flow rate of 0.5 mL·min<sup>-1</sup> was used with 3 mM H<sub>2</sub>SO<sub>4</sub> as mobile phase at 70 °C. Linearity was determined by means of the calculus of the regression. All calibration curves showed a good linear correlation ( $r^2 > 0.999$ ) within the concentration range.

**Table 7.** Standard curves for glycerol oxidation products.

Standard	Retention time	Equation <sup>a)</sup> (y=ax)			
		UV detector		RI detector	
		a	r <sup>2</sup>	a	r <sup>2</sup>
Mesoxalic acid	9.2	3653.786	0.999	1054.025	0.999
Tartronic acid	10.84	5111.204	0.999	1235.887	0.999
Glyceraldehyde	17.19	731.7548	0.999	1483.127	0.999
Glyceric acid	18.54	1213.569	0.999	885.373	0.999
Glycerol	19.26			1244.132	0.999
Glycolic acid	21.43	1379.977	0.999	981.756	0.999
Dihydroxyacetone	23.03	1572.767	0.999	1224.625	0.999

a)Range 0-10 mg·mL<sup>-1</sup>

In order to know the detection limit, the respective concentration was considered to be positive when the S/N ratio in triplicate exceeded the value of 3. A concentration of 0.01 mg·mL<sup>-1</sup> could still be registered by the instrument under this condition. As quantification limit can be registered when the signal to noise ratio is 10:1, see *e.g.*, [81], a concentration of 0.1 mg·mL<sup>-1</sup> could be quantified by the instrument. The Coefficient of variation (CV), which represents the dispersion of the response of UV and RI detectors from seven independent analyses around the mean was calculated and is presented as a percentage in Table 8 and Table 9 respectively. The range is from 2.3 to 4.2 % for the UV detector and from 1.75 to 6.39 % for the RI detector which indicates satisfactory values for precision of the instrument.

**Table 8.** Intra-day precision Test of the HPLC method for the determination of glycerol oxidation products (UV detector)

Standard	UV detector		
	Average of 7 determinations (mV·s)	Standard deviation	%CV
Mesoxalic acid	588.1	14.07	2.39
Tartronic acid	920.36	21.21	2.30
Glyceraldehyde	102.78	4.32	4.20
Glyceric acid	203.22	5.70	2.80
Glycolic acid	177.21	7.01	3.95
Dihydroxyacetone	192.48	6.46	3.35

**Table 9.** Intra-day precision Test of the HPLC method for the determination of glycerol oxidation products (RI detector)

Standard	RI detector		
	Average of 7 determinations (mV·s)	Standard deviation	%CV
Mesoxalic acid	199.97	5.51	2.75
Tartronic acid	226.47	6.79	3.00
Glyceraldehyde	246.01	15.72	6.39
Glyceric acid	384.75	6.76	1.75
Glycolic acid	129.44	5.11	3.94
Dihydroxyacetone	152.24	6.06	3.98

Similarly, the sensitivity test performed at six different concentrations showed acceptable CV values as presented in Table 10.

Fig. 35 shows the pattern around the line of constant response for glyceric acid determination. Values below  $1 \text{ mg} \cdot \text{mL}^{-1}$  starts to exceed the 5 % level of deviation in both detectors. Therefore the method showed reliable quantification over the range of 1 to 10 mg. Values outside the linear range of the detector sensitivity can be considered as the limit of quantification but according to Ribani et al., [81] the value obtained by the signal to noise ratio generally is lower than the one obtained by the sensitivity test.

**Table 10.** Sensitivity analysis of UV and RI detectors.

Compound	UV detector		RI detector	
	Mean Sensitivity (mV·s)[(mg mL <sup>-1</sup> )] <sup>-1</sup>	%CV	Mean Sensitivity (mV·s)[(mg mL <sup>-1</sup> )] <sup>-1</sup>	%CV
Mesoxalic acid	3865.2	5.3	1075.1	3.1
Tartronic acid	5408.3	5.4	1249.5	2.4
Glyceraldehyde	703.0	4.3	1494.8	1.5
Glyceric acid	1223.3	2.1	901.7	3.9
Glycerol			1266.2	3.0
Glycolic acid	1387.9	1.7	995.6	3.2
Dihydroxyacetone	1598.0	2.0	1238.4	1.7

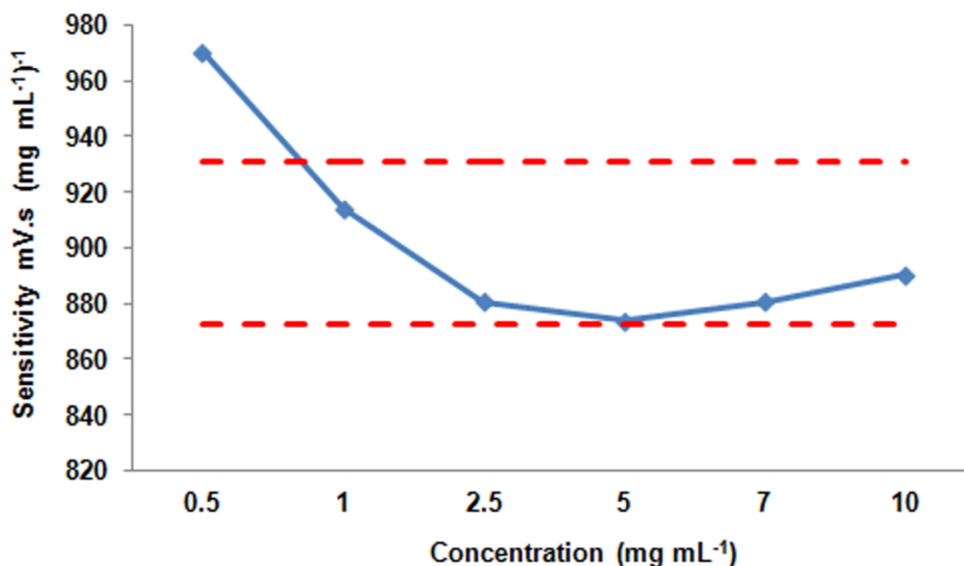


**Fig 35:** Sensitivity test for quantification of glyceric acid in RI detector.

More information about the method application for the identification of glycerol derivatives can be found in a recent publication, *e.g.*, [82].

### 11.3 Analysis of cyclic voltammetric data

Fig. 36 describes the Cyclic voltammogram of the Pt electrode in 0.063 M  $\text{MnO}_2$  and 0.007 M glycerol solution and 0.063M  $\text{MnO}_2$  solution. When using the oxidant alone, the current is non-Faradaic and no glycerol oxidation peak was observed. However, in the presence of reagent and oxidant, with the onset of the electrooxidation reaction, there is a charge transferred across the electrified interface and a Faradaic current flow increases rapidly until, at different particular potentials, a maximum current or peak current, is observed. The current subsequently decreases once a diffusion-limited condition is obtained. When the direction of the applied potential is reversed in the cathodic direction the current decreases until the product of the electrooxidation reaction is reduced at the electrode surface at a particular potential. This step is characterized by a current increment until a maximum cathodic current is reached. After, the current decreases to a diffusion-limited value until the cycle is completed and the direction of the applied potential is reversed. Moreover, the cyclic voltammogram of platinum electrode in presence of  $\text{MnO}_2$  (dash dot line with left y axis) showing that hydrogen evolution takes place (hydrogen adsorption and desorption) and in presence of glycerol and  $\text{MnO}_2$  (solid line and right y axis). The area between -1 and -0.25 V vs Ag/AgCl corresponds to hydrogen evolution while the positive charge in the positive scan corresponds to the oxidation of the hydrogen. The adsorption of  $\text{OH}^-$  and formation of  $\text{PtOH}^-$  occurs at -0.07 V vs Ag/AgCl, followed by a surface oxidation process such as the conversion of  $\text{PtOH}^-$  to form platinum oxide at 0.6 V vs Ag/AgCl. The

reduction of platinum oxide is shown in the reversed scan at 0.11 V vs Ag/AgCl, followed by the oxidation of glycerol at 0.07 V vs Ag/AgCl and hydrogen desorption. As suggested by Roquet et al., glycerol oxidation requires the presence of adsorbed OH<sup>-</sup> groups at the platinum surface, *e.g.* [50]

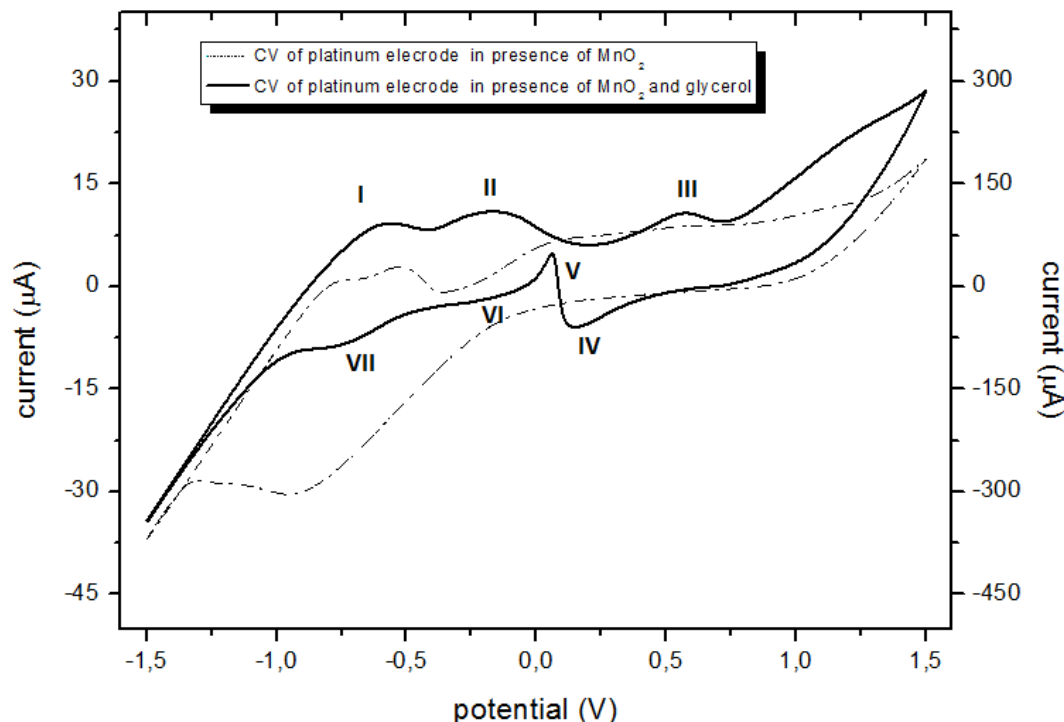


**Fig. 36:** Cyclic voltammogram analysis of Pt electrode in the presence of MnO<sub>2</sub> and glycerol + MnO<sub>2</sub>.

#### 11.4 The analysis of glycerol and MnO<sub>2</sub> reaction order

The order of the reaction with respect to glycerol and MnO<sub>2</sub> is the observed dependence of the reaction rate on the concentration of the specific reactant when the concentrations of all other species in the reaction are constant. To calculate the reaction order of glycerol, a cyclic voltammetry study was performed in 14mM MnO<sub>2</sub> and variation of the reagent concentration from 15-124 mM. Equation (325) was used to calculate the reaction order at specific potentials by means of the analysis of the anodic current at the corresponding concentration.

$$r = (\partial \log I / \partial \log [C_3H_8O_3]) \quad (325)$$

Fig. 37 shows the plot of log current density vs log glycerol concentration for the three peaks. For peaks I and II, no reaction order could be obtained over the range of concentrations studied indicating that the oxidation was inhibited by the reagent concentration due to saturation of active sites and preventing the OH<sup>-</sup> adsorption on Pt surface. However, under the consideration of lower glycerol

concentrations ( $< 33$  mM) it was possible to obtain a reaction order for both peaks (I and II), corresponding to 0.6 and 0.3 respectively. Peak III presented a slope of 0.22. The fractional values demonstrate the complexity of the reaction mechanism and that the rate determining step involves adsorbed species generated during the oxidation, *e.g.* [83].

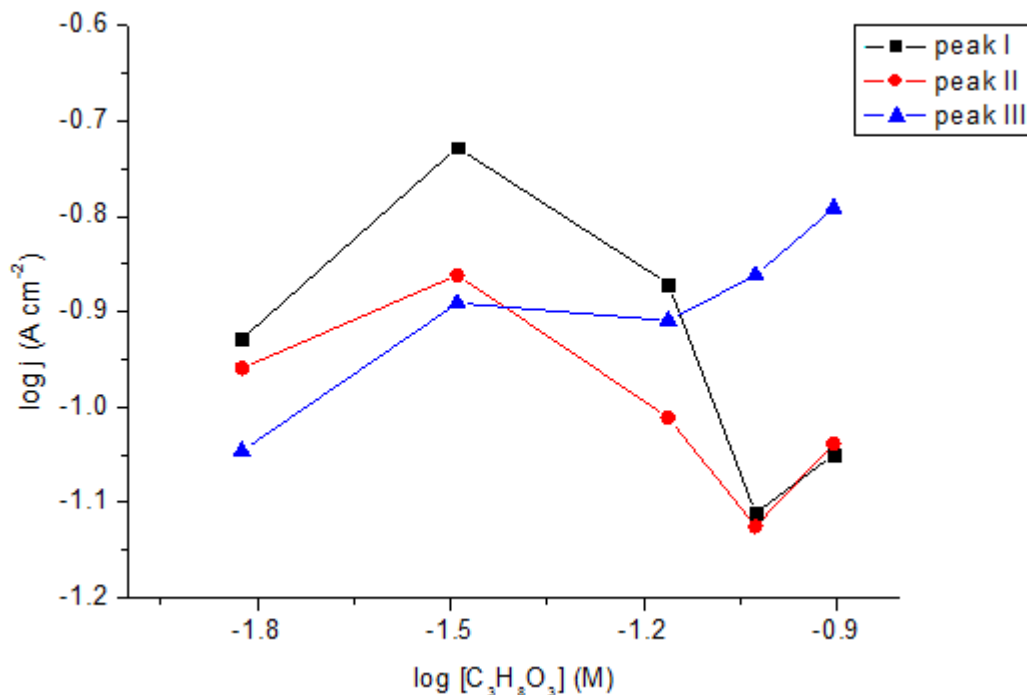


**Fig. 37:** Analysis of the variation of glycerol concentration on the current density ( $j$ ) at different potentials for glycerol solutions (15-124 mM) in 14mM MnO<sub>2</sub>.

Since the anodic oxidation is a heterogeneous process, the rate of the reaction is dependent of the surface concentration of the reactant. The molecular structure of the glycerol molecule influences the electrooxidation rate due to dipole induced the transmission of charge through a chain of atoms in the molecule. The electronic densities of the hydrogen atom of the hydroxyl group and of the C<sub>α</sub> are likely to decrease because the oxygen atom acts as electron acceptor (Fig. 38). As a result, the positive charge of the C<sub>α</sub> facilitates the dehydrogenation step and therefore the oxidation rate *e.g.* [84].

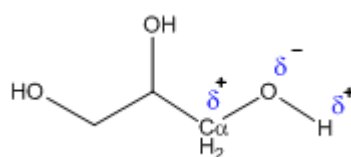


**Fig. 38:** Inductive effect of the glycerol molecule.

For the analysis of  $MnO_2$  reaction order, equation (326) was taken into account:

$$r' = (\partial \log I / \partial \log [MnO_2]) \quad (326)$$

When varying the concentration of  $MnO_2$  between 15 and 124 mM and keeping constant the concentration of glycerol (62 mM), an slope of  $r' = -0.61$ , 0.44 and 0.22 for peaks I, II and III respectively (Fig. 39). The negative sign is related to inhibition of glycerol oxidation by increasing of  $OH^-$  in the media. Increment of  $MnO_2$  concentration shifted the peak to more positive potentials. It is likely that the decreasing in current is due to oversaturation of  $OH^-$  and adsorbed intermediates which prevent the glycerol adsorption on Pt sites.

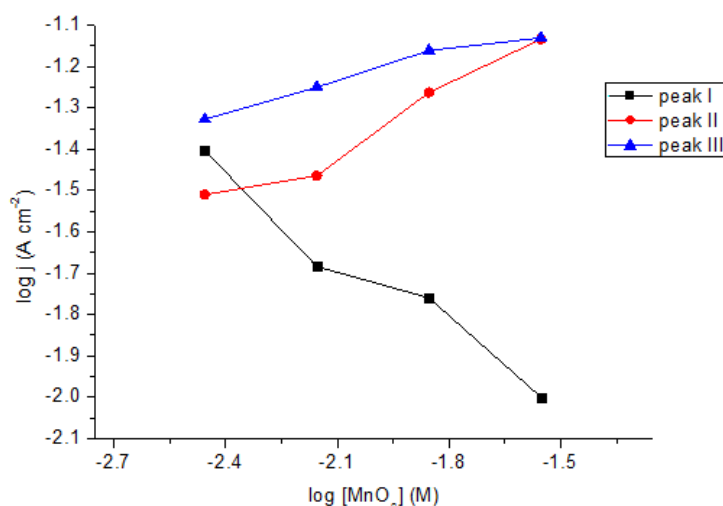


**Fig. 39:** Log of peak current vs log of oxidant concentration for partial oxidation of glycerol.

The analysis of kinetic parameters suggests the presence of a reversible electron transfer with adsorption-diffusion coupling and with a partial reaction order presented in Table 11.

**Table 11.** Reaction order with respect to glycerol and  $MnO_2$  for the electrooxidation of glycerol

$E$ (V) vs Ag/AgCl	$r$ $C_3H_8O_3$	$r'$ $MnO_2$	Expression for the rate of the determining step.
-0.6	0.6	-0.61	$v = k[MnO_2]^{-0.61}[C_3H_8O_3]^{0.6} e^{(nFE/RT)}$
0.105	0.48	0.44	$v = k[MnO_2]^{0.44}[C_3H_8O_3]^{0.48} e^{(nFE/RT)}$
0.75	0.22	0.22	$v = k[MnO_2]^{0.22}[C_3H_8O_3]^{0.22} e^{(nFE/RT)}$

## 11.5 The effect of potential scan limits on cyclic voltammogram

The variation of positive potential limits of scan are presented in Fig. 40, in a range of -1.5 to 1.5 V vs Ag/AgCl using solutions of 0.0625 M glycerol in

0.014M MnO<sub>2</sub> by cyclic voltammetry in platinum electrode at a scan rate of 0.05 V/s and room temperature. It is clearly seen that the increase in potential caused a slightly decrease in the peak current (I) during the anodic sweep. This might indicate that adsorbed glycerol or intermediates are blocking the surface of the platinum electrode.

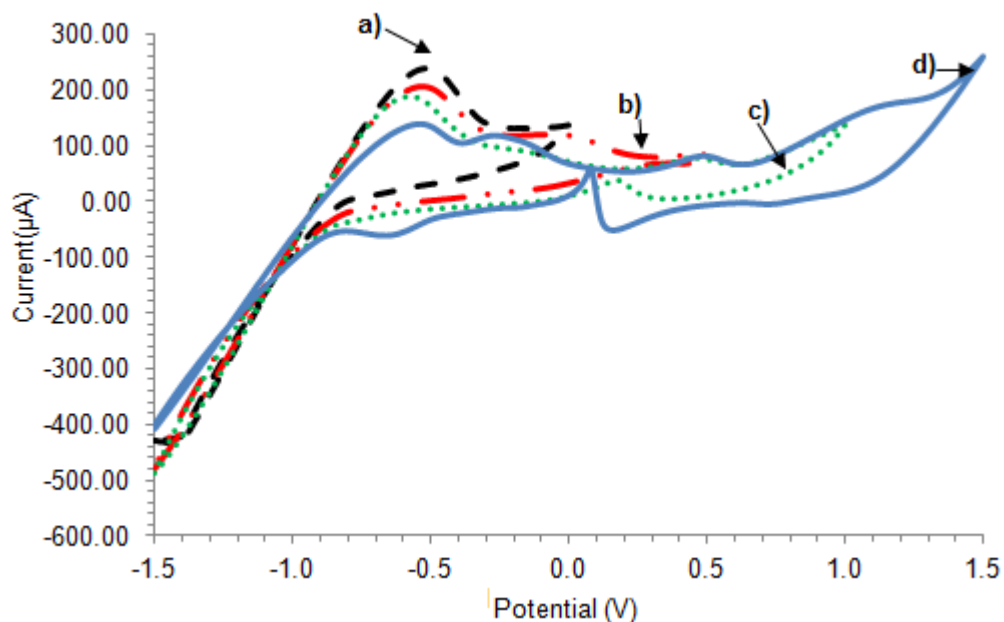


**Fig. 40:** Cyclic voltammogram for glycerol oxidation varying forward potential limit. a) 0 V, b) 0.5 V, c) 1 V, e) 1.5 V in 0.0625 M glycerol + 0.014 M MnO<sub>2</sub> (25 °C, 0.05 V/s).

When the scan limit is 1.5 V vs Ag/AgCl, there is a postwave at -0.235 V vs Ag/AgCl indicating the oxidation of strongly adsorbed reactant. A comparison using a potential limit of 1.3 V vs Ag/AgCl (Fig. 41) clearly shows that the peak on the negative potential is not affected by the adsorption of the reactant. At lower positive potential limits the reactant is weakly adsorbed and an increase in the current of the cathodic peak is observed due to the contribution of both, adsorbed and diffusing glycerol. The enhancement of the current peak in the reverse scan shows that the products are weakly adsorbed.

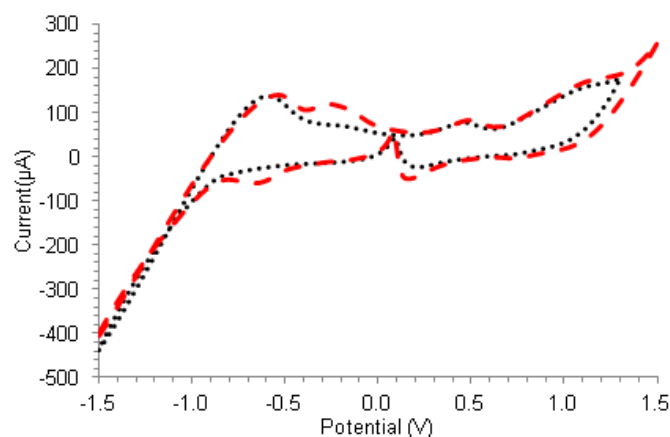


**Fig. 41:** Cyclic voltammogram for glycerol oxidation varying forward potential limit. (dotted line -1.5 to 1.3 V; dashed line (---) -1.5 to 1.5 V) in 0.0625 M glycerol + 0.014 M  $\text{MnO}_2$  (25 °C, 0.05 V/s).

The variation of negative potential limit is presented in Fig. 42. Using potentials of 0 and -0.5 V vs Ag/AgCl showed no oxidation or reduction peaks. Therefore, the oxidation started at more negative potentials. Increasing the negative potential limit enhanced current peaks which were shifted to more positive potentials. Since lower potential limits controls the hydrogen adsorption, as explained in [85], it can be stated that decreasing the potential did not caused an inhibition effect by possible reaction of adsorbed glycerol and the adsorbed hydrogen layer. The peak presented in the reversed scan (around 0.05-0.1V vs Ag/AgCl) using scans from -1.2 V vs Ag/AgCl arose from the reduction of oxides and glycerol oxidation, *e.g.* [86]. The increment on the current of the reverse scan peaks confirmed that the product was weakly adsorbed.

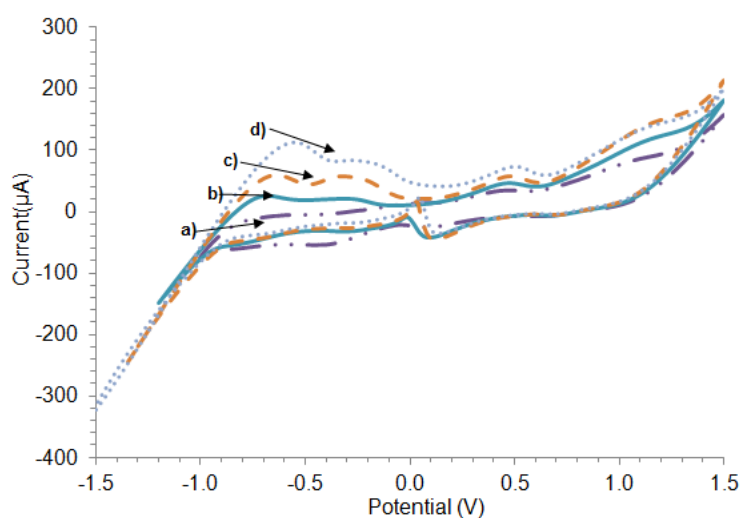


**Fig. 42:** The effect of varying the negative potential limit on cyclic voltammograms at 25 °C and 0.05 V/s. a) -1 V, b) -1.2 V, c) -1.35, d) -1.5 V.

## 11.6 The effect of sweep rate variation on cyclic voltammogram

The variation of sweep rate was studied from 0.01 to 0.08 V/s in 0.0625 M + 0.014 M MnO<sub>2</sub>. The dependence of the peak potential and variation of sweep rate is presented in Fig. 43. The potential for the peak (I) was shifted slightly to more negative potentials at higher sweep rates, while peaks (II) and (III) were shifted to more positive potentials (Fig. 44).

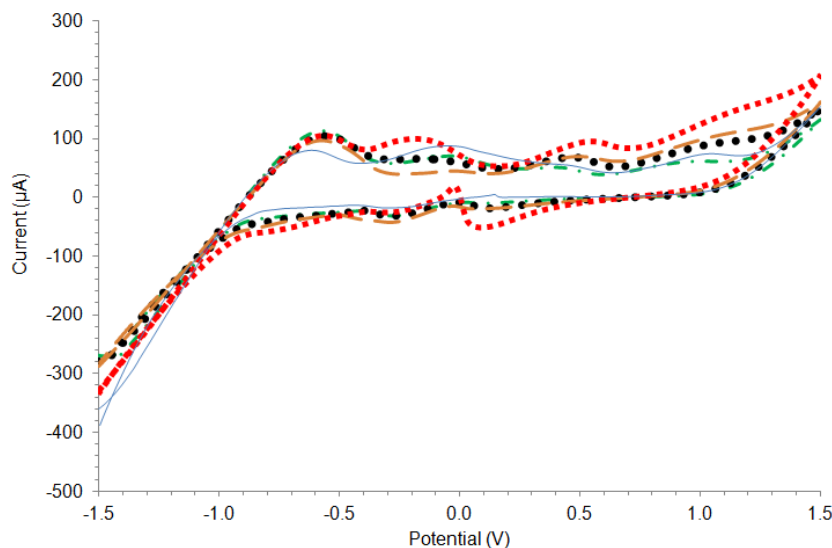


**Fig. 43:** Effect of varying the sweep rate on the voltammograms of a platinum electrode in 0.0625 M glycerol + 0.014 M MnO<sub>2</sub> (25 °C). Solid line: 0.01 V·s<sup>-1</sup>; dash dot line: 0.03 V·s<sup>-1</sup>; round dot line: 0.05 V·s<sup>-1</sup>; long dash line: 0.07 V·s<sup>-1</sup>; square dot line: 0.1 V·s<sup>-1</sup>.

The degree of kinetic reversibility is function of the sweep rate. It is expected that a reaction that is surface-transport-controlled is characterized by a non-variation of peak potential at small sweep rates and a linear variation of peak potential at higher sweep rates, *e.g.* [87]. The linear dependence of the anodic peak current on the corresponding square root of the scan rate showed that the oxidation process is surface-transport-controlled (Fig. 45). However, the fact that a linear relationship was also obtained for a peak current vs sweep rate plot (Fig. 46) suggests that the redox compound is also adsorbed on the electrode surface.

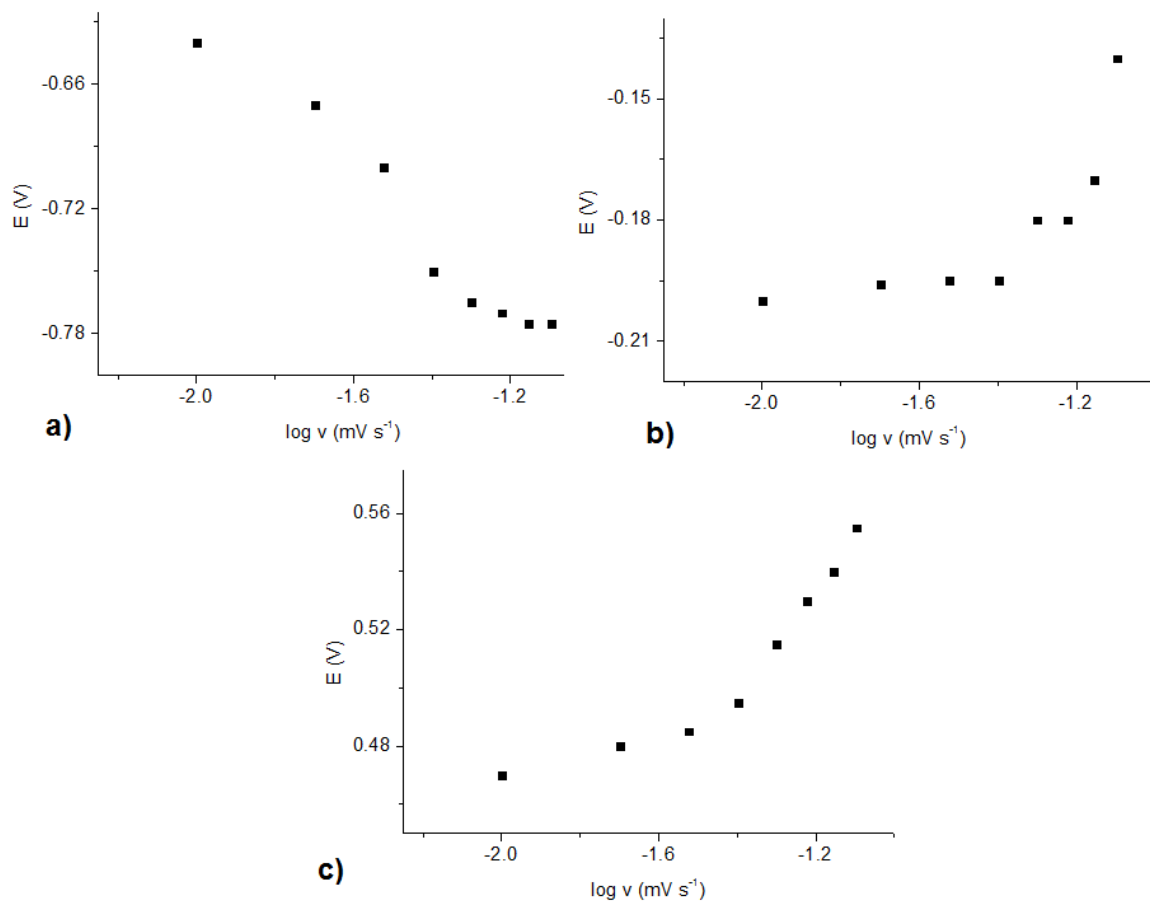


**Fig. 44:** Plot of peak potential against the logarithm of sweep rate for platinum electrode in 0.0625 M glycerol + 0.014 M MnO<sub>2</sub> (25 °C). a) Peak I, b) Peak II, c) Peak III.

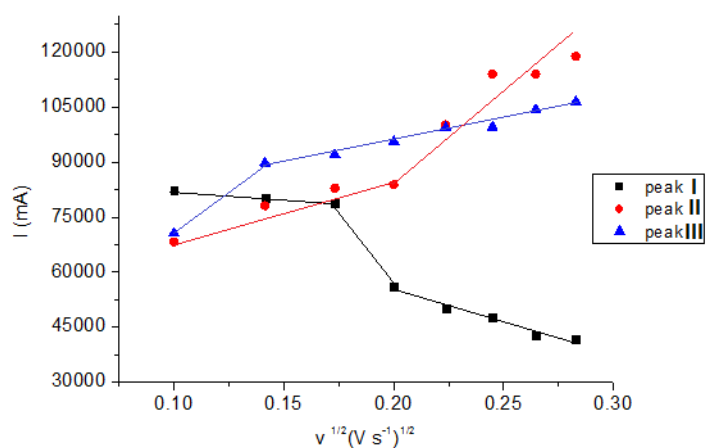


**Fig. 45:** Dependence on anodic peak current on the applied scan rate obtained from cyclic voltammetry.

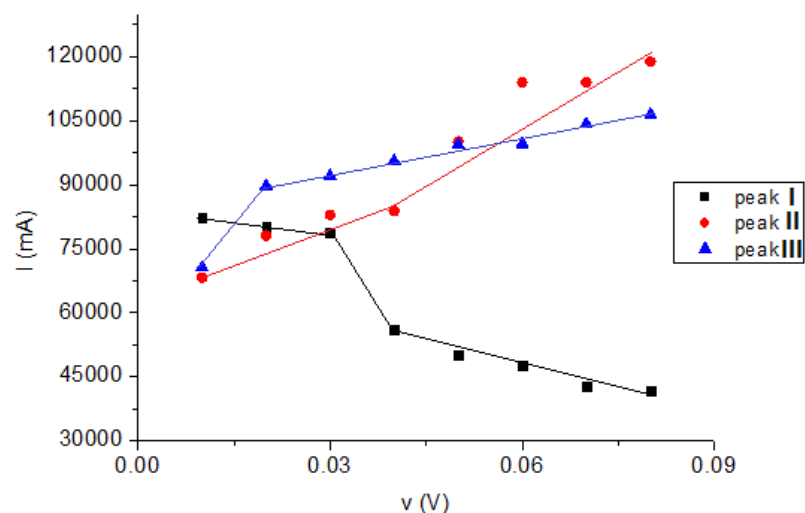


**Fig. 46:** Plot of current peak against sweep rate potential that shows the possibility of adsorbed species.

### 11.7 The effect of temperature on cyclic voltammogram

The variation of temperature in the range of 27 to 60 °C showed that the anodic current increased at higher temperatures. In addition, peaks I and II were shifted to more negative potentials. At 27°C, peaks I and II were found at -0.6, and 0.105 V vs Ag/AgCl respectively and at 60 °C, they appeared at -0.76 and -0.35 V vs Ag/AgCl. The determination of the apparent activation energy ( $\Delta E^*$ ) was performed from the slope values obtained in the plots of  $\log j$  vs.  $T^{-1}$  in the temperature range under study for peaks I and III and below 40 °C for peak II. The values were obtained from the linear regression and are presented in Table 12. Arrhenius plots for glycerol oxidation are presented in Fig. 47.

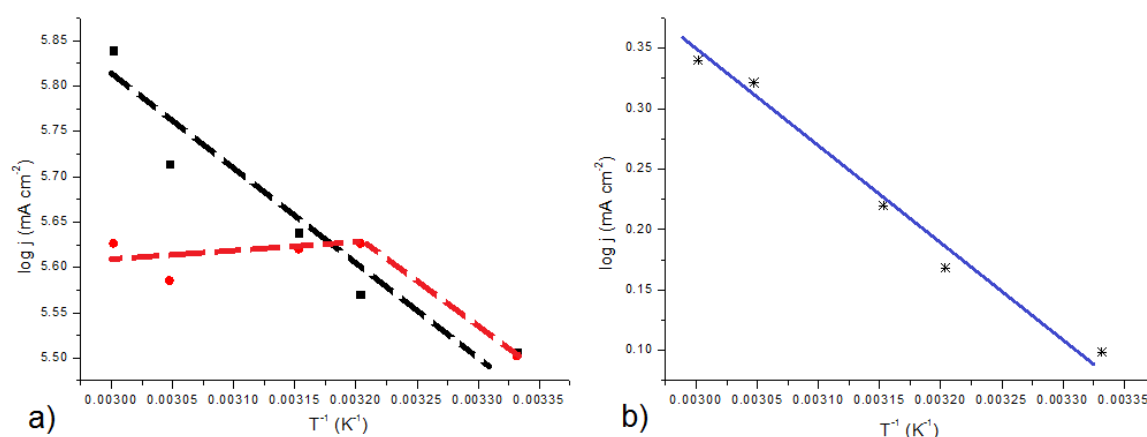


**Fig. 47:** Arrhenius plot for glycerol oxidation. (■) peak I; (●) peak II; (\*) peak III.

**Table 12.** Apparent activation energy ( $\Delta E^*$ ) for the forward scan peaks detected.

Peak	E (V) <sup>a</sup> vs Ag/AgCl	$\Delta E^*$ (kJ·mol <sup>-1</sup> )
I	-0.76	6.19
II	-0.35	7.48
III	0.8	6.52

<sup>a</sup> average of the peak potential at different temperatures

## 11.8 Oxidation at controlled potential by multiple pulse amperometry

The multiple pulse amperometry method was selected as a technique to perform the anodic oxidation for prolonged time at 0.5 V. A current decay was presented immediately after the first hour of reaction as presented in Fig. 48 a), suggesting contamination of the electrode surface by poisonous material that affects the electrode activity. Therefore, two different pulses of +1.5, and -1.5 V were included between the applied potential of 0.5 V allowing the current to be constant during the electrochemical reaction as shown in Fig. 48 b). A list of several experiments performed to evaluate the effect of stirring speed, temperature, reaction time, applied potential and pulses is presented in Appendix B.

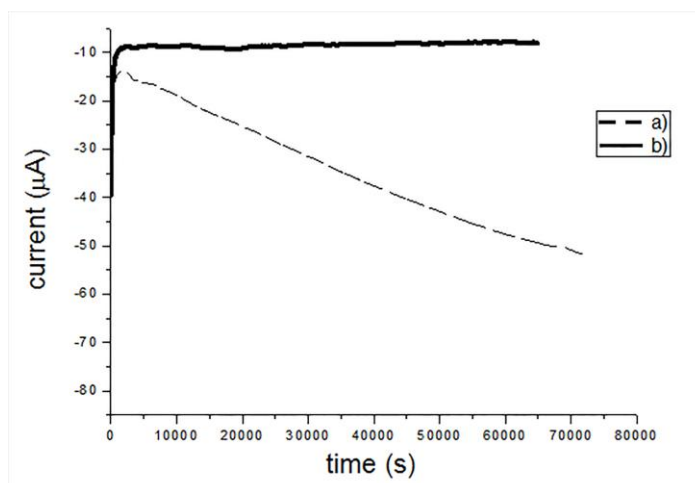


**Fig. 48:** Current vs time plot at controlled potential using multiple pulse amperometry a) without pulse steps of  $\pm 1.5$ V b) including pulse steps of  $\pm 1.5$ V for 1 s each.

The products formed were identified and quantified by means of HPLC using two different detectors (Ultraviolet and Refractive index detectors) to ensure the validity of the results. Agreement between both detectors in the quantification of products was always presented. Fig. 49 presents the variation of products

formed in function of reaction time. Data is presented in dimensionless values considering the initial concentration of glycerol. The fact that dihydroxyacetone was not reported as product suggests that the presence of more hydrogen atoms linked to the  $C_\alpha$  favored the glycerol oxidation as the oxidation of the second carbon did not occurred.

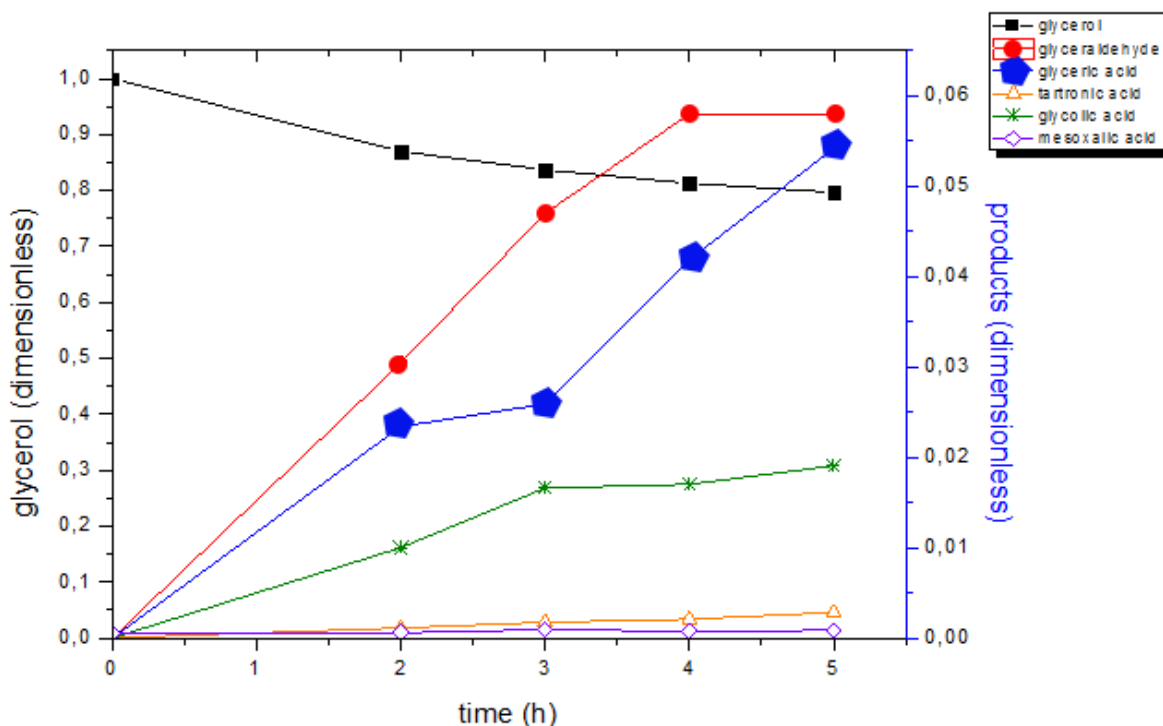


**Fig. 49:** Plot of glycerol and products formed (glyceric acid, glyceraldehyde, glycolic acid, tartronic acid, mesoxalic acid) (dimensionless) vs time of oxidation.

## 11.9 Evaluation of kinetic parameters using mathematical statistic method

As follows from the time analysis of the reaction mixture, mesoxalic and tartronic acids were also detected but their concentration was very low within the monitored time interval (0-5 h) compared to the concentrations of glycerol, glyceraldehyde, glyceric and glycolic acid. For this reason, their concentration was neglected for model analysis and simplification of the mechanism model. Therefore, the mechanism of the anodic glycerin oxidation could be described by the scheme presented previously in Fig. 4.

The kinetic model is represented by the following system of differential equations:

$$\frac{dc_A}{dt} = -k_1 c_A \quad (327)$$

$$\frac{dc_B}{dt} = k_1 c_A - k_2 c_B \quad (328)$$

$$\frac{dc_C}{dt} = k_2 c_B - k_3 c_C \quad (329)$$

$$\frac{dc_D}{dt} = k_3 c_C \quad (330)$$

The mentioned equations (327) to (330) represent a vector differential equation:

$$\dot{\mathbf{C}} = \mathbf{A} \cdot \mathbf{C} \quad (331)$$

$$\mathbf{C}(0) = \mathbf{C}_0 \quad (332)$$

By application of the Laplace transform we get:

$$\mathbf{C}_L - \mathbf{C}_0 = \mathbf{A} \cdot \mathbf{C}_L \quad (333)$$

$$\mathbf{C}_L = (\mathbf{sI} - \mathbf{A})^{-1} \mathbf{C}_0 \quad (334)$$

$$(\mathbf{sI} - \mathbf{A})^{-1} \mathbf{C}_0 = \begin{pmatrix} \frac{C_{A0}}{s+k_1} \\ \frac{C_{A0}k_1}{(s+k_1)(s+k_2)} \\ \frac{C_{A0}k_1k_2}{(s+k_1)(s+k_2)(s+k_3)} \\ \frac{C_{A0}k_1k_2k_3}{s(s+k_1)(s+k_2)(s+k_3)} \end{pmatrix} = \begin{pmatrix} C_{AL} \\ C_{BL} \\ C_{CL} \\ C_{DL} \end{pmatrix} \quad (335)$$

The analytical solution of the previous set of equations is presented in (336) to (339)

$$C_A = C_{A0} e^{-k_1 t} \quad (336)$$

$$C_B = \frac{C_{A0}k_1}{k_1 - k_2} (e^{-k_2 t} - e^{-k_1 t}) \quad (337)$$

$$C_C = C_{A0}k_1k_2 \left[ \frac{e^{-k_1 t}}{(k_3 - k_1)(k_2 - k_1)} + \frac{e^{-k_2 t}}{(k_3 - k_2)(k_1 - k_2)} + \frac{e^{-k_3 t}}{(k_2 - k_3)(k_1 - k_3)} \right] \quad (338)$$

$$C_D = C_{A0} - C_{A0}k_1k_2k_3 \left[ \frac{e^{-k_3 t}}{k_3(k_2 - k_3)(k_1 - k_3)} + \frac{e^{-k_2 t}}{k_2(k_3 - k_2)(k_1 - k_2)} + \frac{e^{-k_1 t}}{k_1(k_3 - k_1)(k_2 - k_1)} \right] \quad (339)$$

where the terms  $C_A$ ,  $C_B$ ,  $C_C$ , and  $C_D$  represents the concentration of glycerol, glyceraldehyde, glyceric acid, and glycolic acid respectively. The evaluation of the kinetic constant rates ( $k_1$ ,  $k_2$  and  $k_3$ ) was done by fitting the experimental data with the integrated kinetic equations (336) to (339). The final values found for  $k_1$ ,  $k_2$  and  $k_3$  were  $0.032 \text{ h}^{-1}$ ,  $0.49 \text{ h}^{-1}$  and  $0.27 \text{ h}^{-1}$  respectively. The evaluation of the rate constants is described in Fig. 50 by comparison with the experimental values. The numerical solution of the differential equations was performed using Runge Kutta of 4th order and is presented in Appendix C.

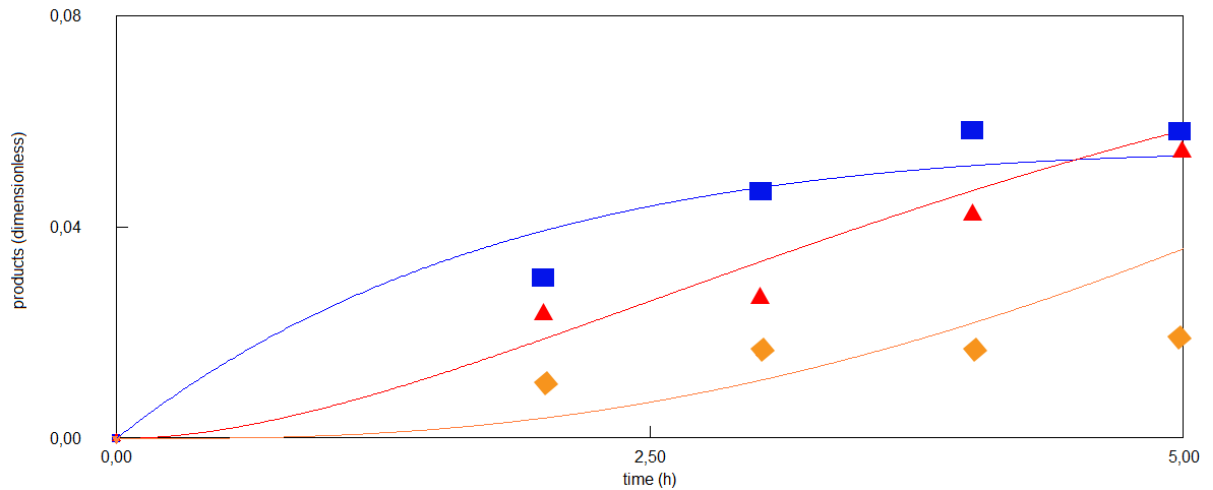


**Fig. 50:** Comparison between numerical results and experimental data for the partial electrochemical oxidation of glycerol. The products are (■) glycerinaldehyde, (▲) glyceric acid, and (◆) glycolic acid.

A concentration - time curve for each competing reaction was observed for the experimental and modeling data. However, a better fit can be achieved by developing more complex models, for example, in the case that a reversible reaction is considered, such as the presented in Fig. 23

The evaluation of the kinetic constant rates was performed using ERA 3.0 software, which uses the weighted sum of squares as objective function in order to minimize the weighted sum of squares of residual deviations. Fig. 51 and Fig. 52 presents the model fitting to experimental data for concentrations of glycerol and products using the rate constants of  $k_1=0.04516 \text{ h}^{-1}$ ,  $k_2=0.4263 \text{ h}^{-1}$ ,  $k_3=3.473 \text{ h}^{-1}$ ,  $k_4=4.3917 \text{ h}^{-1}$ ,  $k_5=6.269 \text{ h}^{-1}$ ,  $k_6=115.176 \text{ h}^{-1}$ ,  $k_7=38.413 \text{ h}^{-1}$ ,  $k_8=4.345 \text{ h}^{-1}$ ,  $k_9=3.674 \text{ h}^{-1}$ ,  $k_{10}=8.576 \text{ h}^{-1}$ .

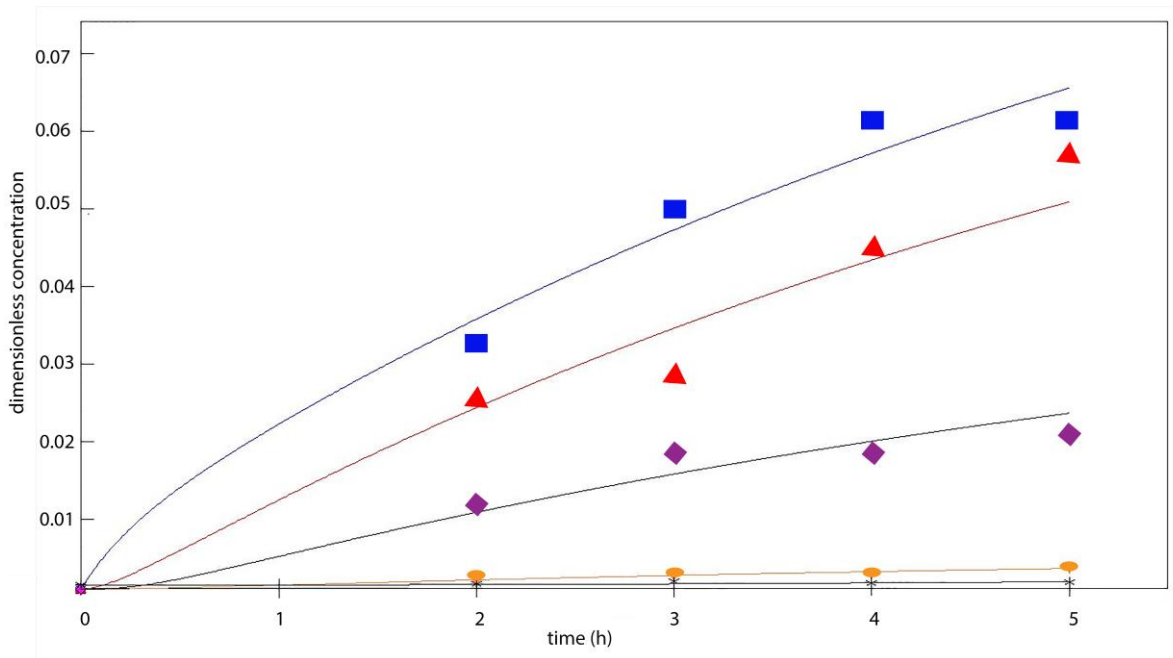


**Fig. 51:** Products concentration profile. Comparison between numerical results and experimental data for the mechanism described in Fig. 23 (■) glyceraldehyde, (▲) glyceric acid, (◆) glycolic acid, (●) tartronic acid, (\*) mesoxalic acid.

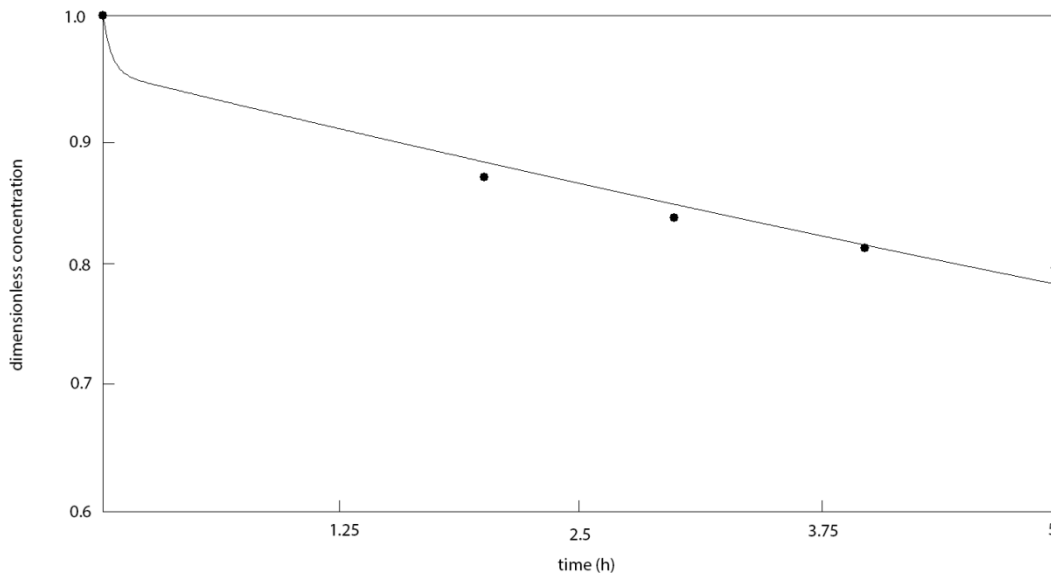


**Fig. 52:** Glycerol concentration profile. Comparison between numerical results and experimental data for the mechanism described in Fig. 23.

In order to test the transfer function proposed in Chapter 9, the previous values of rate constants were used in addition to  $C_{A0}=1 \text{ mol}\cdot\text{m}^{-3}$ . As a result, the state-space representation of the system is converted into the respective transfer functions, which are given by the following set of equations:

From input  $u_I=C_{A0}$  to output:

$$y_1 = C_A \rightarrow G(s) = \frac{s^5 + 184.744s^4 + 3653.0028s^3 + 23865.09s^2 + 48439.5s + 8034.97}{s^6 + 184.79s^5 + 3661.33s^4 + 24026.6s^3 + 49460.26s^2 + 9935.52s - 1.7785 \cdot 10^{-10}} \quad (340)$$

$$y_2 = C_B \rightarrow G(s) = \frac{0.04516s^4 + 8.1669s^3 + 133.813s^2 + 673.1926s + 851.1834}{s^6 + 184.79s^5 + 3661.33s^4 + 24026.6s^3 + 49460.26s^2 + 9935.52s - 1.7785 \cdot 10^{-10}} \quad (341)$$

$$y_3 = C_C \rightarrow G(s) = \frac{0.15684s^3 + 26.6918s^2 + 293.4246s + 673.1243}{s^6 + 184.79s^5 + 3661.33s^4 + 24026.6s^3 + 49460.26s^2 + 9935.52s - 1.7785 \cdot 10^{-10}} \quad (342)$$

$$y_4 = C_D \rightarrow G(s) = \frac{0.98323s^2 + 12.7044s + 36.638}{s^6 + 184.79s^5 + 3661.33s^4 + 24026.6s^3 + 49460.26s^2 + 9935.52s - 1.7785 \cdot 10^{-10}} \quad (343)$$

$$y_5 = C_E \rightarrow G(s) = \frac{37.769s + 323.9067}{s^6 + 184.79s^5 + 3661.33s^4 + 24026.6s^3 + 49460.26s^2 + 9935.52s - 1.7785 \cdot 10^{-10}} \quad (344)$$

$$y_6 = C_F \rightarrow G(s) = \frac{3.6124s + 15.6959}{s^6 + 184.79s^5 + 3661.33s^4 + 24026.6s^3 + 49460.26s^2 + 9935.52s - 1.7785 \cdot 10^{-10}} \quad (345)$$

Accordingly, the zero state response can be determined. For this, we firstly require to perform partial fraction expansion of equations (340) to (345):

$$Y_1(s) = \frac{0.8087}{s} - \frac{0.0003}{s+163.4955} + \frac{0.0003}{s+9.5843} + \frac{0.0003}{s+8.2891} + \frac{0.0002}{s+3.4065} + \frac{0.1908}{s+0.2246} + \quad (346)$$

$$Y_2(s) = \frac{0.0856}{s} - \frac{0.0003}{s+163.4955} - \frac{0.003}{s+9.5843} + \frac{0.0012}{s+8.2891} - \frac{0.0039}{s+3.4065} - \frac{0.0802}{s+0.2246} + \quad (347)$$

$$Y_3(s) = -\frac{0.0031}{s+9.5843} + \frac{0.0015}{s+8.2891} + \frac{0.0002}{s+3.4065} - \frac{0.0691}{s+0.2246} + \frac{0.0677}{s} \quad (348)$$

$$Y_4(s) = \frac{0.0001}{s+3.4065} - \frac{0.0039}{s+0.2246} + \frac{0.0037}{s} \quad (349)$$

$$Y_5(s) = -\frac{0.0004}{s+9.5843} - \frac{0.0001}{s+8.2891} + \frac{0.0037}{s+3.4065} - \frac{0.0358}{s+0.2246} + \frac{0.0326}{s} \quad (350)$$

$$Y_6(s) = -\frac{0.0002}{s+9.5843} + \frac{0.0003}{s+8.2891} - \frac{0.0017}{s+0.2246} + \frac{0.0016}{s} \quad (351)$$

Following, the previous equations in the s-domain are then expressed in the time domain using Inverse Laplace transform tables:

$$y_1(t) = -0.0003e^{-163.4955t} + 0.0003e^{-9.5843t} + 0.0003e^{-8.2891t} + 0.0002e^{-3.4065t} + 0.1908e^{-0.2246t} + 0.8087 \quad (352)$$

$$y_2(t) = 0.0003e^{-163.4955t} - 0.003e^{-9.5843t} + 0.0012e^{-8.2891t} - 0.0039e^{-3.4065t} - 0.0802e^{-0.2246t} + 0.0856 \quad (353)$$

$$y_3(t) = -0.0031e^{-9.5843t} + 0.0015e^{-8.2891t} + 0.0002e^{-3.4065t} - 0.0691e^{-0.2246t} + 0.0677 \quad (354)$$

$$y_4(t) = 0.0001e^{-3.4065t} - 0.0039e^{-0.2246t} + 0.0037 \quad (355)$$

$$y_5(t) = -0.0004e^{-9.5843t} - 0.0001e^{-8.2891t} + 0.0037e^{-3.4065t} - 0.0358e^{-0.2246t} + 0.0326 \quad (356)$$

$$y_6(t) = -0.0002e^{-9.5843t} + 0.0003e^{-8.2891t} - 0.0017e^{-0.2246t} + 0.0016 \quad (357)$$

The set of equations (340) to (345) are unstable to a step input. Appendix D describes the incorporation of PID controller to regulate the response to a stable output. Fig. 53 and Fig. 54 show the output response for oxidation products and glycerol respectively to an input ( $C_{A0}$ ) (impulse input)

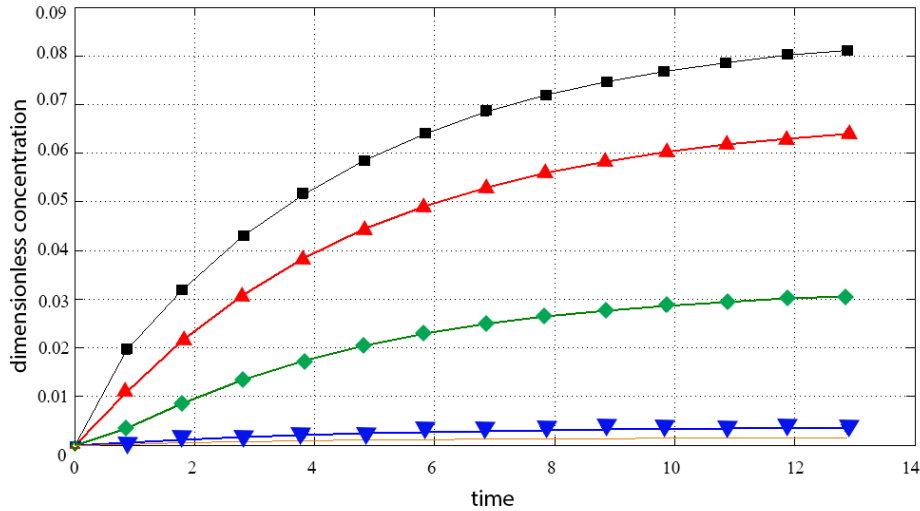


**Fig. 53:** Estimation of the output (products formed ■  $C_B$ ; ▲  $C_C$ ; ▼  $C_D$ ; ◆  $C_E$ ; —  $C_F$ ) after impulse input during anodic oxidation of glycerol.

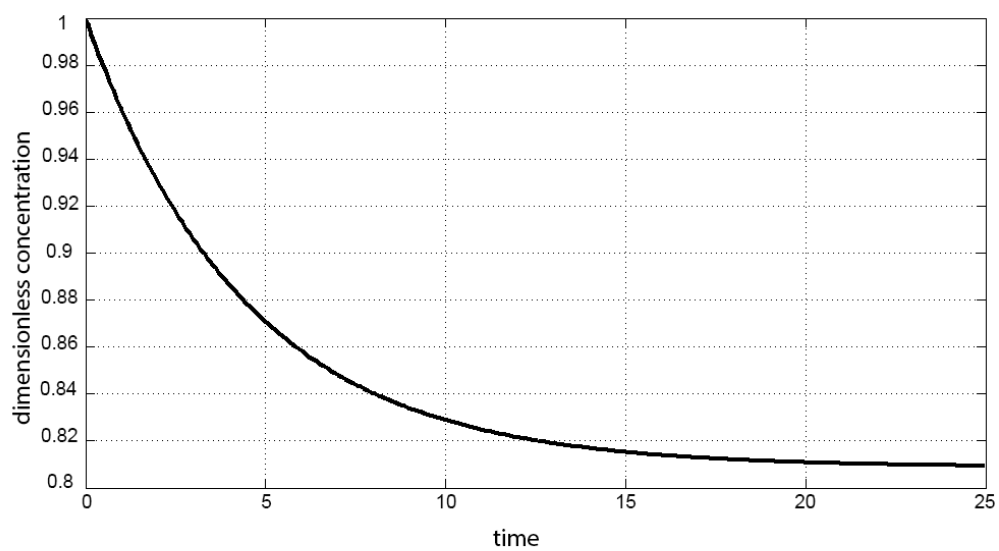


**Fig. 54:** Estimation of the concentration of glycerol (output) to an impulse input during electrooxidation of glycerol.

## 12 CONTRIBUTION OF THE THESIS TO SCIENCE AND PRACTICE AND DISCUSSION

Large amounts of glycerin are produced as a by-product of biodiesel production from vegetable oils and animal fats. The named raw materials are from the chemical point of view triglycerides of fatty acids, unsaturated in the case of vegetable oils and saturated in animal fats. For the utilization of fats and oils in diesel engines it is necessary to replace glycerin with short-chain aliphatic alcohols, most frequently methanol. The replacement is done through transesterification with methanol using alkali hydroxides or their methanlates as catalysts. The reaction gives two layers of limitedly miscible phases, where the upper layer contains predominantly fatty acid methyl esters (i.e. biodiesel), and the lower layer contains glycerin. The quality of the glycerin phase depends on the alkali catalyst used in transesterification, which is neutralized and followed by glycerin refining by vacuum distillation. Increasing production of biodiesel goes hand in hand with large quantities of excess glycerin for which it is crucial to find new innovative applications. It can be used in a number of ways, for example in the production of epichlorohydrin as a monomer of epoxy resins, or as a feed for farm animals. Energetic applications of glycerin comprise biogas production or direct combustion.

Today, special attention is paid to partial oxidation of glycerin, which gives oxidation intermediate products with high utility value. Great efforts in this sense are put into partial oxidation of glycerin to glyceraldehyde, the price of which (p.a. purity) exceeds by several times the price of gold. Glyceraldehyde of such purity is used in cosmetics as a component of very expensive lotions for skin smoothing.

I have described the production of glyceraldehyde from glycerin in detail in the bibliographic search of the thesis and also published in a renowned international chemical journal, Australian Journal of Chemistry, *e.g.* [10]. Partial oxidation of glycerin to glyceraldehyde gives other valuable products, in particular glycolic acid used as a component of protective skin lotions, and also glyceric, tartronic and mesoxalic acid used in pharmaceutical applications. Some of the named acids can find potential application as crosslinking agents in the production of biodegradable polymeric packing materials.

Although the evaluation of the state of the art contains a lot of publications dealing with glyceraldehyde production by means of electrochemistry, these papers give results based only on laboratory-scale testing. According to my best knowledge, there is no record of glyceraldehyde production by electrochemical means on at least pilot plant level. This makes the research into the production of pure glyceraldehyde a very complicated matter but at the same time more

interesting. Most of the publications do not deal in detail with possible mechanism of partial glycerin oxidation and its subsequent quantitative description including experimental verification of the proposed mathematical models. The transfer of experimental data to real industrial operation, even in case of qualified small-scale production, is very demanding; it involves other experimental steps to minimize the “distance” from the experimental conditions to the real operations. The disadvantage of large number of additional experiments is to large extent eliminated by modern approach using theoretical tools of modeling of a dynamic system, which not only allows transferring experimental data to industrial conditions, but also represents a crucial part of the exploitation of the production system which is an indispensable step in implementation of automated control systems of technological processes for a particular manufacturing procedure. The achievement of acceptable yield is conditioned by maintaining the reaction within optimal conditions of both the concentrations of the reaction components and particularly the reaction temperature, which necessarily requires an optimal control system. The complexity of partial oxidation of glycerin to glyceraldehyde can be encapsulated in the following points:

The partial oxidation of glycerin to glyceraldehyde is a series of consecutive reactions, which is in a simplified way depicted in Fig. 4 (p.29) and described by Equations (1-4) (p.30). The time at which the maximal yield is achieved is at the values of rate constants stated in Fig. 5 (p.31) 10 hours, at other values (see Fig. 6) the optimal time exceeds 20 h. The hypothetical example assumes isothermal process which means that all reaction heat is conducted away from the system which is fulfilled in the case of very small conversions in experimental anodic oxidation. The second case is the use of nitrous oxide or other oxidizers. A major problem of partial oxidation of glycerol lies in its low reactivity and high oxidation reactivity of glyceraldehyde, which is expressed by different values of the rate constants of oxidation in the first step of glycerin towards glyceraldehyde and in another when glyceraldehyde is oxidized to the subsequent oxidation products. A simplified mechanism for the partial oxidation of glycerol is described by Equations (15-19) and pages 32-34 of the graphical interpretation (Figures 7-10). Yield of glyceraldehyde depends on the ratio of rate constants for oxidation of glyceraldehyde and glycerin and the initial concentration of oxidizing agent. In this case, as the input value for the model calculations I chose a ratio of values of the specified constants and initial concentrations of nitrous oxide and glycerol.

In order to control the chemical reactor, it is important the estimation of the transfer function, which I calculated on the basis of dynamic models for the anodic oxidation, the oxidation of nitrous oxide for the isothermal case and the non-isothermal system in which imply a higher oxidation conversion of

glycerol. An important indicator of the technology is also the adiabatic temperature difference of the reaction mixture, and it is necessary to know also for the standard formed enthalpy of reaction. The values were estimated from published thermodynamic tables and also from the bond energy using bond enthalpies, achieving a very good agreement in the case of the calculated values of the heat of reaction for both procedures. In conclusion it can be stated that the expected production technology is relatively pure glyceraldehyde using anodic oxidation (cyclic voltammetry and multiple pulse amperometry) or controlled oxidation of nitrous oxide in low concentrations of glycerol.

## 13 RECOMMENDATION FOR INDUSTRIAL APPLICATIONS

The task of optimizing glycerol oxidation results from the need for efficient processing of surplus glycerol generated by the biodiesel industry. Given the considerable quantities of glycerol produced in biodiesel manufacture, two technologies, namely anodic oxidation and use of oxidation agents, are promising as they do not form such by-products that would contaminate the final reaction mixture. These include the use of hydrogen peroxide and nitrous oxide. In order to understand the glycerol oxidation reaction, it is important to proceed with the estimation of thermodynamic and kinetic parameters. The estimation of the adiabatic temperature rise during the glycerol oxidation reaction demonstrated the highly exothermic behavior and as a result, the risk behavior and dangerous situation of explosion while the reaction is proceeding. For this reason, it is necessary that in the specific case, the above value should be estimated and the results of mass, energy balance together with economic evaluation will be used in the design of a pilot plant including its control. As mentioned, the dissertation generally does not solve all the problems of pilot partial oxidation of glycerol but emphasizes what must be taken into account when planning specific practical technology.

Taking into account the results from this work and the current state of the heterogeneous and electrochemical oxidation of glycerol, further research on identification of reactive intermediates and conditions that cause the poisoning effect on electrodes and therefore decrease catalytic activity is suggested. In addition, the precise relationship between glycerol derivatives obtained at specific potentials should be addressed. Moreover, a detailed description of downstream processing for a potential application is considered essential, because in most cases recovery, extraction, purification, and crystallization of the product comprise the major part of the process costs and energy consumption. In relationship to the electrochemical oxidation, complementary analysis of polarographic waves, coulometric studies, steady-state current–voltage relationships, Tafel slopes determination, transfer coefficient, reaction order, and transient behavior at the electrode surface are necessary for the identification of partial steps in the reaction to elucidate the mechanism of the glycerol electro-oxidation process at specific working electrodes and under specific reaction conditions.

## 14 CONCLUSIONS

Among the different methods used for the identification of glycerol derivatives (mesoxalic acid, tartronic acid, glyceraldehyde, glyceric acid, glycolic acid and dihydroxyacetone), HPLC method conditions (mobile phase concentration, temperature, and flow rate) were fully optimized. This aspect is one of the most important to ensure reliable results since the current state of literature does not provide a full descriptive method for the identification of all the previous compounds. Moreover, the simultaneous analysis of these products is complicated by poor resolution resulting in peak overlapping. In order to suppress this phenomenon, the effect of column temperature, flow rate and concentration of aqueous  $H_2SO_4$  (used as mobile phase) was studied. All of these factors demonstrated to influence the separation of glycerol oxidation products on a sulfonated divinylbenzene-styrene resin column. Cyclic voltammetry and Multiple Pulse Amperometry were systematically analyzed to evaluate the effect of platinum electrode in presence of  $MnO_2$  for partial oxidation of glycerol. The description of the reaction mechanism of glycerol oxidation into its products was proposed, including the determination of the vector differential equations describing the anodic oxidation of glycerol with its solution and following simulation calculation.

Proposal of analytical solution of some deterministic models was performed. Design of non-linear kinetics of glycerin oxidation using  $N_2O$  as oxidizing agents was achieved. The evaluation of adiabatic temperature for closing and non closing reaction systems and presentation of the corresponding simulation calculations was carried out. The determination of the physical mathematical model for glycerol oxidation, performance of the linearization of the proposed model and determination of transfer function for control purposes was achieved. It was also developed quantitative experimental methods for the analysis of products reaction blend using liquid chromatography.

Agreement between numerical data (from mathematical modeling), experimental data and output using the respective transfer function and impulse input was observed. As a result, the determined transfer function of the system demonstrated to fully describe the process.

## 15 LITERATURE

- [1] ALENEZI, R., G.A. LEEKE, J.M. WINTERBOTTOM, R.C.D. SANTOS, A.R. KHAN. Esterification kinetics of free fatty acids with supercritical methanol for biodiesel production. *Energy Convers. Manag.* 2010, vol. 51, issue 5, p. 1055-1059.
- [2] BASHA, S.A., K.R. GOPAL, S. JEBARAJ. A review on biodiesel production, combustion, emissions and performance. *Renew. Sustain. Energy Rev.* 2009, vol. 13, 6-7, p. 1628-1634.
- [3] ABETI, M., W.M.A.W. DAUD, M.K. AROUA. Biodiesel production using alumina-supported calcium oxide: An optimization study. *Fuel Process. Technol.* 2010, vol. 91, issue 2, p. 243-248.
- [4] FERELLA, F., G. Mazziotti Di CELSO, I. De MICHELIS, V. STANISCI, F. VEGLIÒ. Optimization of the transesterification reaction in biodiesel production. *Fuel.* 2010, vol. 89, issue 1, p. 36-42.
- [5] JOVANOVIĆ, N., K. KOLOMAZNÍK, V. VAŠEK. Modeling two phases of refining process of animal fat. *Trans. VŠB – Tech. Univ. Ostrava, Mech. Ser.* [online]. 2008, vol. 2, issue 54, p. 43–48.
- [6] KRAHL, J., A. MUNACK, O. SCHRÖDER, H. STEIN, M. DUTZ, J. BÜNGER. Biodiesel and Swedish Low Sulfur Diesel Fuel as Ecologically Compatible Fuels in Modern Diesel Engines. *Fresen. Environ. Bull.* 2003, vol. 12, issue. 6, p. 640-647
- [7] SHARMA, Y.C. and Bhaskar SINGH. An ideal feedstock, kusum (*Schleichera triguga*) for preparation of biodiesel: Optimization of parameters. *Fuel.* 2010, vol. 89, issue 7, p. 1470-1474.
- [8] JÉRÔME, F., J. BARRAULT. Use of hybrid organic-siliceous catalysts for the selective conversion of glycerol. *Eur. J. Lipid Sci. Technol.*. 2010, vol. 113, issue 1, p. 118-134.
- [9] BELL, B.M., J.R. BRIGGS, R.M. CAMPBELL, S.M. CHAMBERS, P.D. GAARENSTROOM, J.G. HIPPLER, B.D. HOOK, K. KEARNS, J.M. KENNEY, W.J. KRUPER, D.J. SCHRECK, C.N. THERIAULT, C.P. WOLFE. Glycerin as a Renewable Feedstock for Epichlorohydrin Production. The GTE Process. *CLEAN - Soil, Air, Water.* 2008, vol. 36, issue 8, p. 657-661. DOI: 10.1002/clen.200800067.
- [10] BELTRÁN-PRIETO, J.C., K. KOLOMAZNÍK, J. PECHA. A Review of Catalytic Systems for Glycerol Oxidation: Alternatives for Waste Valorization. *Aust. J. Chem.* 2013, p. 511-521. DOI: 10.1071/ch12514.

- [11] DA SILVA, M. MACK, J. CONTIERO. Glycerol: a promising and abundant carbon source for industrial microbiology. *Biotechnol. Adv.* 2009, vol. 27, issue 1, p. 30-39.
- [12] ŠVITEL, J., E. ŠTURDÍK. Product yield and by-product formation in glycerol conversion to dihydroxyacetone by *Gluconobacter oxydans*. *J. Ferment. Bioeng.* 1994, vol. 78, issue 5, p. 351-355. DOI: 10.1016/0922-338x(94)90279-8.
- [13] TKÁČ, J., M. NAVRÁTIL, E. ŠTURDÍK, P. GEMEINER. Monitoring of dihydroxyacetone production during oxidation of glycerol by immobilized *Gluconobacter oxydans* cells with an enzyme biosensor. *Enzyme Microb. Technol.* 2001, vol. 28, 4-5, p. 383-388. DOI: 10.1016/s0141-0229(00)00328-8.
- [14] NAVRÁTIL, M., J. TKÁČ, J. ŠVITEL, B. DANIELSSON, E. ŠTURDÍK. Monitoring of the bioconversion of glycerol to dihydroxyacetone with immobilized *Gluconobacter oxydans* cell using thermometric flow injection analysis. *Process Biochem.* 2001, vol. 36, issue 11, p. 1045-1052. DOI: 10.1016/s0032-9592(00)00298-3.
- [15] HEKMAT, D., R. BAUER, J. FRICKE. Optimization of the microbial synthesis of dihydroxyacetone from glycerol with *Gluconobacter oxydans*. *Bioprocess Biosyst. Eng.* 2003, vol. 26, issue 2, p. 109-116. DOI: 10.1007/s00449-003-0338-9.
- [16] LI, M., J. WU, X. LIU, J. LIN, D. WEI, H. CHEN. Enhanced production of dihydroxyacetone from glycerol by overexpression of glycerol dehydrogenase in an alcohol dehydrogenase-deficient mutant of *Gluconobacter oxydans*. *Bioresour. Technol.* 2010, vol. 101, issue 21, p. 8294-8299. DOI: 10.1016/j.biortech.2010.05.065.
- [17] OHREM, H.L., H. VOB. Kinetics of polyol oxidation with *Gluconobacter oxydans*. *Biotechnol. Lett.* 1995, vol. 17, issue 11, p. 1195-1200. DOI: 10.1007/bf00128385.
- [18] WOLF, H. J. *Process for preparing glyceraldehyde from glycerol with methanol dehydrogenase*. IPC:C12N9/04 C12P7/24 (IPC1-7): C12P7/24 Patent 43539871982. Available in: [http://worldwide.espacenet.com/publicationDetails/biblio?DB=worldwide.espacenet.com&II=0&ND=3&adjacent=true&locale=en\\_EP&FT=D&date=19821012&CC=US&NR=4353987A&KC=A](http://worldwide.espacenet.com/publicationDetails/biblio?DB=worldwide.espacenet.com&II=0&ND=3&adjacent=true&locale=en_EP&FT=D&date=19821012&CC=US&NR=4353987A&KC=A)
- [19] HABE, H., T. FUKUOKA, D. KITAMOTO, K. SAKAKI. Biotransformation of glycerol to d-glyceric acid by *Acetobacter*

- tropicalis*. *Appl. Microbiol. Biotechnol.* 2008, vol. 81, issue 6, p. 1033-1039. DOI: 10.1007/s00253-008-1737-2.
- [20] LEE, P.C., W.G. LEE, S.Y. LEE, H.N. CHANG. Succinic acid production with reduced by-product formation in the fermentation of *Anaerobiospirillum succiniciproducens* using glycerol as a carbon source. *Biotechnol. Bioeng.* 2001, vol. 72, issue 1, p. 41-48. DOI: 10.1002/1097-0290(20010105)72:1<41::aid-bit6>3.3.co;2-e.
- [21] BIZZINI, A., C. ZHAO, A. BUDIN-VERNEUIL, N. SAUVAGEOT, J.-C. GIARD, Y. AUFRAY, A. HARTKE. Glycerol is metabolized in a complex and strain-dependent manner in *Enterococcus faecalis*. *J. Bacteriol.* 2009, vol. 192, issue 3, p. 779-785. DOI: 10.1128/jb.00959-09.
- [22] JOSEPH, B., S. MERTINS, R. STOLL, J. SCHAR, K. R. UMESHA, Q. LUO, S. MULLER-ALTROCK, W. GOEBEL. Glycerol Metabolism and PrfA Activity in *Listeria monocytogenes*. *J. Bacteriol.* 2008, vol. 190, issue 15, p. 5412-5430. DOI: 10.1128/jb.00259-08.
- [23] ZHANG, Y., F. GAO, S. ZHANG, Z. SU, G. MA, P. WANG. Simultaneous production of 1,3-dihydroxyacetone and xylitol from glycerol and xylose using a nanoparticle-supported multi-enzyme system with in situ cofactor regeneration. *Bioresour. Technol.* 2011, vol. 102, issue 2, p. 1837-1843. DOI: 10.1016/j.biortech.2010.09.069.
- [24] KETCHIE, W.C., M. MURAYAMA, R.J. DAVIS. Promotional effect of hydroxyl on the aqueous phase oxidation of carbon monoxide and glycerol over supported Au catalysts. *Top. Catal.* 2007, vol. 44, 1-2, p. 307-317. DOI: 10.1007/s11244-007-0304-x.
- [25] CARRETTIN, S., P. MCMORN, P. JOHNSTON, K. GRIFFIN, G.J. HUTCHINGS. Selective oxidation of glycerol to glyceric acid using a gold catalyst in aqueous sodium hydroxide. *Chemical Chem. Commun.* 2002, issue 7, p. 696-697. DOI: 10.1039/b201112n.
- [26] CARRETTIN, S., P. MCMORN, P. JOHNSTON, K. GRIFFIN, C.J. KIELY, G.A. ATTARD, G.J. HUTCHINGS. Oxidation of Glycerol Using Supported Gold Catalysts. *Top. Catal.* 2004, vol. 27, 1-4, p. 131-136. DOI: 10.1023/b:toca.0000013547.35106.0d.
- [27] PORTA, F., L. PRATI. Selective oxidation of glycerol to sodium glycerate with gold-on-carbon catalyst: an insight into reaction selectivity. *J. Catal.* 2004, vol. 224, issue 2, p. 397-403. DOI: 10.1016/j.jcat.2004.03.009.
- [28] DEMIREL-GÜLEN, S., M. LUCAS, P. CLAUS. Liquid phase oxidation of glycerol over carbon supported gold catalysts. *Catal. Today.* 2005, 102-103, p. 166-172. DOI: 10.1016/j.cattod.2005.02.033.

- [29] MALLAT, T., A. BAIKER. Oxidation of Alcohols with Molecular Oxygen on Solid Catalysts. *Chem. Rev.* 2004, vol. 104, issue 6, p. 3037-3058. DOI: 10.1055/sos-sd-036-00028.
- [30] KIMURA, H., K. TSUTO, T. WAKISAKA, Y. KAZUMI, Y. INAYA. Selective oxidation of glycerol on a platinum-bismuth catalyst. *Appl. Catal. A Gen.* 1993, vol. 96, issue 2, p. 217-228. DOI: 10.1016/0926-860x(90)80011-3.
- [31] BIANCHI, C. L., P. CANTON, N. DIMITRATOS, F. PORTA, L. PRATI. Selective oxidation of glycerol with oxygen using mono and bimetallic catalysts based on Au, Pd and Pt metals. *Catal. Today.* 2005, vol. 102-103, p. 203-212. DOI: 10.1016/j.cattod.2005.02.003.
- [32] GARCIA, R., M. BESSON, P. GALLEZOT, P. FORDHAM, R. GARCIA, M. BESSON, P. GALLEZOT. Chemoselective catalytic oxidation of glycerol with air on platinum metals. *Applied Catalysis A: General.* 1995, vol. 127, issue 1-2, p. 161-170. DOI: 10.1016/s0167-2991(96)80226-6.
- [33] HU, W., B. LOWRY, A. VARMA. Kinetic study of glycerol oxidation network over Pt–Bi/C catalyst. *Appl. Catal. B Environ.* 2011, vol. 106, issue 1, p. 123–132, DOI: 10.1016/j.apcatb.2011.05.015.
- [34] WORZ, N., A. BRANDNER, P. CLAUS. Platinum–Bismuth-Catalyzed Oxidation of Glycerol: Kinetics and the Origin of Selective Deactivation. *J. Phys. Chem. C.* 2010, vol. 114, issue 2, p. 1164-1172. DOI: 10.1021/jp909412h.
- [35] HU, W., D. KNIGHT, B. LOWRY, A. VARMA. Selective Oxidation of Glycerol to Dihydroxyacetone over Pt–Bi/C Catalyst: Optimization of Catalyst and Reaction Conditions. *Ind. Eng. Chem. Res.* 2010, vol. 49, issue 21, p. 10876-10882. DOI: 10.1021/ie1005096.
- [36] RODRIGUES, E.G., M.F.R. PEREIRA, X. CHEN, J.J. DELGADO, J.J.M. ÓRFÃO. Influence of activated carbon surface chemistry on the activity of Au/AC catalysts in glycerol oxidation. *J. Catal.* 2011, vol. 281, issue 1, s. 119-127. DOI: 10.1016/j.jcat.2011.04.008.
- [37] ZOPE, B.N., R.J. DAVIS, M. HRONEC, Z. CVENGROSOVA, J. TULEJA, J. ILAVSKY, T. MALLAT, Z. BODNAR, A. BAIKER, S. BENNETT, S. KALIQ, P. JOHNSTON, K. GRIFFIN. Inhibition of gold and platinum catalysts by reactive intermediates produced in the selective oxidation of alcohols in liquid water. *Green Chem.* 2011, vol. 13, issue 12, p. 308-317. DOI: 10.1201/9780203911013.ch15.
- [38] GUERRERO-PEREZ, M.O., J.M. ROSAS, J. BEDIA, J. RODRIGUEZ-MIRASOL, T. CORDERO. Recent Inventions in Glycerol Transformations

- and Processing. *Recent Patents Chem. Eng.* 2010, vol. 2, issue 1, p. 11-21. DOI: 10.2174/1874478810902010011.
- [39] BESSON, M., P. GALLEZOT. Selective oxidation of alcohols and aldehydes on metal catalysts. *Catal. Today.* 2000, vol. 57, 1-2, s. 127-141. DOI: 10.1016/s0920-5861(99)00315-6.
- [40] NIE, R., D. LIANG, L. SHEN, J. GAO, P. CHEN, Z. HOU. Selective oxidation of glycerol with oxygen in base-free solution over MWCNTs supported PtSb alloy nanoparticles. *Appl. Catal. B Environ.* 2012, vol. 127, p. 212-220. DOI: 10.1016/j.apcatb.2012.08.026.
- [41] KOROVCHENKO, P., C. DONZE, P. GALLEZOT, M. BESSON. Oxidation of primary alcohols with air on carbon-supported platinum catalysts for the synthesis of aldehydes or acids. *Catal. Today.* 2007, vol. 121, issue 1-2, s. 13-21. DOI: 10.1016/j.cattod.2006.11.007.
- [42] KOLTHOFF, I. M. A. I. MEDALIA. The Reaction between Ferrous Iron and Peroxides. I. Reaction with Hydrogen Peroxide in the Absence of Oxygen. *J. Am. Chem. Soc.* 1949, vol. 71, issue 11, p. 3777-3783. DOI: 10.1021/ja01179a057.
- [43] MANINI, P., P.La PIETRA, L. PANZELLA, A. NAPOLITANO, M. D'ISCHIA, T. OLPP. Glyoxal formation by Fenton-induced degradation of carbohydrates and related compounds. *Carbohydr. Res.* 2006, vol. 341, issue 11, p. 1828-1833. DOI: 10.1055/sos-sd-025-00285.
- [44] CIRIMINNA, R., M. PAGLIARO. One-Pot Homogeneous and Heterogeneous Oxidation of Glycerol to Ketomalonic Acid Mediated by TEMPO. *Adv. Synth. Catal.* 2003, vol. 345, issue 3, p. 383-388. DOI: 10.1002/adsc.200390043.
- [45] SHUL'PIN, G.B., Y.N. KOZLOV, L.S. SHUL'PINA, T.V. STRELKOVA, D. MANDELLI. Oxidation of Reactive Alcohols with Hydrogen Peroxide Catalyzed by Manganese Complexes. *Catalysis Letters.* 2010, vol. 138, 3-4, p. 193-204. DOI: 10.1007/s10562-010-0398-9.
- [46] ROSS, Sidney D, Manuel FINKELSTEIN, Eric J RUDD. *Anodic oxidation.* 1<sup>st</sup> ed. New York: Academic Press, 1975, 339 p. Organic chemistry, v. 32. ISBN 01-259-7650-X.
- [47] SCHNAIDT, J., M. HEINEN, D. DENOT, Z. JUSYS, R. J. BEHM. Electrooxidation of glycerol studied by combined in situ IR spectroscopy and online mass spectrometry under continuous flow conditions. *J. Electroanal. Chem.* 2011, vol. 661, issue 1, p. 250-264. DOI: 10.1016/j.jelechem.2011.08.011.

- [48] KWON, Y., S.C.S. LAI, P. RODRIGUEZ, M.T.M. KOPER. Electrocatalytic Oxidation of Alcohols on Gold in Alkaline Media: Base or Gold Catalysis?. *J J. Am. Chem. Soc.* 2011, vol. 133, issue 18, p. 6914-6917. DOI: 10.1021/ja200976j.
- [49] KYRIACOU, D., T.P. TOUGAS. Preparation of glyceric acid by anodic oxidation of glycerol at a silver oxide electrode. *J. Org. Chem.* 1987, vol. 52, issue 11, p. 2318-2319. DOI: 10.1021/jo00387a045.
- [50] ROQUET, L., E.M. BELGSIR, J.-M. LÉGER, C. LAMY. Kinetics and mechanisms of the electrocatalytic oxidation of glycerol as investigated by chromatographic analysis of the reaction products: Potential and pH effects. *Electrochim. Acta.* 1994, vol. 39, issue 16, p. 2387-2394. DOI: 10.1016/0013-4686(94)e0190-y.
- [51] LANG, Walther. *Manufacture of organic compounds by oxidation* CPC:C25B3/02. Patent 8080951905, Available in:  
[http://worldwide.espacenet.com/publicationDetails/biblio?DB=worldwide.espacenet.com&II=0&ND=3&adjacent=true&locale=en\\_EP&FT=D&date=19051226&CC=US&NR=808095A&KC=A](http://worldwide.espacenet.com/publicationDetails/biblio?DB=worldwide.espacenet.com&II=0&ND=3&adjacent=true&locale=en_EP&FT=D&date=19051226&CC=US&NR=808095A&KC=A)
- [52] MANEA, F., C. RADOVAN, I. CORB, A. POP, G. BURTICA, P. MALCHEV, S. PICKEN, J. SCHOONMAN. Electrochemical Oxidation and Determination of Oxalic Acid at an Exfoliated Graphite-Polystyrene Composite Electrode. *Sensors.* 2007, vol. 7, issue 4, p. 615-627. DOI: 10.3390/s7040615.
- [53] MARSHALL, A.T. R.G. HAVERKAMP. Production of hydrogen by the electrochemical reforming of glycerol–water solutions in a PEM electrolysis cell. *Int. J. Hydrogen Energy.* 2008, vol. 33, issue 17, p. 4649-4654. DOI: 10.1016/j.ijhydene.2008.05.029.
- [54] NAGAI, M., M. YOSHIDA, H. TOMINAGA. Reprint of “Tungsten and nickel tungsten carbides as anode electrocatalysts”. *Electrochim. Acta.*, 2007, vol. 53, issue 2, p. 1030-1036 [cit. 2014-12-08]. DOI: 10.1016/j.electacta.2007.09.036.
- [55] GONZÁLEZ, M.J., C.T. HABLE, M.S. WRIGHTON. Electrocatalytic Oxidation of Small Carbohydrate Fuels at Pt–Sn Modified Electrodes. *J. Phys. Chem. B.* 1998, vol. 102, issue 49, p. 9881-9890. DOI: 10.1021/jp982792d.
- [56] ZHOU, W.J., S.Q. SONG, W.Z. LI, Z.H. ZHOU, G.Q. SUN, Q. XIN, S. DOUVARTZIDES, P. TSIKARAS. Direct ethanol fuel cells based on PtSn anodes: the effect of Sn content on the fuel cell performance. *J. Power*

- Sources*. 2005, vol. 140, issue 1, p. 50-58. DOI: 10.1016/j.jpowsour.2004.08.003.
- [57] ZENG, J., J. YANG, J. Yang LEE, W. ZHOU. Preparation of Carbon-Supported Core-Shell Au-Pt Nanoparticles for Methanol Oxidation Reaction: The Promotional Effect of the Au Core. *J. Phys. Chem. B*. 2006, vol. 110, issue 48, s. 24606-24611. DOI: 10.1021/jp0640979.
- [58] WELLS, J. E., D.E. BABCOCK, W.G. FRANCE. The Nature of Electrode Reactions. I. Factors Affecting the Electrochemical Reduction of N-Nitrosomethylaniline 1. *J. Am. Chem. Soc.* 1936, vol. 58, issue 12, s. 2630-2632. DOI: 10.1021/ja01303a071.
- [59] CORRIOU, Jean-Pierre. *Process control: theory and applications*. 1<sup>st</sup> ed. New York: Springer, 2004, 752 p. ISBN 18-523-3776-1.
- [60] STEPHANOPOULOS, George. *Chemical process control: an introduction to theory and practice*. 1<sup>st</sup> ed. Englewood Cliffs, N.J.: Prentice-Hall, 1984, 696 p. ISBN 01-312-8629-3.
- [61] ROQUET, L., E.M. BELGSIR, J.-M. LÉGER, C. LAMY. Kinetics and mechanisms of the electrocatalytic oxidation of glycerol as investigated by chromatographic analysis of the reaction products: Potential and pH effects. *Electrochim. Acta*, 1994, vol. 39, issue 16, p. 2387-2394. DOI: 10.1016/0013-4686(94)e0190-y.
- [62] SEBORG, Dale E, Thomas EDGAR, Duncan MELLICHAMP. *Process dynamics and control*. 2nd ed. Hoboken, NJ: Wiley, 2004, 713 p. ISBN 04-710-0077-9.
- [63] BEQUETTE, B. *Process control: modeling, design, and simulation*. 1<sup>st</sup> ed. Upper Saddle River, N.J.: Prentice Hall PTR, 2003, 769 p. ISBN 01-335-3640-8.
- [64] DOMALSKI, E.S. Selected Values of Heats of Combustion and Heats of Formation of Organic Compounds Containing the Elements C, H, N, O, P, and S. *J. Phys. Chem. Ref. Data*. 1972, vol. 1, issue 2. DOI: 10.1063/1.3253099.
- [65] COTTRELL, T. L. *The Strengths of Chemical Bonds* 2<sup>nd</sup>. Butterworths Scientific Pub, 1958. ISBN 9781124078052.
- [66] Common Bond Energies (D) and Bond Lengths (r). YODER, C. Available online in:  
[http://www.wiredchemist.com/chemistry/data/bond\\_energies\\_lengths.html](http://www.wiredchemist.com/chemistry/data/bond_energies_lengths.html), April, 28, 2014

- [67] Bond enthalpy (Bond energy). CLARK J. Available online in: <http://www.chemguide.co.uk/physical/energetics/bondenthalpies.html>, 10-Feb-2014.
- [68] MAJER, Vladimir, Vaclav SVOBODA, Henry KEHIAIAN. H.V, *Enthalpies of vaporization of organic compounds : a critical review and data compilation*. 1<sup>st</sup> ed. Boston: Blackwell Scientific, 1985, 300 p. ISBN: 9780632015290
- [69] RIGHETTI, M.C, G SALVETTI, E. TOMBARI. Heat capacity of glycerol from 298 to 383K. *Thermochim. Acta*. 1998, vol. 316, issue 2, p. 193-195 DOI: 10.1016/s0040-6031(98)00302-5.
- [70] HIMMELBLAU, David Mautner, James B. RIGGS. *Basic principles and calculations in chemical engineering*. 8th ed. Upper Saddle River, NJ: Prentice Hall, 2012, 945 p. ISBN 01-323-4660-5.
- [71] JIN, H., B. SUBRAMANIAM. Exothermic oxidations in supercritical CO<sub>2</sub>: effects of pressure-tunable heat capacity on adiabatic temperature rise and parametric sensitivity. *Chem. Eng. Sci.* 2003, vol. 58, issue 9, p. 1897-1901. DOI: 10.1016/s0009-2509(03)00011-3.
- [72] PAGLIARO, M., R. CIRIMINNA, H. KIMURA, M. ROSSI, C. Della PINA. From Glycerol to Value-Added Products. *Angew. Chem. Int. Ed. Engl.* 2007, vol. 46, issue 24, p. 4434-4440. DOI: 10.1002/anie.200604694.
- [73] CLARIDGE C.A. and D. HENDLIN, "Oxidation of glycerol by *Streptococcus faecalis*," *J. Bacteriol.*, 1962 vol. 84, issue 6, p. 1181–1186.
- [74] WYMAN Charles, *Handbook on Bioethanol: production and utilization*. 1<sup>st</sup> ed. Washington, DC: Taylor, CRC Press, Applied Energy Technology Series, 1996, 424 p. ISBN 15-603-2553-4.
- [75] BULUSU, S., G. A. MILLS, V. WALKER. Analysis of Organic Acids in Physiological Fluids by High Performance Liquid Chromatography. *J. Liq. Chromatogr.* 1991, vol. 14, issue 9, p. 1757-1777. DOI: 10.1080/01483919108049652.
- [76] SNYDER, Lloyd R, J KIRKLAND, Joseph L GLAJCH. *Practical HPLC method development*. 2nd ed. New York: Wiley, 1997, 765 p. ISBN 04-710-0703-X.
- [77] Enthalpy of fusion table. Available online in: <http://www.phs.d211.org/Science/smithcw/AP%20Chemistry/Posted%20Tables/Enthalpy%20Vaporization%20and%20Fusion.pdf>, June, 26, 2014.
- [78] NIST Standard Reference Data, Enthalpy of formation table, 2006. Available online in:

<http://www.rtmsd.org/cms/lib/PA01000204/Centricity/Domain/123/NISTThermodynamicTables.pdf>, June, 25,2014

- [79] CHEN, H, B FANG, Z HU. Simultaneous HPLC determination of four key metabolites in the metabolic pathway for production of 1,3-propanediol from glycerol. *Chromatographia*. 2007, vol. 65, 9-10, p. 629-632. DOI: 10.1016/s0009-5893(07)82072-8.
- [80] KWON, Y., M.T.M. KOPER. Combining Voltammetry with HPLC: Application to Electro-Oxidation of Glycerol. *Anal. Chem.* 2010, vol. 82, issue 13, p. 5420-5424. DOI: 10.1021/ac101058t.
- [81] RIBANI, M., C.H. COLLINS, C.B.G. BOTTOLI. Validation of chromatographic methods: Evaluation of detection and quantification limits in the determination of impurities in omeprazole. *J. Chromatogr. A*, 2007, vol. 1156, 1-2, p. 201-205. DOI: 10.1016/j.chroma.2006.12.080.
- [82] BELTRÁN-PRIETO J.C., J. PECHA, V. KAŠPÁRKOVÁ, K. KOLOMAZNÍK, Development of an HPLC method for the determination of glycerol oxidation products, *J. Liq. Chromatogr. Relat. Technol.*, 2013, vol. 36, issue. 19, p. 2758–2773,
- [83] VELÁZQUEZ-PALENZUELA, A., F. CENTELLAS, J.A. GARRIDO, C. ARIAS, R. M. RODRÍGUEZ, E. BRILLAS, P. CABOT. Kinetic analysis of carbon monoxide and methanol oxidation on high performance carbon-supported Pt–Ru electrocatalyst for direct methanol fuel cells. *J. Power Sources*, 2011, vol. 196, issue 7, p. 3503-3512. DOI: 10.1016/j.jpowsour.2010.12.044.
- [84] TAKKY, D., B. BEDEN, J.-M. LEGER, C. LAMY. Evidence for the effect of molecular structure on the electrochemical reactivity of alcohols. *J. Electroanal. Chem. Interfacial Electrochem.* 1985, vol. 193, 1-2, p. 159-173. DOI: 10.1016/0022-0728(85)85060-9.
- [85] LAMY, C. Electrocatalytic oxidation of organic compounds on noble metals in aqueous solution. *Electrochim. Acta*. 1984, vol. 29, issue 11, p. 1581-1588. DOI: 10.1016/0013-4686(84)85012-4.
- [86] SCHELL, M., Y. XU, Z. ZDRAVESKI. Mechanism for the Electrocatalyzed Oxidation of Glycerol Deduced from an Analysis of Chemical Instabilities. *J. Phys. Chem.* 1996, vol. 100, issue 49, p. 18962-18969. DOI: 10.1021/jp961195t.
- [87] LYONS, M.E.G., G.P. KEELEY. The Redox Behaviour of Randomly Dispersed Single Walled Carbon Nanotubes both in the Absence and in the Presence of Adsorbed Glucose Oxidase. *Sensors*. 2006, vol. 6, issue 12, p. 1791-1826. DOI: 10.3390/s6121791.

## APPENDIX A

HPLC chromatogram of some anodic oxidation experiments.

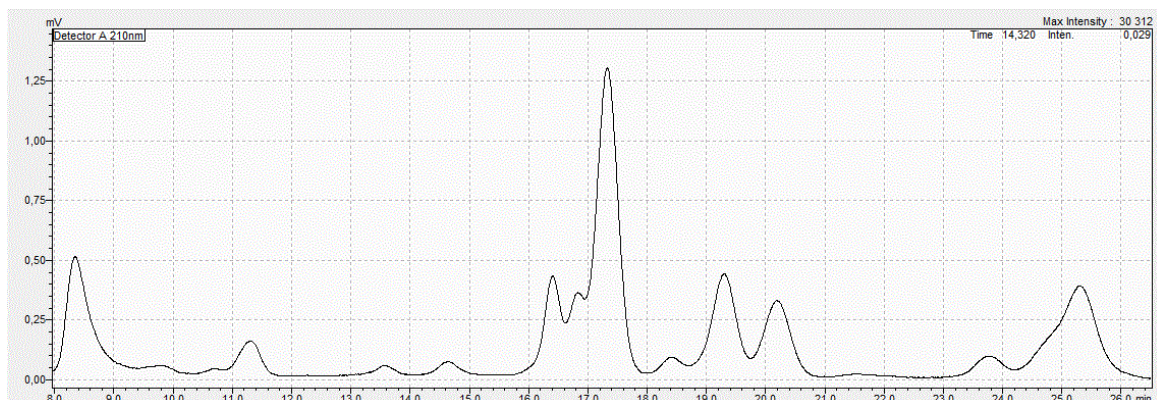


**Fig. 55:** Technique: Multiple pulse amperometry, E1:1.05V, t1=2s, E2:-1.5V, t2=1s, E3:1.5V, t3=1s, reaction time 2h

Compound	Concentration (mg·mL <sup>-1</sup> )
Glyceraldehyde	0.06
Glyceric acid	0.0066
Glycolic acid	0.0095
Mesoxalic acid	0.0029
Tartronic acid	0.00044

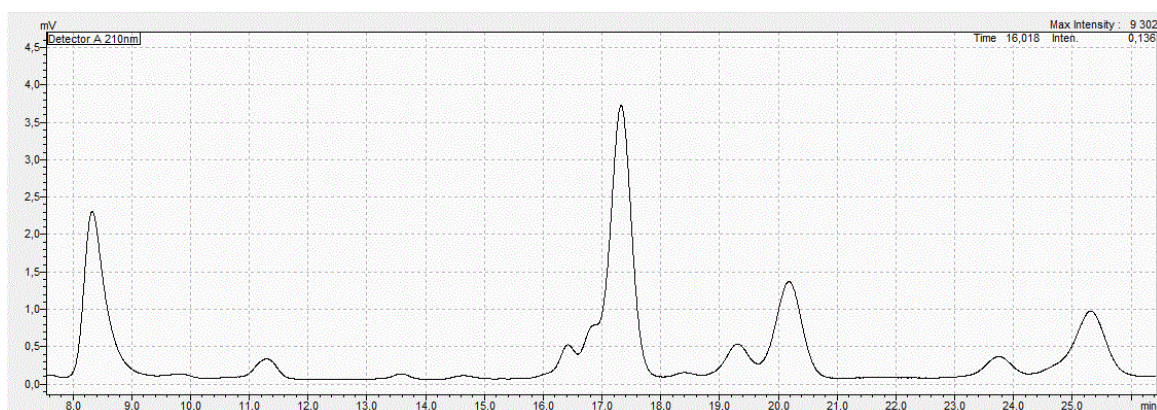


**Fig. 56:** Technique: Multiple pulse amperometry, E1:1.05V, t1=2s, E2:-1.5V, t2=1s, E3:1.5V, t3=1s, reaction time 5h

Compound	Concentration (mg·mL <sup>-1</sup> )
Glyceraldehyde	0.187
Glyceric acid	0.029
Glycolic acid	0.02
Mesoxalic acid	0.014
Tartronic acid	0.001

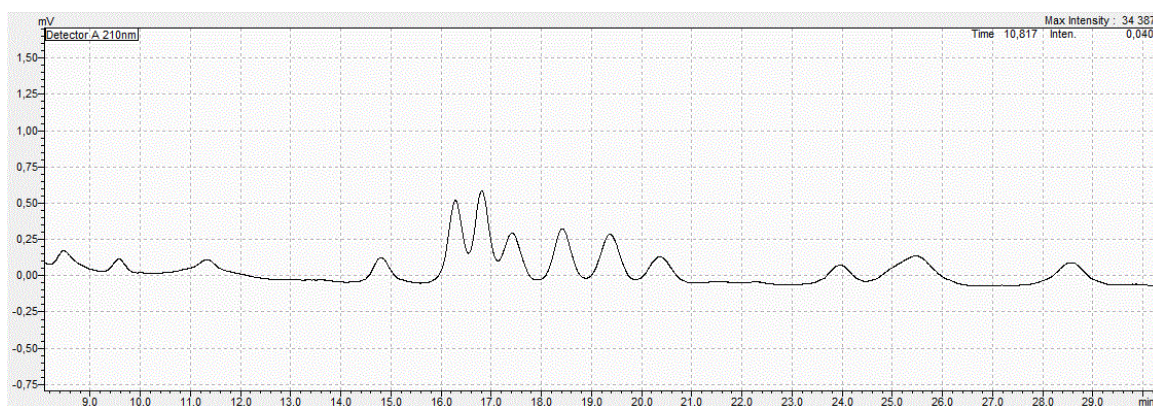


**Fig. 57:** Technique: Multiple pulse amperometry, E1:0.7V, t1=2s, E2:-1.5V, t2=1s, E3:1.5V, t3=1s, reaction time 16h

Compound	Concentration ( $\text{mg}\cdot\text{mL}^{-1}$ )
Glyceraldehyde	0.014
Glyceric acid	0.004
Glycolic acid	0.005
Mesoxalic acid	0.003
Tartronic acid	0.0005

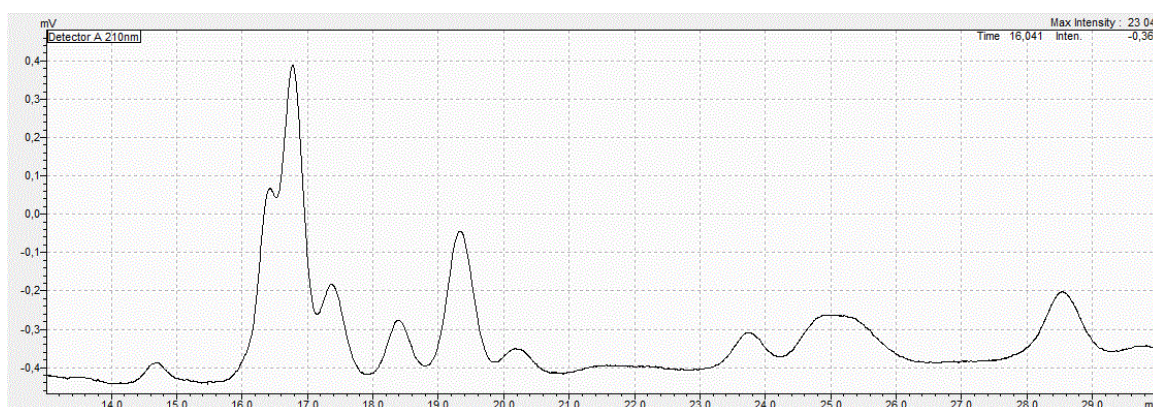


**Fig. 58:** Technique: Multiple pulse amperometry, E1:0.7V, t1=2s, E2:-1.5V, t2=1s, E3:1.5V, t3=1s, reaction time 11h

Compound	Concentration ( $\text{mg}\cdot\text{mL}^{-1}$ )
Glyceraldehyde	0.01
Glyceric acid	0.001
Glycolic acid	0.003
Mesoxalic acid	0.002
Tartronic acid	0.0002

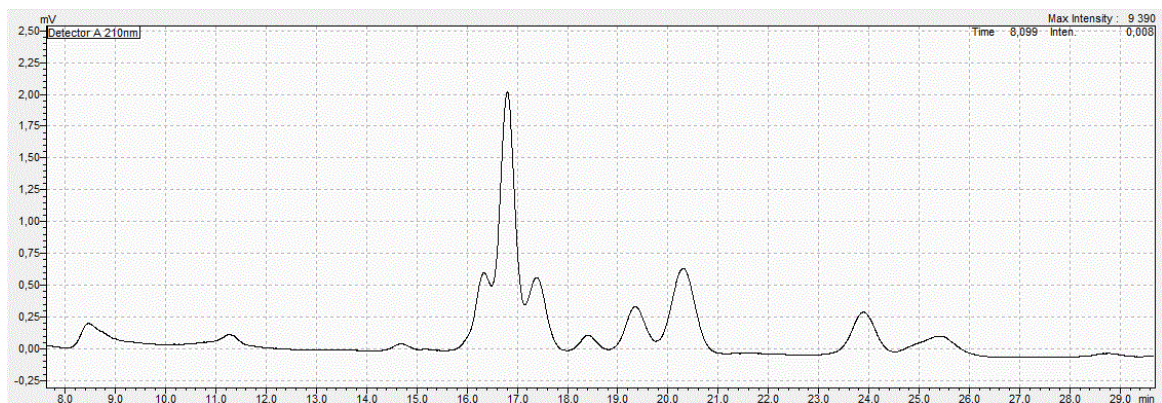


**Fig. 59:** Technique: Multiple pulse amperometry, E1:1.05V, t1=2s, E2:1.5V, t2=1s, E3:0.7V, t3=1s, reaction time 13h

Compound	Concentration (mg·mL <sup>-1</sup> )
Glyceraldehyde	0.0252
Glyceric acid	0.012
Glycolic acid	0.004
Mesoxalic acid	0.002
Tartronic acid	0.0003

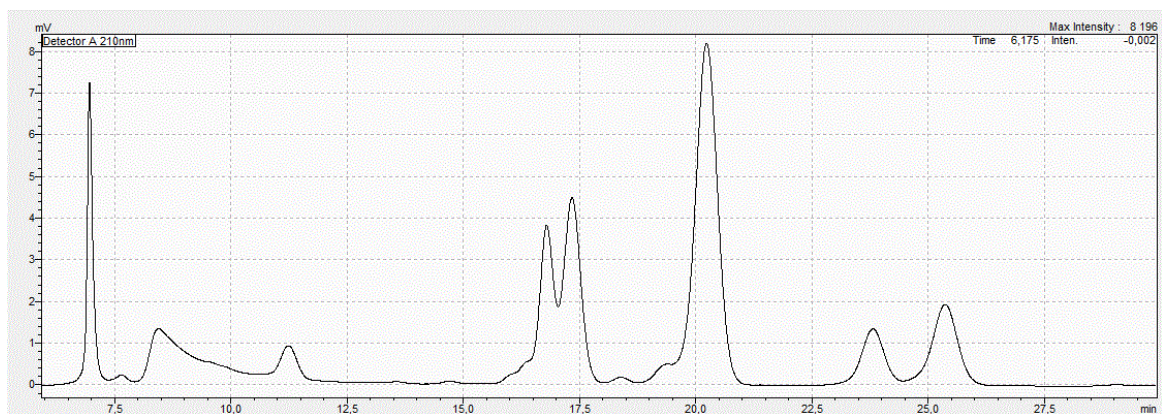


**Fig. 60:** Technique: Multiple pulse amperometry, E1:1.05V, t1=2s, E2:-1.5V, t2=1s, E3:1.5V, t3=1s, reaction time 14h, 100 rpm, 63 °C

Compound	Concentration (mg·mL <sup>-1</sup> )
Glyceraldehyde	0.21
Glyceric acid	0.20
Glycolic acid	0.048
Mesoxalic acid	0.017
Tartronic acid	0.003

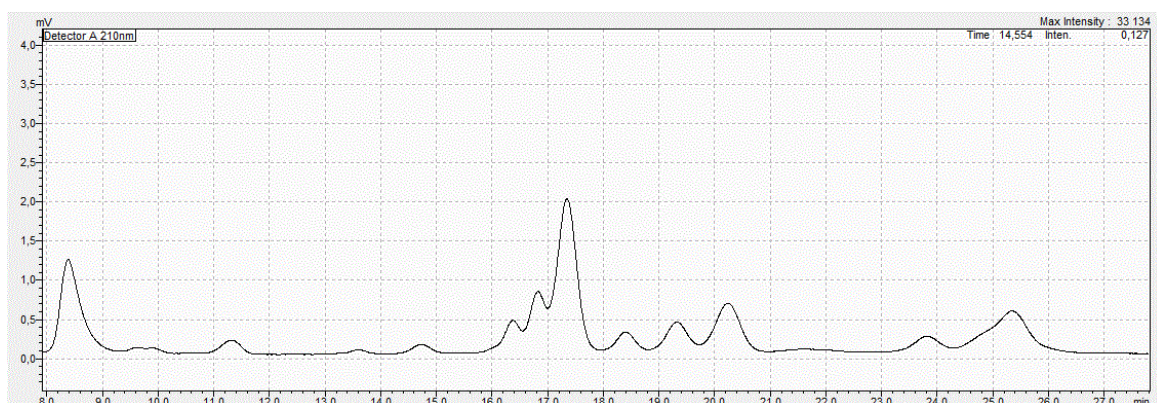


**Fig. 61:** Technique: Multiple pulse amperometry, E1:1.05V, t1=2s, E2:-1.5V, t2=1s, E3:1.5V, t3=1s, reaction time 7h

Compound	Concentration (mg·mL <sup>-1</sup> )
Glyceraldehyde	0.088
Glyceric acid	0.014
Glycolic acid	0.014
Mesoxalic acid	0.007
Tartronic acid	0.001

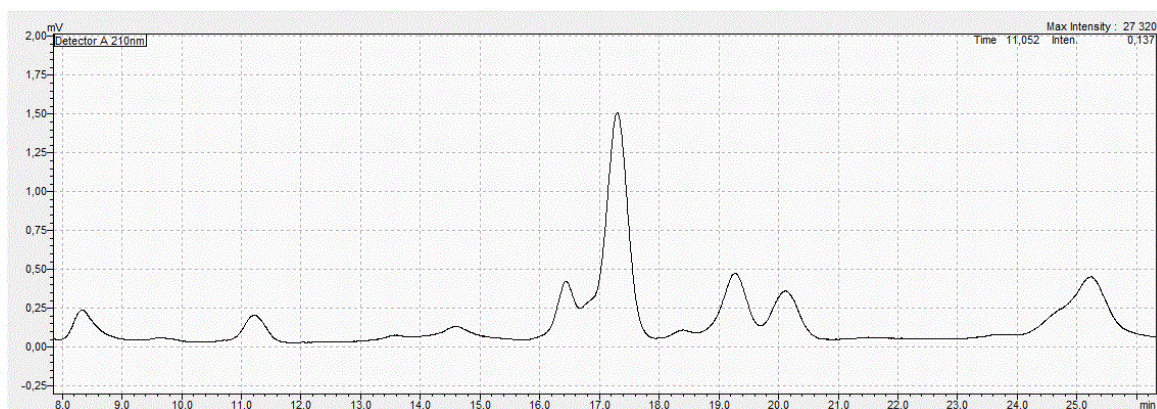


**Fig. 62:** Technique: Multiple pulse amperometry, E1:1.05V, t1=2s, E2:-1.5V, t2=1s, E3:1.5V, t3=1s, reaction time 4h

Compound	Concentration (mg·mL <sup>-1</sup> )
Glyceraldehyde	0.230
Glyceric acid	0.049
Glycolic acid	0.032
Mesoxalic acid	0.023
Tartronic acid	0.002

## APPENDIX B

List of selected experiments performed for the evaluation of parameters affecting the anodic oxidation of glycerol and influence on selectivity and conversion to glyceraldehyde

Glycerol	stirring speed	T	E1	t1	E2	t2	E3	t3	time	glyceraldehyde	
										selectivity	conversion
(mg/mL)	(rpm)	°C	(V)	(s)	(V)	(s)	(V)	(s)	(h)	(%)	(%)
5,533	100	65	1,05	2	-1,5	1	1,5	1	14	31,33	1,54
5,533	250	63	1,05	2	-1,5	1	1,5	1	9	0,27	0,015
5,533	100	70	1,05	2	-1,5	1	1,5	1	12	0,62	0,03
5,533	100	55	1,05	2	-1,5	1	1,5	1	8	0,22	0,012
5,2	100	63	1,05	2	-1,5	1	1,5	1	14	52,3	4,31
5,2	100	63	1,05	2	-1,5	1	1,5	1	7	54,11	3,02
5,496	100	63	1,05	2	-1,5	1	1,5	1	14	34,23	3,23
5,496	100	63	1,05	2	-1,5	1	1,5	1	7	45,5	1,77
5,723	100	65	1,05	2	-1,5	1	1,5	1	27	22	4,25
5,532	100	65	1,05	2	-1,5	1	1,5	1	15	50,33	4,71
5,51	100	65	1,05	2	-1,5	1	1,5	1	2	34,87	0,92
5,51	100	65	1,05	2	-1,5	1	1,5	1	5	37,6	2,56
5,51	100	65	1,05	16	-1,5	8	1,5	8	14	42,8	2,83
5,51	100	63	1,05	2	-1,5	1	1,5	1	6	75,7	3,98
5,51	100	63	1,05	2	-1,5	1	1,5	1	3	56,3	2,34
5,7	100	63	1,05	18	-1,5	4	1,5	4	11,5	66,8	3,89
5,51	100	63	1,05	2	-1,5	1	1,5	1	6	23,74	2,21
5,7	100	63	1,05	2	-1,5	1	1,5	1	4	31,8	2,67
5,932	100	63	1,05	2	-1,5	1	1,5	1	2	14,6	1,03
5,932	100	63	1,05	2	-1,5	1	1,5	1	5	42,5	2,93
5,7	100	63	1,05	22	-1,5	2	1,5	2	11,5	30,51	4,03
1,498	100	63	1,05	2	-1,5	1	1,5	1	2	9,04	0,46
1,498	100	63	1,05	2	-1,5	1	1,5	1	1	6,78	0,19
5,592	100	63	1,05	2	-1,5	1	1,5	1	4	31,79	1,22
0,715	100	63	1,05	2	-1,5	1	1,5	1	2	10,88	0,48
5,595	100	63	1,05	2	-1,5	1	1,5	1	15	66,55	5,897
5,595	100	63	1,05	2	-1,5	1	1,5	1	43	20	5,29
5,662	100	63	1,05	2	-1,5	1	1,5	1	19	71,6	7,68
0,71	100	63	1,05	2	-1,5	1	1,5	1	7	65,8	5,37
0,697	100	63	1,05	2	-1,5	1	1,5	1	20,7	25,88	7,52
0,697	100	63	1,05	2	-1,5	1	1,5	1	9	53,76	9,99

## APPENDIX C

Program developed in Matlab for the simulation of chemical reaction in series  
 $A \rightarrow B \rightarrow C \rightarrow D$

```
%Simulation of a type of glycerol oxidation  A-->B-->C-->D
% k1  k2  k3
% A-GLYCEROL , dca/dt=-k1*ca
% B-GLYCERALDEHYDE , dcb/dt=k1*ca-k2*cb
% C-GLYCERIC ACID, dcc/dt=k2*cb-k3*cc
% D-GLYCOLIC ACID, dcd/dt=k3*cc

% time increment (min)
h=0.5;
%time
t0=0;
%period (min)
time=20;
% value of K1 (min^-1)
k1=0.04;
%value of k2 (min^-1)
k2=0.18;
%value of k3 (min^-1)
k3=0.01;

%initial conditions:
ca0=1;
cb0=0;
cc0=0;
cd0=0;
ce0=0;

%FOR THE DETERMINATION OF COMPONENT A

t1=t0;
t1=[t0:h:time]';
ca1 = 0*t1;
ca1(1) = ca0;
i = 1;

while(i<max(size(t1)))
fn1a=-k1*ca1(i);
t2=t1(i)+(h/2);
```

```

ca2=ca1(i)+((h*fn1a)/2);
fn2a=-k1*ca2;
t3=t1(i)+(h/2);
ca3=ca1(i)+((h*fn2a)/2);
fn3a=-k1*ca3;
t4=t1(i)+h;
ca4=ca1(i)+fn3a*h;
fn4a=-k1*ca4;
j=i+1;
ca1(j)=ca1(i)+((h/6)*(fn1a+2*fn2a+2*fn3a+fn4a));
i=i+1;
end
plot(t1,ca1,'blue')
hold on

```

**%FOR THE DETERMINATION OF COMPONENT B**

```

t1=t0;
t1=[t0:h:time]';
cb1 = 0*t1;
cb1(1) = cb0;
i = 1;

while(i<max(size(t1)))
fn1b=k1*ca1(i)-k2*cb1(i);
fn1a=-k1*ca1(i);
t2=t1(i)+(h/2);
cb2=cb1(i)+((h*fn1b)/2);
ca2=ca1(i)+((h*fn1a)/2);
fn2b=k1*ca2-k2*cb2;
fn2a=-k1*ca2;
t3=t1(i)+(h/2);
cb3=cb1(i)+((h*fn2b)/2);
ca3=ca1(i)+((h*fn2a)/2);
fn3b=k1*ca3-k2*cb3;
fn3a=-k1*ca3;
t4=t1(i)+h;
cb4=cb1(i)+fn3b*h;
ca4=ca1(i)+fn3a*h;
fn4b=k1*ca4-k2*cb4;
j=i+1;
cb1(j)=cb1(i)+((h/6)*(fn1b+2*fn2b+2*fn3b+fn4b));
i=i+1;

```

```

end
plot(t1,cb1,'black')

%FOR THE DETERMINATION OF COMPONENT C

t1=t0;
t1=[t0:h:time]';
cc1 = 0*t1;
cc1(1) = cc0;
i = 1;

while(i<max(size(t1)))
fn1c=k2*cb1(i)-k3*cc1(i);
fn1b=k1*ca1(i)-k2*cb1(i);
fn1a=-k1*ca1(i);
t2=t1(i)+(h/2);
cc2=cc1(i)+((h*fn1c)/2);
cb2=cb1(i)+((h*fn1b)/2);
ca2=ca1(i)+((h*fn1a)/2);
fn2c=k2*cb2-k3*cc2;
fn2b=k1*ca2-k2*cb2;
fn2a=-k1*ca2;
t3=t1(i)+(h/2);
cc3=cc1(i)+((h*fn2c)/2);
cb3=cb1(i)+((h*fn2b)/2);
ca3=ca1(i)+((h*fn2a)/2);
fn3c=k2*cb3-k3*cc3;
fn3b=k1*ca3-k2*cb3;
t4=t1(i)+h;
cc4=cc1(i)+fn3c*h;
cb4=cb1(i)+fn3b*h;
fn4c=k2*cb4-k3*cc4;
j=i+1;
cc1(j)=cc1(i)+((h/6)*(fn1c+2*fn2c+2*fn3c+fn4c));
i=i+1;
end

plot(t1,cc1,'red')

% FOR THE DETERMINATION OF COMPONENT D

t1=t0;
t1=[t0:h:time]';

```

```

cd1 = 0*t1;
cd1(1) = cd0;
i = 1;

while(i<max(size(t1)))
fn1d=k3*cc1(i);
fn1c=k2*cb1(i)-k3*cc1(i); %
fn1b=k1*ca1(i)-k2*cb1(i); %
fn1a=-k1*ca1(i);
t2=t1(i)+(h/2);
cc2=cc1(i)+((h*fn1c)/2);
cb2=cb1(i)+((h*fn1b)/2);
ca2=ca1(i)+((h*fn1a)/2);
fn2d=k3*cc2;
fn2c=k2*cb2-k3*cc2;
fn2b=k1*ca2-k2*cb2;
t3=t1(i)+(h/2);
cc3=cc1(i)+((h*fn2c)/2);
cb3=cb1(i)+((h*fn2b)/2);
fn3d=k3*cc3;
fn3c=k2*cb3-k3*cc3;
t4=t1(i)+h;
cc4=cc1(i)+(fn3c*h);
fn4d=k3*cc4;
j=i+1;
cd1(j)=cd1(i)+((h/6)*(fn1d+2*fn2d+2*fn3d+fn4d));
i=i+1;
end

plot(t1,cd1,'cyan')

data_glycerol_oxidation=[ t1 ca1 cb1 cc1 cd1 ]

%for confirmation sum must be equal to the initial amount (ca0)
sum=ca1+cb1+cc1+cd1

xlabel ('time[h]')
ylabel ('concentration')
title ('Simulation of glycerol oxidation')
hleg1 = legend('glycerol','glyceraldehyde','glyceric acid', ...
'glycolic acid');

```

## APPENDIX IV

### Incorporation of PID controllers

The set of equations (340) to (345) described in page 92 are unstable as depicted by the response to a step input of the respective transfer functions, as showed in the figure 63 a) and b)

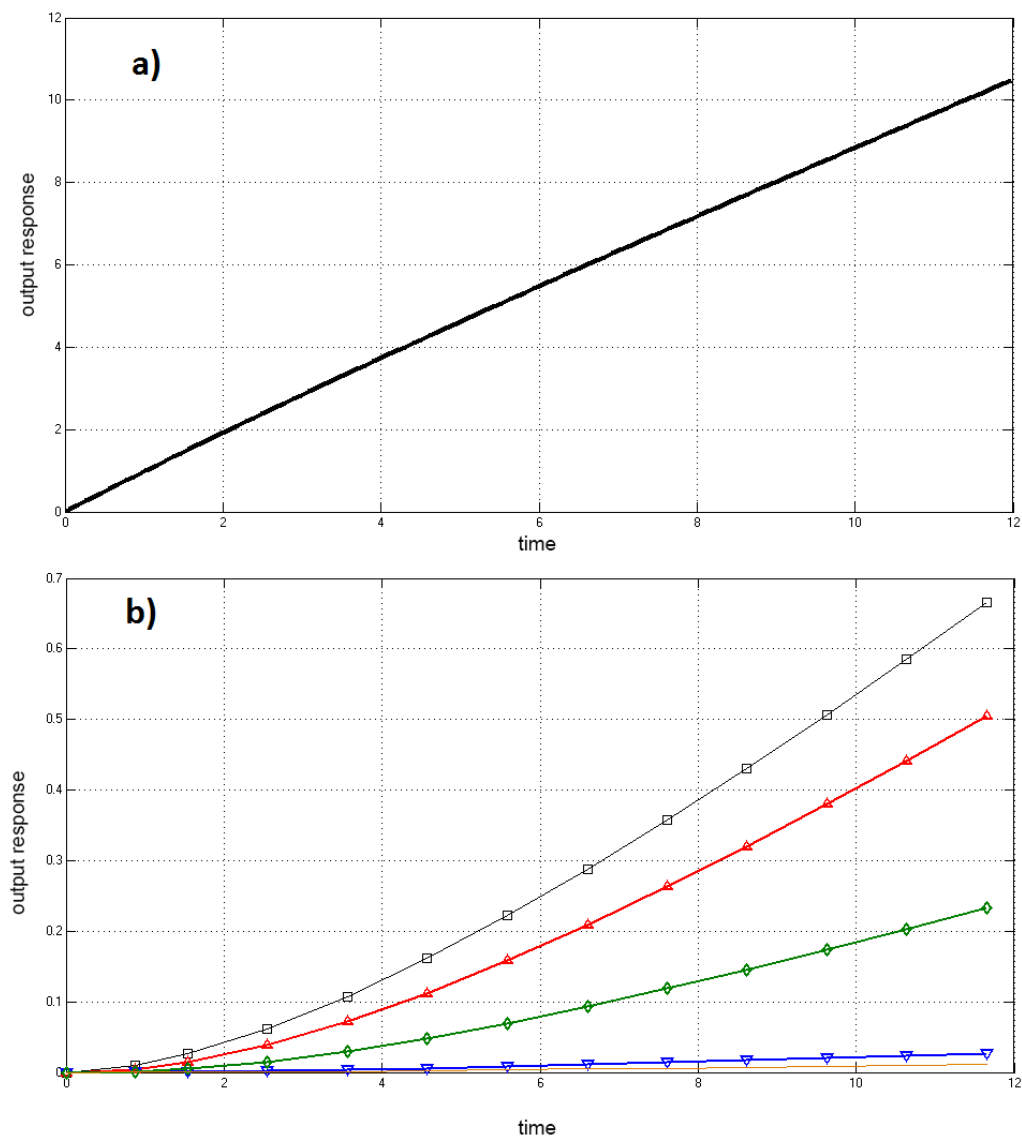


**Fig. 63:** Step response of the system considering the estimated transfer functions for glycerol reacted (a) and products formed (b) ( $\square C_B$ ;  $\blacktriangle C_C$ ;  $\blacktriangledown C_D$ ;  $\blacklozenge C_E$ ;  $— C_F$ )

As a result, it is required the incorporation of PID controllers that can regulate the response to a stable output. A continuous-time PID controller with first-order

derivative filter was considered based on the formula  $+I\frac{1}{s} + D\frac{N}{1+N\frac{1}{s}}$ , where the tuning parameters are P (proportional gain), I (integral gain), D (derivative gain) and N (filter coefficient). The values of the parameters P, I D and N obtained after tuning procedure are presented in Table 13.

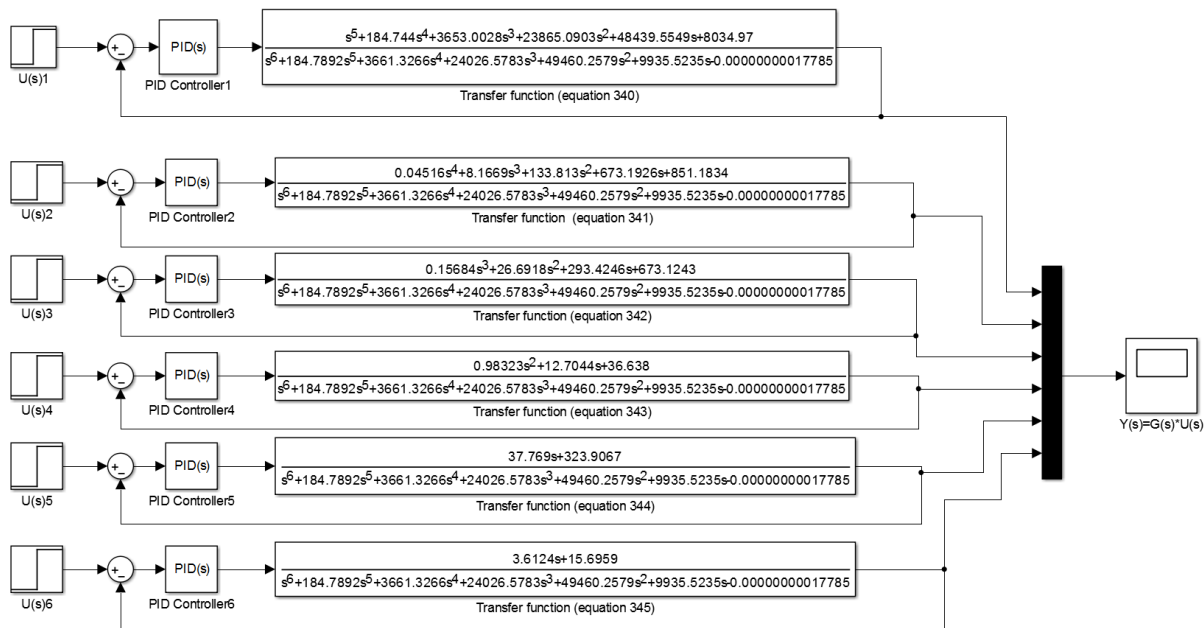


**Fig. 64:** Proposal of closed-loop PID controllers for the stabilization of the anodic oxidation system.

**Table 13.** Closed-loop calculations of controller parameters

PID controller	Controller parameters			
	Proportional (P)	Integral (I)	Derivative (D)	Filter coefficient (N)
1	1,11	0,009	-0,52	2,12
2	5,94	0,027	29,15	0,53
3	8,25	0,033	25,12	0,99
4	120,18	0,407	378,52	0,831
5	14,57	0,049	42,66	1,428
6	289,47	0,981	876,93	1,06

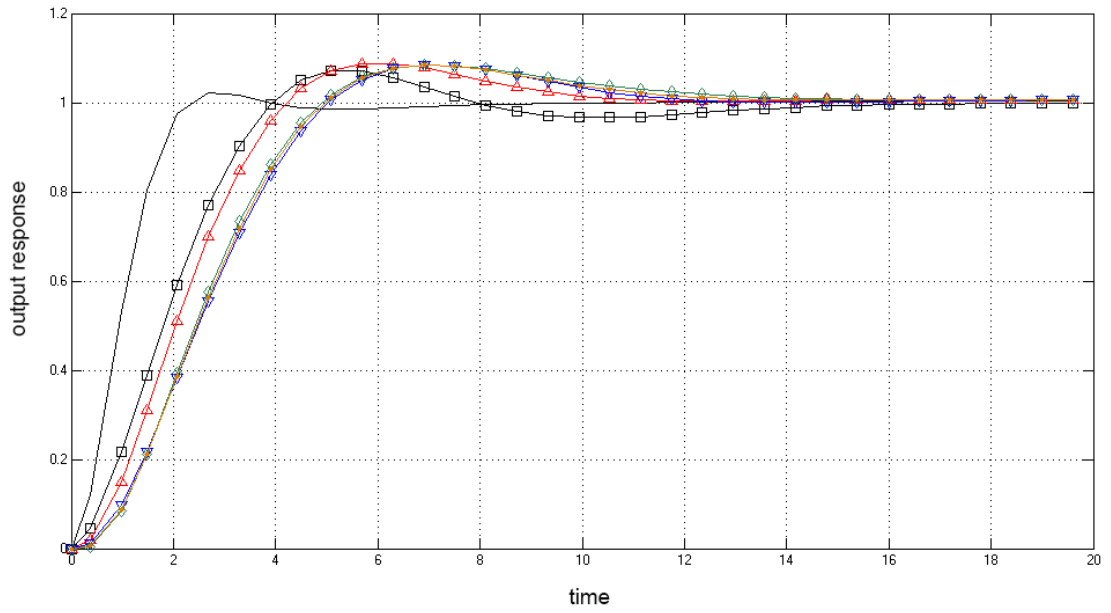


**Fig. 65:** Dynamic response of feedback loop. Estimation of the output response (solid line: glycerol; products formed  $\square C_B$ ;  $\blacktriangle C_C$ ;  $\blacktriangledown C_D$ ;  $\blacklozenge C_E$ ;  $— C_F$ ) after step input

# LIST OF PUBLICATIONS OF THE AUTHOR

## Publications in international journals with impact factor

J.C. BELTRÁN-PRIETO, R. VELOZ-RODRÍGUEZ, M.C. PÉREZ-PÉREZ, J.L. NAVARRETE-BOLAÑOS, E. VÁZQUEZ-NAVA, H. JIMÉNEZ-ISLAS, J.E. BOTELLO-ÁLVAREZ, Chromium recovery from solid leather waste by chemical treatment and optimisation by response surface methodology, *Chemistry and Ecology*, 2012, vol. 28, issue 1, p. 89–102.

G. PARAVANOVA, B. HAUSNEROVA, J. C. BELTRÁN-PRIETO. Determination of Dispersion Efficiency of Cement Suspensions by Method of Centrifugation, *Journal of Applied Polymer Science*, 2013, vol. 129, issue 1, p. 464–471.

J.C. BELTRÁN-PRIETO, J. PECHA, V. KAŠPÁRKOVÁ, K. KOLOMAZNÍK, Development of an HPLC method for the determination of glycerol oxidation products, *Journal of Liquid Chromatography & Related Technologies*, 2013, vol. 36, issue 19, p. 2758-2773.

J.C. BELTRAN-PRIETO; K. KOLOMAZNÍK; R. VELOZ-RODRÍGUEZ. Removal of chromium from tannery waste water using waste building material, *Fresenius Environmental Bulletin*, 2013, vol. 22, issue 2a, p. 573-578

G. PARAVANOVA, B. HAUSNEROVA, J.C. BELTRÁN-PRIETO. The action principle of organic plasticizers in cement suspensions determined from centrifugation, *Polymer Composites*, 2013, vol. 34 issue 9, p. 1483-1488.

J.C BELTRÁN-PRIETO, K. KOLOMAZNÍK AND J. PECHA, A Review of Catalytic Systems for Glycerol Oxidation: Alternatives for Waste Valorization, *Australian Journal of Chemistry*, 2013, vol. 66, issue 5, p.511-521.

G. PARAVANOVA, B. HAUSNEROVA, J.C. BELTRÁN-PRIETO, Rheological properties of calcium carbonate suspensions determined from centrifugation. *Chemické listy*, 2014 vol. 108, issue 1, p. s32- s34

J. C. BELTRÁN PRIETO, R. SLAVÍK, K. KOLOMAZNÍK, Electrooxidation of Glycerin by Potential Sweep Technique and Controlled Potential Electrolysis, *International Journal of Electrochemical Science*, 2014, vol. 9, p. 6910-6923.

J.C. BELTRÁN PRIETO, R. SLAVÍK, K. KOLOMAZNÍK, Non-isothermal modeling of glycerol oxidation reaction and estimation of thermodynamic parameters, *Russian Journal of General Chemistry*, 2014, Vol. 84, issue 11

## **Publications in Journals without Impact factor and Conference proceedings**

J.C. BELTRÁN-PRIETO, K. KOLOMAZNÍK, Optimization of alkaline hydrolysis of chrome shavings for chromium oxide recovery”, International Journal of Arts and Sciences 2012, vol. 5 issue 4, p. 1-13, ISSN 1944-6934

.C. BELTRÁN-PRIETO, J. PECHA, V. KAŠPÁRKOVÁ, K. KOLOMAZNÍK “Determination of Glycerol Derivatives by High-Performance Liquid Chromatography”, Advances in Environment, Biotechnology and Biomedicine, 47-52, Proceedings of the 1st WSEAS International Conference on Energy and Environment Technologies and Equipment (EEETE '12) ISBN: 978-1-61804-122-7, Published by WSEAS Press. Editors: Prof. Drahomira Pavelkova, Prof. Jiri Strouhal, Assoc. Prof. Marie Pasekova

J.C. BELTRÁN PRIETO, R. SLAVÍK, K. KOLOMAZNÍK, Effect of Platinum Electrode on Partial Oxidation of Glycerol and Optimization by Central Composite Design, Recent Advances in Energy and Environmental Management. Proceedings of the 8th International Conference on Energy & Environment (EE '13), 2013, ISSN: 2227-4359. Published by WSEAS Press. Editors: Valeri Mladenov, Tasho Tashev, Hui Wang, Ivan Kralov, Sergey Stankevich, Pelin Yildiz, Jon Burley.

J.C. BELTRÁN PRIETO, R. VELOZ-RODRÍGUEZ, Optimization of Chromium Adsorption using Central Composite Design, Recent Advances in Continuum Mechanics, Hydrology and Ecology, Proceedings of the 8th International Conference on Water Resources, Hydraulics & Hydrology (WHH '13) . 2013, ISBN: 978-960-474-313-1, Editors: Valeri Mladenov, Ivan Kralov, Tasho Tashev, Francisc Popescu, José Ignacio Hernández López, Giri Kattel, Ana Maria Tavares Martins

J.C. BELTRÁN PRIETO, R. SLAVÍK, K. KOLOMAZNÍK , Study of the electrooxidation of Glycerol on Platinum Electrodes by Cyclic Voltammetry and Multiple Pulse Amperometry, 7th International Conference on Environmental Engineering and Management Integration Challenges for Sustainability, 18 – 21 September 2013, Vienna, Austria, ISBN: 978-973-621-418-9

J.C. BELTRÁN PRIETO, K. KOLOMAZNÍK, Mathematical Modeling of Heat Loss of a Sphere in Contact with a Well Stirred Fluid in ISCS 2013: Interdisciplinary Symposium on Complex Systems, Chapter 14, Series: Emergence, Complexity and Computation, Vol. 8, Sanayei, Ali; Zelinka, Ivan; Rossler, Otto E. (Eds.) ISBN 978-3-642-45437-0

J.C. BELTRÁN PRIETO, R. SLAVÍK, K. KOLOMAZNÍK, J.PECHA, Mechanism and kinetic studies on the synthesis of glyceraldehyde via anodic oxidation of glycerol, 21st International Congress of Chemical and Process Engineering CHISA 2014 Prague 23-27 August 2014 Prague, Czech Republic, ISBN: 978-80-02-02555-9

J.C. BELTRÁN PRIETO, R. SLAVÍK, K. KOLOMAZNÍK, Optimization of electrochemical oxidation of glycerol for glyceric acid production, International Journal of Energy and Environment, 2013, vol. 7 issue 5, p. 229-235,

J.C. BELTRÁN PRIETO, R. SLAVÍK, K. KOLOMAZNÍK, J.PECHA, Evaluation of Kinetics and Reaction Mechanism of Partial Oxidation of Glycerol, International Journal of Automation and Power Engineering, 2014, vol. 3, issue 1, p. 72 -74.

## **CURRICULUM VITAE AUTOR**

Name and title: Juan Carlos Beltrán Prieto, M.Sc.  
Day and place of birth: 9.9.1984, Cortazar México  
Address: Nam. T.G. Masaryka 3050 760 01, Zlín  
E-mail: prieto@fai.utb.cz

### **Education:**

2010– recent Tomas Bata University in Zlín. Faculty of Applied Informatics. Doctoral studies, Automatic control and Informatics.  
2007 – 2009 Technological Institute of Celaya, Department of Biochemical Engineering, Master studies.  
2002 – 2007 Technological Institute of Celaya, Department of Biochemical Engineering, Bachelor studies.

### **Participation in Research Projects**

ED2.1.00/03.0089 - Centrum bezpečnostních, informačních a pokročilých technologií (CEBIA-Tech) (2011-2014, MSM/ED), Výzkumný program 3 - Alternativní zdroje energie. Junior researcher.

Treatment of waste water and chromium solid waste from leather industry. Technological Institute of Celaya (2004-2010)

Effect of CSF-1 treatment in bone marrow transplantation. Queensland Institute of Medical Research, Brisbane, Australia (2006)

Recovery and reuse of tannins from the leather industry. Center for Applied Innovation and Competitive Technologies (CIATEC) (2004)

### **Language skills**

English – highly proficient in spoken and written  
Czech – basic communication skills